Dissertation

submitted to the

Combined Faculties for the Natural Sciences and for Mathematics

of the Ruperto-Carola University of Heidelberg, Germany

for the degree of

Doctor of Natural Sciences

UNDERSTANDING THE ROLE OF SPHINGOSINE 1-PHOSPHATE IN REGULATING THE MICROGLIA AND GLIOMA INTERACTIONS

Presented by

M.Sc. Rakesh Sharma

Born in: Chennai, India

Oral examination: 10th of April, 2019

UNDERSTANDING THE ROLE OF SPHINGOSINE 1-PHOSPHATE IN REGULATING THE MICROGLIA AND GLIOMA INTERACTIONS

Referees:

Prof. Dr. Peter Angel

Dr. Björn Tews

To my family

Abstract

Glioblastoma multiforme (GBM) are the most common highly malignant and most devastating brain tumors, with a 5-year survival rate below 10%. Based on molecular-genetic factors, GBM are sub-grouped into four distinct genetic subclasses, namely Proneural, Neural, Classical and Mesenchymal based on subtype metagene score and aberrations in genes including *PDGFRA*/*IDH1*, *EGFR*, and *NF1*. Within a GBM tumor, microglia/macrophages make up the largest population of tumor-infiltrating cells, contributing to at least one-third of the total tumor mass. Glioma cells recruit and exploit microglia for their proliferation and invasion ability, and transform microglia into an anti-inflammatory, i.e. tumor-supportive, phenotype.

Substantial evidence suggests that Sphingosine-1-phosphate (S1P), a pleotropic bioactive sphingolipid metabolite, is involved in glioma cell migration and invasion and functions as an important mitogen for glioma cells. S1P is formed inside the cell by two sphingosine kinases, *SPHK1* and *SPHK2*. TCGA Analysis of the expression of Sphingosine Kinase 1 (*SPHK1*) in different subgroups of GBM revealed that *SPHK1* expression correlated to poor survival outcome in GBM, among which the mesenchymal subtype showed the highest expression of *SPHK1*. Previous literature also suggested that the mesenchymal subtype showed a selective enrichment of microglia/macrophage- related genes. Thus, it was hypothesized that glioma-derived S1P, the secretory metabolite of SPHK1, could play an important role in regulating the microglia/macrophage – glioma crosstalk.

Using an iBidi Culture-Insert 3-well co-culture system, primary murine microglia co-cultured with glioma cells overexpressing human *SPHK1*, displayed an enhanced expression of pro-tumorigenic related microglial genes, as shown by an increased mRNA expression of Arginase 1 (*Arg1*) and Macrophage scavenger receptor 1 (*Msr1*). The selective inhibition of SPHK1 by the small-molecule inhibitor SKI-II, or knockdown of SPHK1 in glioma cells, inhibited the pro-tumorigenic phenotype of microglia, as shown by a decreased mRNA expression of *Arg1* and *Msr1*, decreased production of IL-10 and significant increased production of pro-inflammatory cytokines such as TNFα and IL-6. Furthermore, inhibition of SPHK1 in gliomas also resulted in decreased activation of key signaling events that regulate anti-inflammatory phenotype, with

subsequent activation of pro-inflammatory pathways in microglia/ macrophages. Inhibition of the sphingosine 1-phosphate receptors by FTY720 also shifted the activation state of microglia towards a pro-inflammatory phenotype.

In addition, S1P regulated the microglial phenotype by altering NF-κB signaling, a key pro-inflammatory pathway. S1P was able to reduce LPS induced pro-inflammatory polarization of microglia, by inhibiting the NF-κB pathway. S1P abrogated the LPS induced M1 phenotype via signaling through S1PR1 and activation of the non-canonical TLR4 pathway, possibly via activation of the TBK1/ IRF3 signaling. In summary, these results support the role of glioma-secreted S1P in maintaining the anti-inflammatory phenotype of microglia that promotes tumor progression and invasion.

Zusammenfassung

Glioblastoma multiforme (GBM) sind die häufigsten hochmalignen und verheerendsten Hirntumoren mit einer 5-Jahres-Überlebensrate unter 10%. Basierend auf molekulargenetischen Faktoren werden GBM in vier verschiedene genetische Subklassen eingeteilt, nämlich Proneural, Neural, Classical und Mesenchymal, basierend auf Subtyp-Metagene-Score und Aberrationen in Genen, einschließlich *PDGFRA* / *IDH1*, *EGFR* und *NF1*. Innerhalb eines GBM-Tumors bilden Mikroglia / Makrophagen die größte Population von Tumor-infiltrierenden Zellen, dieses beträgt mindestens ein Drittel der gesamten Tumormasse. Gliomzellen rekrutieren und nutzen Mikroglia für ihre Proliferations- und Invasionsfähigkeit und transformieren Mikroglia in einen entzündungshemmenden, d. h. tumorunterstützenden Phänotyp.Wesentliche Hinweise legen nahe, dass Sphingosin-1-phosphat (S1P), ein pleiotroper, bioaktiver Sphingolipid-Metabolit, an der Migration und Invasion von Gliomzellen beteiligt ist und als wichtiges Mitogen für Gliomzellen fungiert. S1P wird in der Zelle von zwei Sphingosinkinasen, *SPHK1* und *SPHK2*, gebildet. Die TCGA-Analyse der Expression der Sphingosinkinase 1 (*SPHK1*) in verschiedenen Untergruppen von GBM zeigte, dass die SPHK1-Expression mit einem schlechten Überlebens-Ergebnis in GBM korrelierte, wobei der mesenchymale Subtyp die höchste Expression von *SPHK1* zeigte. Frühere Literatur deutete auch darauf hin, dass der mesenchymale Subtyp eine selektive Anreicherung von Mikroglia / Makrophagen-verwandten Genen zeigte. Daher wurde die Hypothese aufgestellt, dass Gliom-abgeleiteter S1P, der sekretorische Metabolit von *SPHK1*, eine wichtige Rolle bei der Regulierung des Mikroglia / Makrophagen-Gliom-Übersprechens spielen könnte.

Unter Verwendung eines iBidiKultur-Insert-3-Well-Co-Kultursystems zeigten primäre murineMikroglia, die mit Gliomzellen, die humanes *SPHK1* überexprimieren, co-kultiviert wurden, eine verstärkte Expression von pro-tumorigenen verwandten Mikroglia-Genen, wie durch eine erhöhte mRNA-Expression von Arginase 1 (Arg1) und Makrophagen-Scavenger-Rezeptor 1 (Msr1) gezeigt wurde. Die selektive Hemmung von *SPHK1* durch den niedermolekularen Inhibitor SKI-II oder die Depletion von *SPHK1* in Gliomzellen hemmte den pro-kanzerogenen Phänotyp von Mikroglia, wie durch eine verminderte mRNA-Expression von Arg1 und Msr1 gezeigt wurde, verringerte die Produktion von IL-10 und erhöhte signifikant die

Produktion von proinflammatorischenCytokinen wie TNFα und IL-6. Darüber hinaus führte die Hemmung von *SPHK1* in Gliomen auch zu einer verminderten Aktivierung von Schlüsselsignalereignissen, die den entzündungshemmenden Phänotyp regulieren, mit anschließender Aktivierung proinflammatorischer Signalwege in Mikroglia / Makrophagen. Die Hemmung der Sphingosin-1-Phosphat-Rezeptoren durch FTY720 verschob auch den Aktivierungszustand von Mikroglia in Richtung eines proinflammatorischen Phänotyps.Darüber hinaus regulierte S1P den mikroglialen Phänotyp durch Veränderung der NF-κB-Signalgebung, einem wichtigen entzündungsfördernden Signalweg. S1P war in der Lage, die LPS-induzierte proinflammatorische Polarisation von Mikroglia durch Hemmung des NF-κB-Signalwegs zu reduzieren. S1P verhinderte den LPS-induzierten M1-Phänotyp durch Signalgebung durch S1PR1 und Aktivierung des nicht-kanonischen TLR4-Wegs, möglicherweise über die Aktivierung der TBK1 / IRF3-Signalisierung. Zusammenfassend unterstützen diese Ergebnisse die Rolle von Gliom-sekretiertem S1P bei der Aufrechterhaltung des anti-inflammatorischen Phänotyps von Mikroglia, der die Tumorprogression und -invasion fördert.

Table of Contents

Abstract vii

Zusammenfassung ix

Table of figures xiv

1. Introduction 2

1.1 Glioblastoma multiforme 2

1.2 Brain tumor microenvironment 3

1.2.1 Endothelial cells 4

1.2.2 Astrocytes 4

1.2.3 Dendritic cells 5

1.3 Microglia in the CNS 6

1.3.1 Activation/ polarization states of microglia 8

1.3.2 Microglia/ macrophages in malignant gliomas 12

1.4 TLR4 activation upon LPS stimulation 15

1.5 Sphingosine 1-phopshate signaling 16

1.5.1 Sphingosine Kinases 17

1.5.2 Sphingosine 1-Phosphate Receptors 18

1.5.3 Role of S1P in cancer 20

2. Materials and Methods 22

2.1 Materials 22

2.2 Methods 32

2.2.1 Animal cell culture 32

2.2.2 Western blot analysis 36

2.2.3 Trizol based RNA isolation 38

2.2.4 RNA isolation using kit 38

2.2.5 First strand cDNA synthesis 39
2.2.6 Quantitative Real time Reverse transcriptase Polymerase Chain Reaction (qRT-PCR) 39
2.2.7 ELISA 40
2.2.8 Flow Cytometry 40
2.2.9 Plasmid DNA isolation 41
2.2.10 Transformation in E.coli competent cells 41
2.2.11 Statistical analysis 41
3. Results 42
3.1 High SPHK1 expression correlates with poor-survival outcome in GBM and an increased expression in mesenchymal subgroup of GBM 42
3.2 SPHK1 expression is positively correlated to microglial gene signature 44
3.3 Validation of microglia isolation by flow cytometry 46
3.4 Silencing of SPHK1 in gliomas induces a pro-inflammatory phenotype in microglia/ macrophages. 47
3.5 Over-expression of SPHK1 in glioma enhances the M2 phenotype of microglia/ macrophages. 51
3.6 Inhibition of SPHK1 in a co-culture system shifts microglia/ macrophages to an M1 phenotype. 55
3.7 Inhibition of SPHK1 in gliomas modulates important signaling pathways that regulate M1-M2 polarization of microglia/ macrophages 59
3.8 Antagonism of Sphingosine 1-Phosphate receptors by FTY720 induces a pro-inflammatory phenotype of microglia/ macrophages 62
3.9 S1P inhibits LPS mediated M1 phenotype of microglia/ macrophages 67
4. Discussion 74
4.1 High SPHK1 expression influences gene expression class in GBM and correlates to increased microglial gene signature 74

4.2 Modulation of SPHK1 activity in gliomas influences the polarization of microglia 76
4.3 FTY720 treatment stimulates a pro-inflammatory signature of microglia/ macrophages .. 79
4.4 Sphingosine 1-phosphate induces an anti-inflammatory phenotype in microglia/ macrophages via S1PR1 81
4.5 Future Outlooks 82
5. Abbreviations 84
6. References 88
7. Acknowlegdement 104

Table of figures

Figure 1: The brain tumor microenvironment encompasses various cell types harboring diverse phenotypes and functions.

Figure 2: Identification and characterization of microglia

Figure 3: Distinct activation states of microglia/ macrophages.

Figure 4: The role of tumor associated microglia/macrophages (TAMs) under the influence of glioma.

Figure 5: The relationship of ceramide – sphingosine 1-phosphate rheostat in cancer.

Figure 6: High SPHK1 expression correlates with poor-survival outcome in GBM and an increased expression in mesenchymal subgroup of GBM

Figure 7: SPHK1 expression is positively correlated to microglial gene signature.

Figure 8: Validation of microglia population by flow cytometry.

Figure 9: Validation of knockdown of SPHK1 in glioma cells.

Figure 10: Silencing of SPHK1 in gliomas induces a pro-inflammatory phenotype in microglia/ macrophages.

Figure 11: Verification of overexpression of SPHK1 in glioma cells.

Figure 12: Over-expression of SPHK1 in glioma enhances the M2 phenotype of microglia/ macrophages.

Figure 13: Inhibition of SPHK1 in gliomas modulates gene expression profile of microglia from anti-inflammatory phenotype to a pro-inflammatory phenotype

Figure 14: SKI-II treatment in gliomas induces significant changes in the secretion of inflammatory factors

Figure 15: Inhibition of SPHK1 in gliomas shifts macrophage response to an M1 phenotype.

Figure 16: SKI-II treatment in glioma modulates important signaling pathways that regulate M1-M2 polarization of primary microglia

Figure 17: SKI-II treatment in glioma regulates key signaling pathways that defined the M1-M2 polarization of macrophages

Figure 18: Inhibition of Sphingosine 1-phosphate receptors by FTY720 modulates gene expression profile of microglia by inducing a pro-inflammatory phenotype.

Figure 19: FTY720 treatment induces significant changes in the secretion of inflammatory factors in microglia

Figure 20: Antagonism of Sphingosine 1-Phosphate receptors by FTY720 in microglia modulates important signaling pathways that regulate M1-M2 polarization

Figure 21: S1P inhibits LPS mediated M1 phenotype of microglia/ macrophage

Figure 22: S1P modulates NF-κB activity in microglia/ macrophages via S1PR1

1. Introduction

1.1 Glioblastoma multiforme

Malignant glioblastoma are highly aggressive types of brain tumors in the central nervous system and account for almost 80% of all malignant brain neoplasms[1]. These include tumors generally associated with cytologically malignant, mitotically active, necrotic-prone neoplasms typically associated with rapid pre- and postoperative disease evolution and a fatal outcome[2]. As of today no successful treatment exists, offering GBM patients an average survival time of about 12-15 months after diagnosis, despite surgical tumor resection, radio-, and chemotherapy[3].

The rationales for failure of GBM treatment are diverse. One feature of GBM is the highly invasive growth pattern into the brain parenchyma which prevents complete surgical resection of the tumor. Even though GBM can be visualized using a high contrast MRI to identify tumor lesions, tumor cells migrate deep into the brain parenchyma and far beyond, making it difficult to detect by MRI. Recurring GBM after surgical resection often re-emerge close to the region of the resected primary tumor, but also at locations distant from the original tumor location and can cross over to the contra-lateral hemisphere[4]. Another cause for the failure of treatment is the genetic and cellular inter- and intra-tumor heterogeneity of GBMs[5–7].

The 2016 World Health Organization (WHO) classification of tumors of the central nervous system classified CNS tumors based on molecular parameters, in addition to previously incorporated histological features of the tumor[8]. The new classification restructured the identification of malignant glioblastoma (GBM), which currently includes both the genotype (*Isocitrate dehydrogenase 1*, *IDH1* mutation status) and phenotype in diagnosing these tumors. GBM are classified based on genotype either as IDH wildtype (about 90% of cases), IDH mutant, or NOS (for which IDH evaluation has to be performed) [8,9]. Additionally *epitheloid glioblastoma* has been introduced as a new variant, while the *adenoid*, *granular cell*, *metaplastic*, *heavily lipidized glioblastoma*, and *glioblastoma with a primitive neuronal component* has been included as new patterns[8,9].

Despite being morphologically similar, different GBM tumors result in different outcomes that are partially defined by various tumor molecular fingerprints[10]. Based on global DNA methylation patterns of glioblastoma, adult GBM could be subdivided into three distinct

epigenetic subgroups, one among these that correlated to mutations in *IDH1* gene[10]. The *IDH1* mutation is a gain of function modification that results in production of a novel onco-metabolite, 2-hydroxyglutarate (2HG) that hampers the normal cellular methylation machinery that consequently leads to an increased global methylation called CpG island methylator phenotype (CIMP). Likewise, gene expression profiling of GBM identified four distinct subgroups of GBM, named Proneural, Neural, Classical and Mesenchymal[5,10]. Tumors with *IDH1* mutation and $CIMP^+$ tumors can be segregated into the proneural expression profile, while other proneural subtypes are characterized by abnormalities in platelet derived growth factor receptor alpha (*PDGFRA*)[7,10]. The classical subgroup is characterized by mutation of epidermal growth factor receptor (*EGFR*), and the mesenchymal tumors characterized by neurofibromin (*NF1*) mutations[7].

Recent studies have shown that the mesenchymal subtype of GBMs display a high degree of necrosis, and a higher microglia/ macrophage infiltration, emphasizing the role of tumor microenvironment in strongly influencing both transcriptional regulators and gene expression class[7,11,12].

1.2 Brain tumor microenvironment

The tumor microenvironment (TME) consists of many different non-tumorigenic cells in addition to tumor cells that include endothelial cells, pericytes, fibroblasts, and immune cells. While normal brain is considered to be an "immune-privilege" organ in the body, the microenvironment in the brain has distinctive features that distinguish them from other organs of the brain [13]. These important features include a unique composition of the extra-cellular matrix (ECM), characteristic tissue-specific resident cell types including microglia, astrocytes, neurons, and a blood brain barrier (BBB) that protects the brain from invading pathogens, circulating immune cells and factors within the blood[13,14]. However, in certain brain tumors, the BBB is often compromised leading to infiltration of several immune cell types from the peripheral blood. Moreover, recent studies have challenged the understanding of immune privilege, where it has been illustrated that CNS possess a functional lymphatic system within the meninges, and CNS-derived antigens can stimulate an immune response in the cervical lymph nodes[13,14].

1.2.1 Endothelial cells

The tumor vasculature, formed by the interaction of endothelial cells, astrocytes, and pericytes, has distinctive functions in the tumor (**Figure 1**). The vasculature connects the tumor to the blood systems supplying it with nutrients and oxygen[3]. GBM tumors often exhibit high microvascular proliferation and abnormal angiogenesis frequently found in surrounding areas of pseudopalisading necrosis, and is often characterized by a response to hypoxia in the neoplastic microenvironment[15]. Multiple angiogenic pathways are upregulated in tumor cells, mediated in part by hypoxia, but also in stromal cells[3]. Several studies demonstrate multiple interactions/ crosstalk between glioma and endothelium, which involves important pathways such as VEGF signaling and Ang1/Tie2 signaling axis[15]. Secondly, the vasculature also constitutes a specialized niche for the glioma initiating stem-like cells, the so-called perivascular niche, suggesting that perivascular stem cell niches play a significant role in brain tumor pathology[16].

1.2.2 Astrocytes

Astrocytes, the most abundant member of the glial family are found within and around tumors and have been shown to play important role in the CNS response to tumor growth[17]. In the healthy brain astrocytes play an integral role in providing structural support to neurons, participating in synaptic activity and neurotransmitter uptake, supplying nutrition, as well as a role in the formation and maintining the structural integrity of the BBB[17,18]. Astrocytic end-feet processes form a network of fine lamellae ensheathing endothelial cells, thus maintaining a contact with pericytes through the basal lamina and forming the neurovascular unit with neurons[18,19]. Using gap junctions, multiple astrocytes can connect to larger networks and transport molecules, such as nutrients from blood vessels to neurons[20].

Upon brain damage or disease (such as GBM), astrocytes actively respond by altering their morphology and transcriptional profile, a process termed reactive astrogliosis that lead to the breakdown of the BBB and increased vascular permeability[17]. Reactive astrocytes can proliferate and secrete different factors that promote glioma growth and brain metastases[17,20]. The tumor cells establish functional gap junctions with astrocytes and reprogram them by providing cGAMP to induce a pro-inflammatory phenotype, characterized by production of various cytokines (for e.g. IFN-α and TNFα). Consecutively, these cytokines promote metastases by stimulating STAT1 and NF-κB signaling in tumor cells (**Figure 1**)[13]. Reactive astrocytes in

glioma also secrete stromal-derived factor 1 (SDF1), which can cause increased glioma cell proliferation and have been found to mediate glioma cell invasion by the activation of matrix metalloproteinase (MMP) 9[21,22]. A gene expression profiling of glioma-associated astrocytes revealed that these cells express potential pro-tumorigenic genes such as *Spp1*, *Ctgf*, and *Vgf*[23].

1.2.3 Dendritic cells

Dendritic cells, the myeloid- derived antigen presenting cells (APCs) put forward tumor antigens to T cells stimulating an anti-tumor immune response. These responses can be further enhanced by factors that are secreted by tumor cells into the microenvironment, such as reactive oxygen species (ROS) or danger-associated molecular patterns (DAMPs)[13,24]. These anti-tumor immune responses orchestrate antigen-specific responses by activating $CD4^+$ helper T cells and $CD8^+$ effector T cells[24]. Increased invasion of $CD8^+$ effector T cells into the tumor tissue has been correlated with prolonged survival in patients[25]. However, several studies have shown that numbers of $CD4^+$ and $CD8^+$ T cells are decreased in high-grade glioma, and that these cells show abnormal and decreased functionality[26]. In turn, studies have shown that glioma grade positively correlates with the numbers of infiltrating regulatory T cells (Tregs) and that depletion of $CD8^-$ /$CD4^+$/$FoxP3^+$Tregs from experimental gliomas resulted in increased survival of mice[27]. These cells have been implicated in participating in the establishment of an immunosuppressive milieu and preventing correct activation of immune cells, such as macrophages/monocytes and $CD4^+$ or $CD8^+$ T cells[27].

The majority of invading immune cells within brain tumors are microglia/ macrophages, which will be described more in detail later[28,29]. As opposed to initial thoughts that brain tumors were considered protected from immune surveillance by BBB, recent studies showed that activated immune cells cross the leaky BBB that is disrupted by the tumor[30]. Among other immune cells that invade the tumor, neutrophils also play an important role in gliomagenesis. Neutrophils have been shown to promote glioblastoma progression and chemoresistance by causing increased expansion of the glioma stem cell niche via upregulation of S1004A in tumor cells[31].

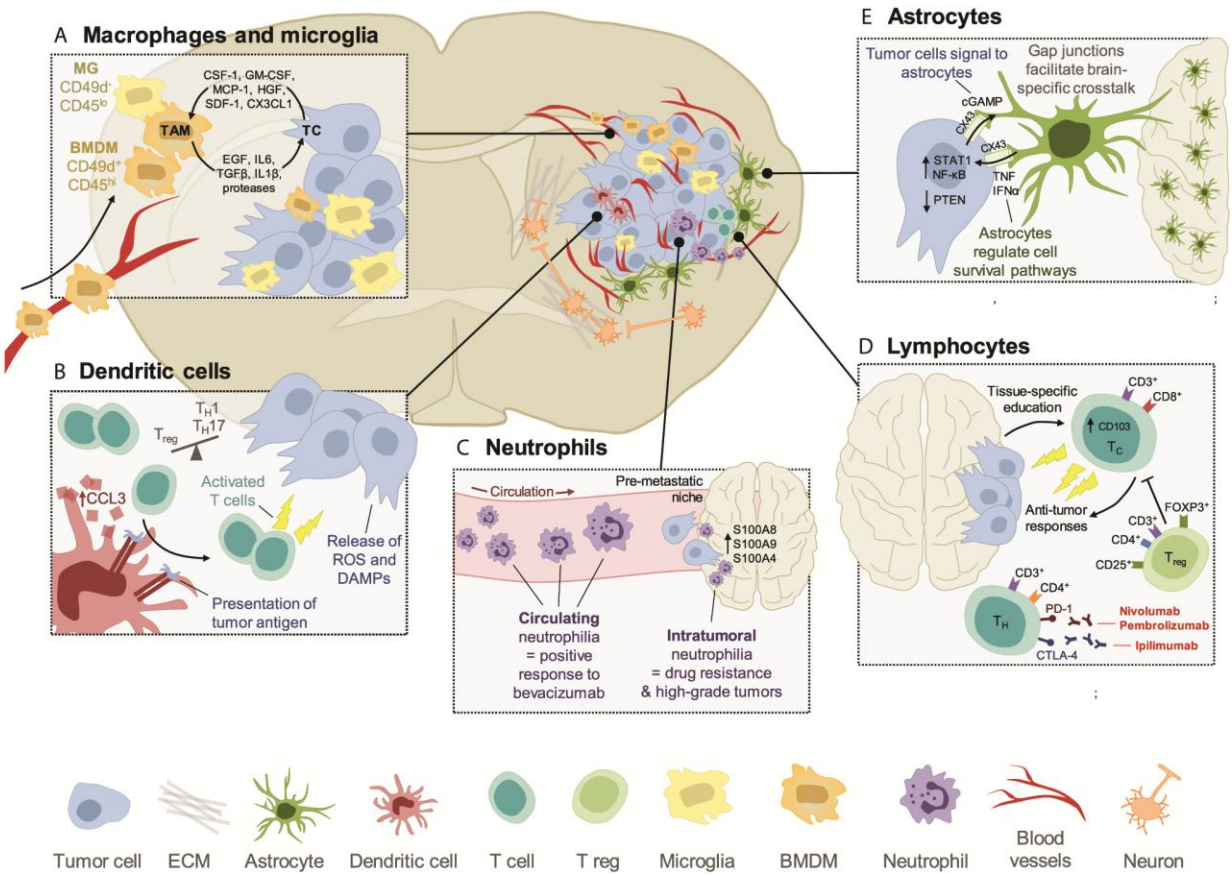

Figure 1: The brain tumor microenvironment encompasses various cell types harboring diverse phenotypes and functions.

Brain tumors are made up of diverse cell types. They can be grouped into peripherally-derived immune cells (lymphocytes, macrophages, neutrophils and dendritic cells) and specialized organ-resident cell types (microglia, astrocyes). Depending on the affected tissue, local positioning within tumors and disease stage, the cells in the TME can feature different activation states that are able to exert pro-tumoral or anti-tumoral activities. (Image is adopted and modified from Quail and Joyce, 2017)[13].

1.3 Microglia in the CNS

Like resident macrophages that function as the first responders to injury or infection in various tissues of the body, microglia and perivascular macrophages (PVM) represent the resident tissue macrophages of the CNS[32]. Microglia are glial origin, yolk-sac derived, monocyte-lineage cells that function as key immune regulators in the central nervous system (CNS), and play a crucial role in normal functioning and maintenance of the CNS[33]. They constitute about 10% of the CNS cells in the brain and spinal cord where they form a unique three-dimensional lattice, in which

individual microglial cells occupies it own defined territory[34]. Microglia are highly ramified cells that are under constant surveillance by extending its fine motile extensively branched processes, to detect and respond to extracellular signals by altering their morphology and phenotype, thereby maintaining brain homeostasis[32,34].

Microglia were originally identified by Franz Nissl in 1899, but later and characterized by Pio del Rio-Hortega in 1919[35]. Rio-Hortega conceptualized the definition of microglia, which were published in "*Cytology and Cellular Pathology of the Nervous System*", edited by Wilder Penfield in 1932[36,37]. He identified several key functions of microglia, formulated through a series of studies published in the early 1920s where he identified micrgoglial cells using a modified silver carbonate impregnation (**Figure 2**)[37]. His findings stated the following: 1) microglia enter the brain during early development. 2) microglial cells are of mesodermal origin (known today to originate from primitive yolk-sac derived macrophages[38]) and present an amoeboid morphology. 3) They utilize the blood vessels and the shit matter tracts as migrating tracts to enter different regions of the brain. 4) In mature brains, they transform into a branched, ramified morphology (known today as resting or M0 microglia[38]), and respond to external stimuli and pathological events by undergoing morphological and phenotypical transformation 5) They occupy their own unique defined territory in the brain, and are dispersed throughout the entire brain. 6) These cells have the ability to migrate, proliferate and phagocytose (**Figure 2**)[36,37].

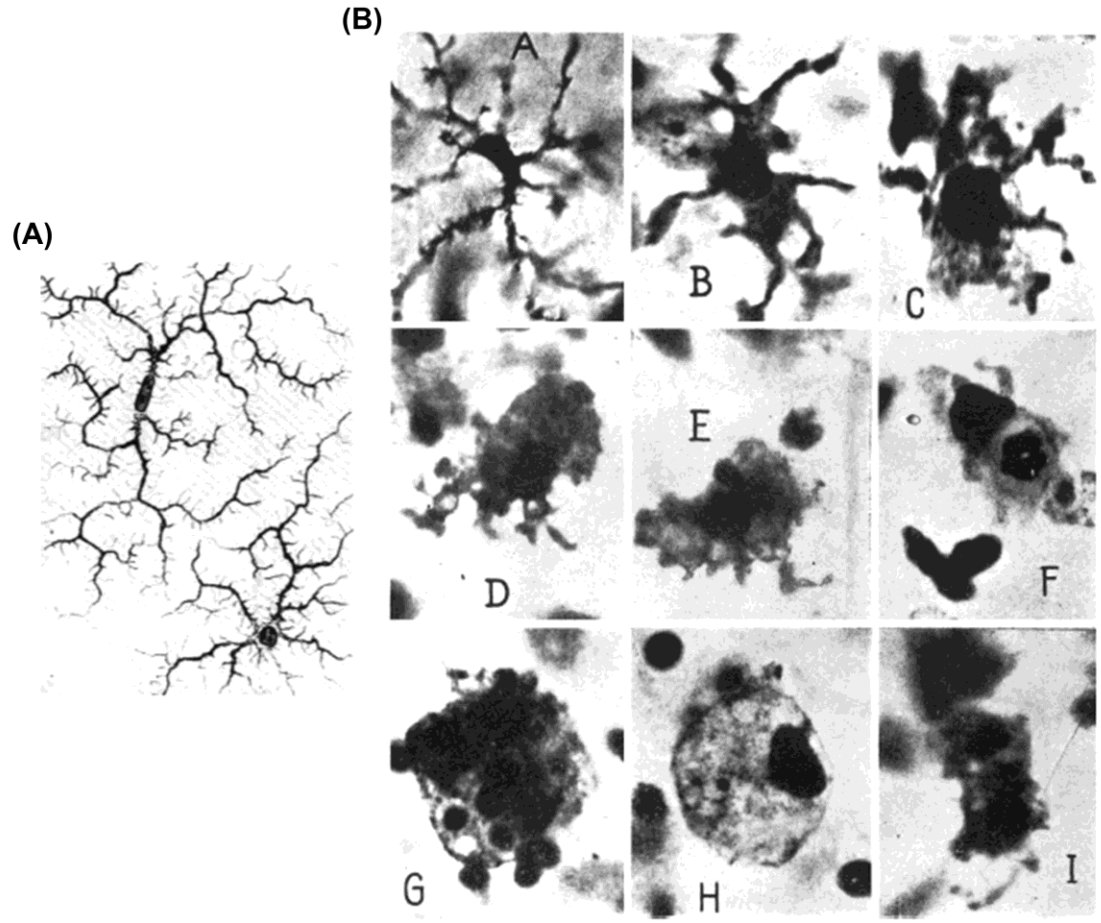

Figure 2: Identification and characterization of microglia

(A) An image of ramified microglial cells as illustrated by Rio-Hortego. (B) Evolution of microglia during its phagocytic activity. A, cell with thick wall, rough prolongations; B, cells with short prolongation and enlarged cell body; C, hypertrophic cell with pseudopodia; D and E, amoeboid and psuedopodic forms; F, cell with phagocytosed leukocyte; G, cell with numerous phagoctosed erythrocytes; H, fat-granule cell; G, cell in mitotic division. (Image is adopted and modified from Kettenmann et al, 2011[37]).

1.3.1 Activation/ polarization states of microglia

As previously observed by Rio-Hortega, microglia exists in a resting and a complex activation state[37]. Although microglia are described 'resting', they are constantly in active surveillance randomly scanning their neighboring domains even in its native state, by forming finger-like protrusions which can grow and shrink by 2-3 μm/min[35,39,40]. The resting state (also called M0

phenotype) is differentiated by low expression of macrophage-related surface markers, such as major histocompatibility markers (MHCII) and CD45[41].

Microglia transform into an 'activation' state following a neuronal insult, such as ischemia, infection and trauma, or in the presence of inflammatory mediators, by which they lose their ramified morphology and assume an amoeboid form[35,41]. Depending on the type of external stimuli it encounters, this activated state can be broadly classified into two individual states of microglia, namely the classical activation (M1 phenotype) and alternative activation (M2 phenotype).

1.3.1.1 Classical activation of microglia

Classical activation represents a pro-inflammatory reaction that mediate inflammatory tissue damage, which is triggered by pro-inflammatory agents such as lipopolysaccharide (LPS) and interferon gamma (IFN-γ) (**Figure 3**)[42,43]. M1 activated microglia produce reactive oxygen species as a result of reduced nicotinamide adenine dinucleotide phosphate (NADPH) oxidase activation (respiratory burst), and increased production of proinflammatory cytokines such as tumor necrosis factor alpha (TNFα), interleukin-6 (IL-6) and interleukin 1 beta (IL-1β)[44,45].

M1 cells also elicit the activation of the pathogenic T_h1 subset and T_h17 subset polarizations that promote cellular immune function and cause inflammation and autoimmune diseases, such as inflammatory bowel disease and collage-induced arthritis[46,47]. The production of proinflammatory IL-12 promotes T_h1 effector cell differentiation, IL-23 is important for constant IL-17 expression, an important cytokine associated with increased levels of polymorphonuclear leukocyte (PMN) recruitment, which is ultimately results in the differentiation of pathogenic T_h17 cells[47,48]. Toll like receptors (TLR) and C-type lectin receptors (CLR) on microglia respond to secreted inflammatory signals, triggering the expression of target genes through activation of signaling cascades including NF-κB, JNK, ERK1/2 and p38[47].

1.3.1.2 Alternative activation of microglia

On the contrary, alternative activation of microglia represents the anti-inflammatory phenotype (also called M2 phenotype) that mediates allergic, cellular and humoral responses to parasitic and extracellular pathogens. Initially alternatively activated microglia/ macrophages were classified based on expression of the mannose receptor (CD206); but since then a number of

studies have identified an assortment of different markers representing an M2 specific phenotype[35,42]. Among the most characterized and described markers is the enzyme arginase 1 (Arg1) that converts arginine to polyamines, proline, and ornithines that consequently leads to wound healing and matrix deposition[48]. Strikingly, Arg1 competes with iNOS that also utilizes arginine as its substrate to produce nitric oxide[48]. Thus upon alternative activation by IL10 or IL-4/IL-13, Arg1 can effectively inhibit the activity of iNOS consequently leading to the decreased production of nitric oxide and thereby resulting in a suppression of M1 phenotype. Thus, the expression of iNOS vs Arg1 determines the fate of microglia/ macrophages, thereby providing a relatively simpler technique to distinguish M1 and M2 phenotypes. Other markers used for describing M2 cells include Ym1, a heparin-binding lectin, FIZZ1, which promotes deposition of extracellular matrix, and CD206. Although alternative microglia/ macrophages are represented with these specific subset of markers, it provides only an over-simplification of the overall diversity of M2 phenotypes[42,49].

An alternative approach to categorize the function and phenotype of M2 cells is on the basis of the cytokines that induce them. The prototypical cytokine IL-4 was initially described as the mediator of alternative activation. Microglia/ macrophages that respond to both IL-4 and the closely related cytokine IL-13 has been classified as 'M2a', that mainly function to suppress inflammation and show increased phagocytic activity and production of growth factors such as insulin growth factor-1 (IGF-1) and IL-10 (**Figure 3**). IL-4 and IL-13 signal through IL-4Rα potentially leading to anti-inflammatory functions, such as Arg1 upregulation, inhibition of NF-κB isoforms, and production of scavenger receptors for phagocytosis[38,42,49].

M2b, the type II alternative activation is induced following exposure to immunoglobulin Fc gamma receptors (FcγRs) (CD16, CD32 or CD64) and immune complexes on LPS or IL-1β primed microglia/ macrophages (**Figure 3**). Although they do not express the classical markers of the alternative activation, such as Arg1, FIZZ1 and Ym1, they display an IL-10^{High}, IL-12^{Low} M2 cytokine profile, along with increased HLA-DR expression, elevated levels of MHCII, CD32 and CD86. These attributes has been associated with increased phagocytic activity and their ability to stimulate T cells towards a T_h2 response, suggesting that M2b might be a potential regulator or initiator of the M2 response in general[38,42,49].

The third state of alternative activation classified as 'M2c' (acquired deactivation) is based on exposure of IL-10, glucocorticoids, or transforming growth factor beta (TGF-β) to microglia/macrophages (**Figure 3**). This results in increased expression of TGF-β, sphingosine kinase 1 (SPHK1) and CD163. Although described as a 'deactivated' state, they seem to be involved in tissue remodeling and matrix deposition after inflammation has been suppressed[38,42,49]. One additional type of M2 activated type, the so-called tumor-associated microglia/ macrophage, will be described in detail below.

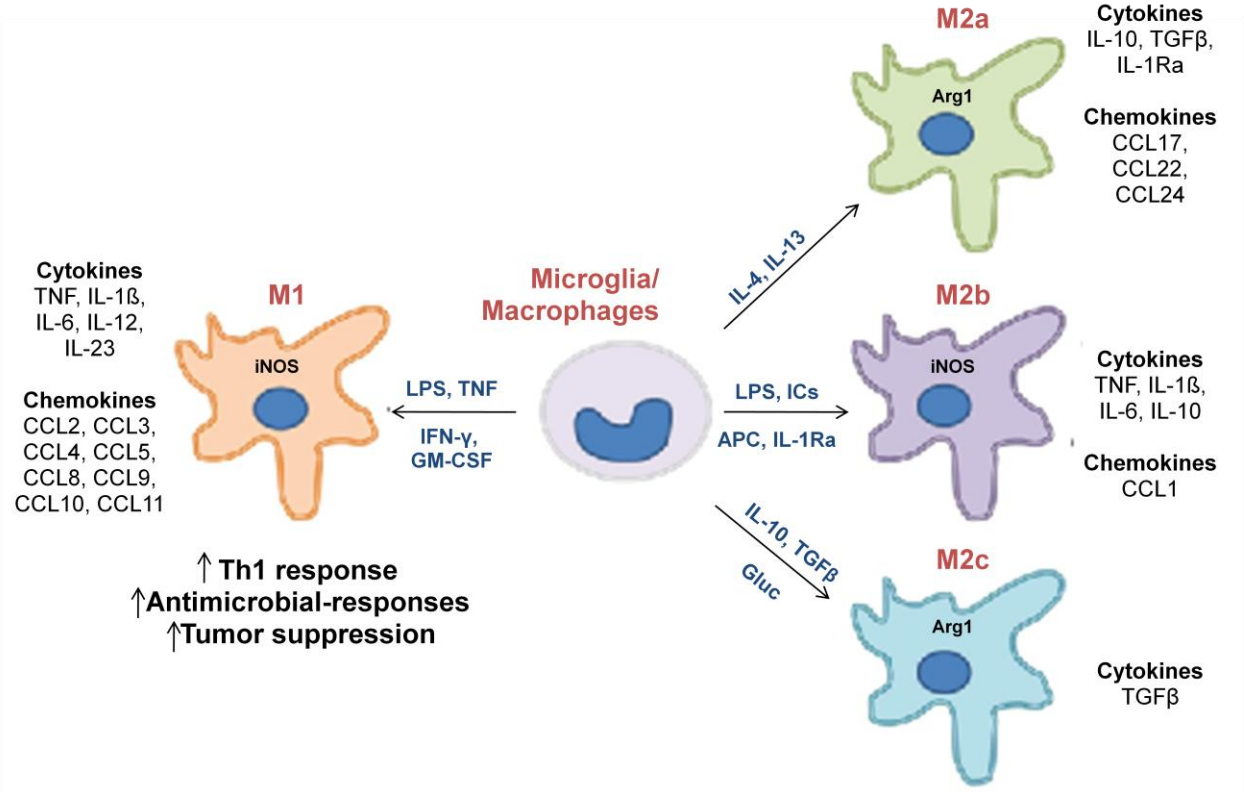

Figure 3: Distinct activation states of microglia/ macrophages.

Microglia/ macrophages can be transformed into proinflammatory (M1), or into immunosuppressive (M2) phenotype. Stimuli are received from the microenvironment, either by surrounding lymphocytes and other immune cells, or by microbial products when the tissue encounters a damage or infection. In turn, microglia/ macrophages respond by transcriptional activation of specific set of genes and secretion of cytokines and chemokines. IC, immune complexes; APC, apoptotic cells; Gluc, glucocorticoids. (Image is adopted and modified from Duque et al., 2014)[48].

1.3.2 Microglia/ macrophages in malignant gliomas

Within a glioma, brain-resident microglia and peripheral macrophages constitute the largest population of tumor-infiltrating cells, contributing at least up to 30% of the cells in the tumor tissue[16,50–52]. These glioma-associated microglia/ macrophages (GAMs) accumulate both around intact glioma tissue and necrotic areas, and their abundance establishes a microenvironment that influences glioma proliferation and invasiveness[50,53]. One study stated that depletion of microglia using clodronate-loaded liposomes resulted in glioma growth and invasion, in an *ex-vivo* organotypic brain slice culture model[54]. Consequently, these results were further validated *in-vivo* using a transgenic mice model that expresses the herpes simplex virus thymidine kinase gene specifically expressed on $Cd11b^+$ microglial cells (CD11b-HSVTK mice), that when treated with ganciclovir results in microglia depletion[55]. Tumor-bearing mice depleted of microglia and reconstituted with wildtype bone marrow (that resulted in reduction in microglial population by 30%) collectively diminished glioma growth, suggesting that microglia possess pro-tumorigenic functions and actively support tumor growth[55].

GAMs also play an important role in promoting glioma cell invasion by the degradation of the extracellular matrix (ECM), support tumor angiogenesis, and mediate an immunosuppressive milieu[51,53,55]. Microglia exploit the membrane type 1 matrix metalloproteases (MT1-MMP), a potent membrane-inserted proteinase that is involved in focal degradation of the ECM (**Figure 4**)[55,56]. MT1-MMP expression is upregulated in microglial cells in presence of glioma cells, while MT1-MMP deficient tumor-bearing mice impaired glioma growth resulting in substantially smaller tumors [55]. GAMs also affect tumor angiogenesis and indirectly influence tumor growth. Signaling through the receptor for advanced glycation end product (RAGE), a membrane protein that binds glycosylated macromolecules is important for the process[57]. RAGE ablation reduces angiogenesis, by downregulating the expression of VEGF, an important pro-angiogenic factor that prevented normal vessel formation. These effects were rescued when reconstituted with wild-type microglia or macrophages in RAGE deficient mice that resulted in normalized tumor angiogenesis[57].

GAMs synthesize and release various factors that promote glioma proliferation and/or migration (**Figure 4**). Microglia secretes stress-inducible protein 1 (STI1, a cell surface ligand for cellular prion (PrP(C)) that promoted the proliferation and migration of glioma through the activation of

MMP-9 in a (PrP(C)) dependent manner[58]. Likewise, microglia also secretes TGF-β that enhances glioma growth, invasion, angiogenesis and immunosuppression[59]. Additionally, glioblastoma and microglial interactions mediated through epidermal growth factor receptor (EGFR) and colony stimulating factor 1 receptor (CSF-1R) enhanced glioblastoma invasion[60]. Interestingly, two independent studies showed that blockade of CSF1R by PLX3397 or BLZ945, both blood penetrable drugs blocked glioma progression, and suppressed the pro-tumorigenic phenotype of microglia[60,61]. CSF-1, the ligand secreted by glioma cells, and responsible for activation of the CSF-1R signaling in microglia, function as an important chemoattractant for GAMs. Similarly, CCL2 is another chemoattractant released by glioma cells, which activates the CCL2 Receptor signaling in microglia, resulting in secretion of IL-6 and thereby promoting glioma invasiveness (**Figure 4**)[60].

GAMs determine its effects on glioma proliferation based on its molecular profile and phenotypic status. As previously described states of microglia being predominantly M1 (classical activation) or M2 (alternative activation), several studies show that microglia/macrophages induce an M2 phenotype when it encounters glioma cell[53–55,62]. GAMs acquires the M2 phenotype by upregulating several pro-tumorigenic or immunosuppressive markers such as increased production of anti-inflammatory molecules (e.g. TGF-β1, ARG1, and IL-10), and molecules supporting tissue remodeling and angiogenesis (e.g. VEGF, MMP2, MMP9, and MMP14)[63]. Peripheral blood mononuclear cells (PBMCs) harvested from either normal or glioma patients acquired an immuno-suppressive phenotype (M2)[64]. These included reduced expression of CD14, increased expression of anti-inflammatory cytokine IL-10 and TGF-β, and increased phagocytic activity[64]. Similarly, glioma cancer stem cells (gCSCs) conditioned media polarized microglia toward an M2 phenotype, as exhibited by reduced phagocytic activity, increased secretion of IL-10 and TGF- β, and decreased ability to stimulate T-cell proliferation[65].

Conversely, GAMs also display M1 characteristics that produce pro-inflammatory molecules, such as TNFα, IL1β, and CXCL10[63,66]. Interestingly, a study showed that IL-6 deficient mice displayed reduced glioma growth, and microglial IL-6 is upregulated by glioma stem cells and not from the bulk tumor[67]. The exact mechanisms of glioma-microglia/macrophage interaction still remain unresolved.

Current glioma therapies, such as surgery, chemo-, and radiotherapy, that directly target the tumor cells, have failed due to several reasons, such as the highly invasive growth, radio- and chemo-resistance of glioma-initiating cells, and the cellular and genetic inter- and intra-tumor heterogeneity[5,68,69]. In this light, GAMs might serve as a potential target for future anti-glioma therapies. A recent study showed that inhibition of microglia activity by minocycline extended the survival of glioma bearing miceby suppressing TLR2 mediating signaling and subsequent MMP9 expression[70]. In conclusion, these studies highlight the possibility of targeting the immune fraction within the tumor and could provide novel therapeutic approaches for glioma therapy.

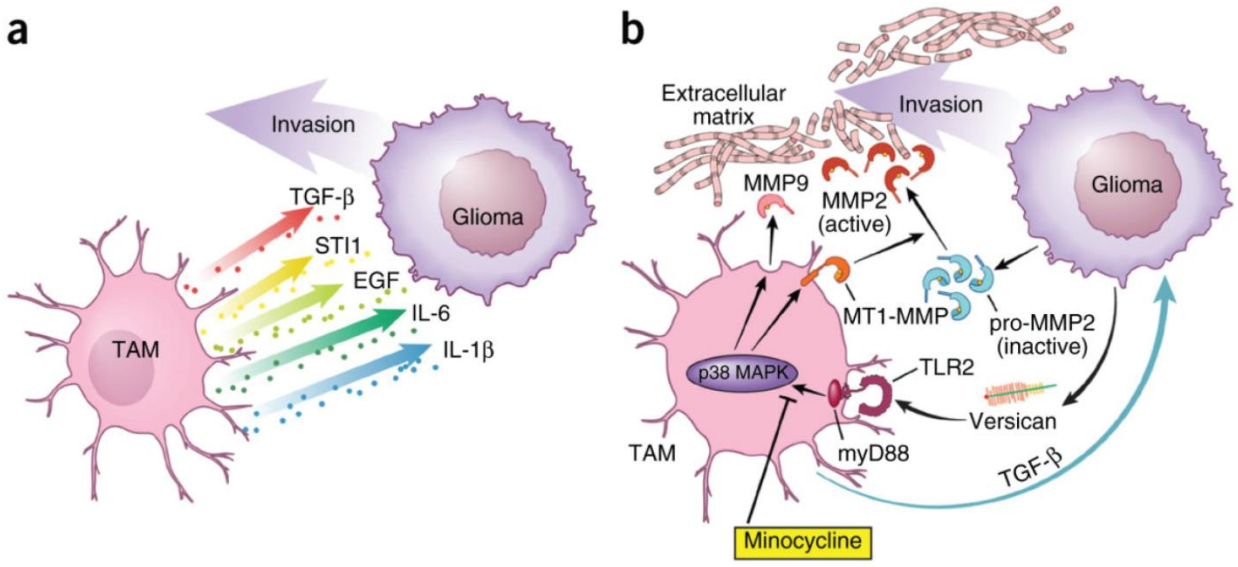

Figure 4: The role of tumor associated microglia/macrophages (TAMs) under the influence of glioma.

(**a**) TAMs synthesize and release various factors that promote glioma proliferation and/or invasion. (**b**) Microglia secretes TGF-β, which promotes the glioma cells to secrete Pro-MMP2, which is then cleaved into active MMP2 by microglia-expressed MT1-MMP. Microglia induces the expression of MT1-MMP by secretion of versican from glioma cells. Versican activates TLR2 and p38- MAPK signaling in microglial cells, which leads to expression of MT1-MMP on microglial cells. TLR2 signaling in microglia also initiates MMP9 secretion. (Image adapted and modified from Hambardzumyan et al., 2016)[71].

1.4 TLR4 activation upon LPS stimulation

Among several pathways that regulate the pro-inflammatory phenotype of microglia/ macrophages, TLR4 signaling plays an important role in response of these immune cells to pathogens. Briefly, upon ligand binding at the cell surface, TLR4 receptors homodimerize and undergo conformational changes. This results in the recruitment of TIR-domain-containing adapter molecules to the cytoplasmic face of TLR4 through homophilic interactions between the TIR-domains[72]. There exists four TIR-domain-containing adapter molecules associated to two divergent signaling cascades known to mediate TLR4 signaling: Myeloid differentiation factor 88 (MyD88); MyD88-adapter-like (Mal) protein, also known as TIR-domain-containing adapter protein (TIRAP); TIR-domain-containing adapter inducing interferon-β (TRIF); TRIF-related adapter molecule (TRAM). TLR4 necessitates all four of these adapters to elicit an immune response[72,73].

TLR4 activation engages two distinct intracellular signaling pathways: (i) the TIRAP–MyD88 dependent pathway, which triggers early NF-κB activation and induction of proinflammatory cytokines, such as IL-12; and (ii) the TRIF–TRAM pathway, which induces the activation of the interferon regulatory factor-3 (IRF3) transcription factor that consequently leads to the subsequent expression of type I interferons (IFNs) and the anti-inflammatory cytokine (IL-10)[72,74]. The majority of the LPS induced activation of TLR4 signaling is mediated via the MyD88-dependent pathway, resulting in a coordinated transcriptional activation of proinflammatory cytokines and chemokines, such as production of TNF, which in cooperation with IFNγ in an autocrine manner triggers the microglial proinflammatory population[75]. Conversely, the MyD88-independent pathway requires the inactivation of p110δ of the phosphatidylinositol-3-OH kinase (PI(3)K) resulting in the induction of dendritic cell (DC) maturation resulting in the expression of IFNs and IL-10[74,76]. The TRIF-dependent pathway also stimulates TNF-α production and secretion, subsequently leading to late phase NF-κB activation through IRF3 and TNF-α secretion[72].

The LPS mediated stimulation of TLR4 signaling results in the activation of several transcriptional factors that can be broadly classified into three subgroups[77]. The first category consists of transcriptional factors that are constitutively expressed and stimulated by signal-dependent post-transcriptional modifications. In basal conditions, these transcription factors exist

in the cytoplasm, and signal-dependent activation results in their translocation to the nucleus. This class (class I) includes proteins that play an important role in inflammation, such as NF-kB, IFN-regulatory factors (IRFs), and cAMP-responsive-element-binding protein 1 (CREB1)[77,78].

The second category of transcription factors (class II) are induced during the initial response to LPS. These transcription factors, such as CCAAT/enhancer-binding protein δ (C/EBPδ) control the gene expression of other important cytokines during the secondary response to LPS that lasts over an extended period of time[77,78]. The third category of transcription factors (class III) involves the expression of lineage-specific transcriptional regulators that are stimulated during microglia differentiation. These include PU.1 and C/EBPβ, runt-related transcription factor 1 (RUNX1) and IRF8 that arbitrate cell type-specific responses to inflammatory signals by inducing a chromatin state on microglia-specific inducible genes[77,78].

LPS dependent transcriptional activation of genes also depends on coregulators, including coactivators and corepressors, which are transcriptional regulators that are specifically to their target genes. Several of these coregulators possess histone-modifying features that result in chromatin remodeling at site-specific target gene promoters, that include phosphorylation of histone 3 at serine 10, which facilitate in recruitment of NF-kB to specific inflammatory genes, deubiquitination of histone 2A at lysine 119, which inhibit a specific subset of LPS- inducible genes[79], and demethylation of trimethylated histone 3 at lysine 27, a requirement for the stimulation of specific inflammatory genes[80].

1.5 Sphingosine 1-phopshate signaling

Sphingolipids are ubiquitous components of the lipid bilayer of eukaryotic cells whose metabolism is regulated by numerous signaling molecules, including ceramide (N-acyl sphingosine), sphingosine, and sphingosine 1-phosphate (S1P)[81]. Sphingosine 1-phosphate (S1P), a pleiotropic bioactive lipid is derived from Sphingosine, an eighteen carbon amino-alcohol with an unsaturated hydrocarbon chain that forms the backbone of most sphingolipids[82,83]. Sphingosine was named in 1884 by J.L.Thudichum after the Greek mythological creature, the Sphinx owing to their enigmatic nature[84]. Initially, S1P was thought to be produced by cells solely as an intermediate aiding in the exit of sphingosine from cells, by the phosphorylation and subsequent degradation of sphingosine to S1P, but since its discovery several studies have indicated that S1P plays an important role in regulating cell growth[85],

intracellular calcium motility[86], suppressing programmed cell death[87], and controlling a plethora of significant physiological and pathophysiological processes[82]. S1P and its homologous phosphorylated long-chain sphingoid bases (LCBP) have also been detected in plants (*Arabidopsis*)[88], worms (*C. elegans),* flies *(Drosophila melanogaser*)[89], slime mould (*Dictyostelium discoideum*[90]*)* and yeast (*Saccharomyces cerevisiae)*[91], where LCBPsthat are thought to be a rate-limiting step in regulating the cellular content and production of bioactive sphingolipid metabolites, which further indicated the significance of S1P as a signaling molecule in both lower and higher organisms[89].

S1P levels in cells are tightly regulated in a spatial-temporal manner by the balance of its synthesis and degradation. Sphingosine kinase (SPHK) that catalyzes the phosphorylation of sphingosine in the presence of ATP, regulates the synthesis and balance of S1P within the cell[82]. While, the degradation of S1P is mediated by two different enzymes: S1P phosphatases that catalyze the reversible de-phosphorylation of S1P back to sphingosine, and pyridoxal phosphate-dependent S1P lyase that irreversibly degrades S1P to hexadecenal and phospho-ethanolamine. Identification of specific cell-surface S1P receptors have further illustrated the complex nature of this simple molecule that exhibit both paracrine and autocrine functions[82].

1.5.1 Sphingosine Kinases

SphKs are an evolutionarily conserved, distinct class of diacylglycerol kinases that contain five conserved domains and are expressed in humans, mice, yeast and plants, with homologues in worms and flies. Two eukaryotic isozymes have been identified, which are known as SphK1 and SphK2[82]. These enzymes predominantly exhibit its activity localized to cytosolic fractions, although small amounts are associated with membranes and the nucleus. Although both the isoforms catalyze the same biochemical reactions, they originate from different genes and display different substrate specificities, tissue distributions, and subceullar localization, which indicate that they carry out distinct cellular functions and might be regulated differently[92]. Sphk1 and Sphk2 share 80% similarity and 45% overall sequence identity. It is unclear whether these enzymes are located within organelles or if they are loosely bound to cellular membranes, although Lcb4, the main enzyme that catalyzes the formation of long-chain base phosphates has been shown to be localized in the Golgi, late endosomes and endoplasmic reticulum (ER) was identified in yeast[93,94]. Despite belonging to the family of diacylglycerol kinases, SphKs contain

a unique catalytic domain, consisting of a consensus ATP-binding site (SGDGXK(R)) that show close resemblance to the highly conserved glycine-rich loop involved in binding the nucleotide in the catalytic site of many protein kinases[82].

Sphk1 activity can be regulated by various signals, including growth factors, cytokines, hormones, ligation of the IgE and IgG receptors, and many GPCR ligands that results in the extracellular signal regulated kinase (ERK)-mediated phosphorylation of Sphk1 at position serine 225. Phosphorylation and activation of Sphk1, which is also regulated by its interactions with several other proteins, promotes its translocation from the cytosol to the plasma membrane, where its coverts sphingosine, present in the lipid bilayer to S1P[95]. For example, a study showed that the calcium and integrin-binding protein 1 (CIB1) mediates the translocation of SphK1 to the plasma membrane in response to calcium fluxes through a calcium-myristoyl switch[96]. Several other proteins have been implicated to interact with SphK1, resulting in its increased activity and thereby mediating S1P generation and Sphk1 associated anti-apoptosis[95].

Contrary to the localization of Sphk1 in the cytosol, SphK2 subcellular localization varies according to cell type and cell density[97]. Sphk2 possess nuclear localization (NLS), and export signals (NES) that regulates DNA synthesis, epigenetic modifications via interaction with and modulation of HDAC1/2[98,99]. Sphk2 under stress conditions localizes to the endoplasmic reticulum (ER) that propels the sphingosine salvage pathway driven by ER-localized S1P phosphatases and ceramide synthase, ultimately leading to ceramide-induced apoptosis[100]. Although lacking an identifiable mitochondrial targeting signal, SphK2 when localized in the mitochondria has been shown to promote apoptosis via S1P and BAK-dependent membrane permeabilization and cytochrome c release[101].

1.5.2 Sphingosine 1-Phosphate Receptors

S1P signals primarily through five cognate highly specific orphan G protein coupled receptors (GPCR), S1PR1, S1PR2, S1PR3, S1PR4, and S1PR5, previously referred to as endothelial differentiation gene (EDG)-1, -5, -3, -6, and -8[82]. These receptors are ubiquitously expressed and couple to various G proteins that regulates important downstream cellular processes such as proliferation, migration, cytoskeletal organization, adherens junction assembly, and morphogenesis. This bestows S1P with the ability to enhance their repertoire in regulating diverse physiological processes, including angiogenesis and vascular maturation, heart

development and immunity in a highly specific manner, depending on the relative expression of S1P receptors and G proteins[82]. The receptor subtypes S1PR1, S1PR2 and S1PR3 are widely expressed and constitute the dominant receptors expressed in the cardiovascular system. S1PR1 is also expressed on lymphocytes where they regulate their egress from secondary lymphatic organs. S1PR4 are expressed at low levels in the lymphoid system, and S1PR5 is expressed in the white matter tracts of the CNS[102].

S1P receptors differentially activate the small GTPases of the Rho family, particularly Rho and Rac, which are downstream of the heterotrimeric G proteins and are important for cytoskeletal rearrangements and directed cell movement[82]. S1PR1 primarily couples through Gi/o that has been associated with activation of Ras and the ERK signaling that promotes proliferation; activation of PI3K and protein kinase B (PKB/Akt) to prevent apoptosis and promote survival; induction of PI3K and Rac to promote migration, enhance endothelial barrier function and induce vasodilation; activation of protein kinase C (PKC) and phospholipase C (PLC) to increase intracellular free calcium required for many cellular processes. Furthermore, signaling through Gi/o suppresses adenylyl cyclase activity to reduce cyclic adenosine monophosphate (cAMP). S1PR2 primarily couples to Gq that further activates the small GTPase Rho and Rho-associated kinase (ROCK) to inhibit migration, reduce endothelial barrier function and induce vasorestriction[102].

Several well characterized agonists and antagonists of S1PRs have been described in literature. Among these, S1PR agonist FTY720 (fingolimod/ Gilenya; Novartis), an immunomodulatory drug was approved by the U.S. Food and Drug Administration as a first line oral therapy for relapsing remitting multiple sclerosis (MS)[103]. Although FTY720 acts as an agonist at picomolar to nanomolar concentrations on S1PR1 and S1PR3-5, it also acts as a functional antagonist for S1P1 by inducing receptor endocytosis and degradation of this receptor. This indiscrimination may be responsible for the adverse effects, such as acute bradycardia (decreased heart rate) and hypertension, seen in fingolimod-treated patients[103]. Fingolimod also blocks lymphocyte egress from secondary lymphoid organs to the peripheral blood circulation by antagonizing S1PR. In conclusion, S1P and its five GPCRs play a crucial role in the development and function of the immune, cardiovascular and nervous systems[104].

1.5.3 Role of S1P in cancer

S1P has been implicated in various stages of cancer pathogenesis, including anti-apoptotic phenotype, metastasis, escape from senescence and resistance to chemotherapy and radiation therapy. In contrast to S1P, which is associated with cell growth and survival, its precursors sphingosine and ceramide, are associated with cell growth arrest and apoptosis[105]. There exists a ceramide – sphingosine 1-phosphate rheostat that maintains this balance in response to cellular and environmental stimuli. Sphk1 is a critical regulator of this rheostat, as it produces pro-growth and anti-apoptotic S1P, and also reduces levels of pro-apoptotic ceramide and sphingosine, thereby aiding cancer progression and survival (**Figure 5)**. Further, sphingolipid metabolism is often dysregulated in cancer, and Sphk1 is significantly overexpressed in multiple types of cancer including stomach, lung, kidney, colon breast and glioblastoma[105].

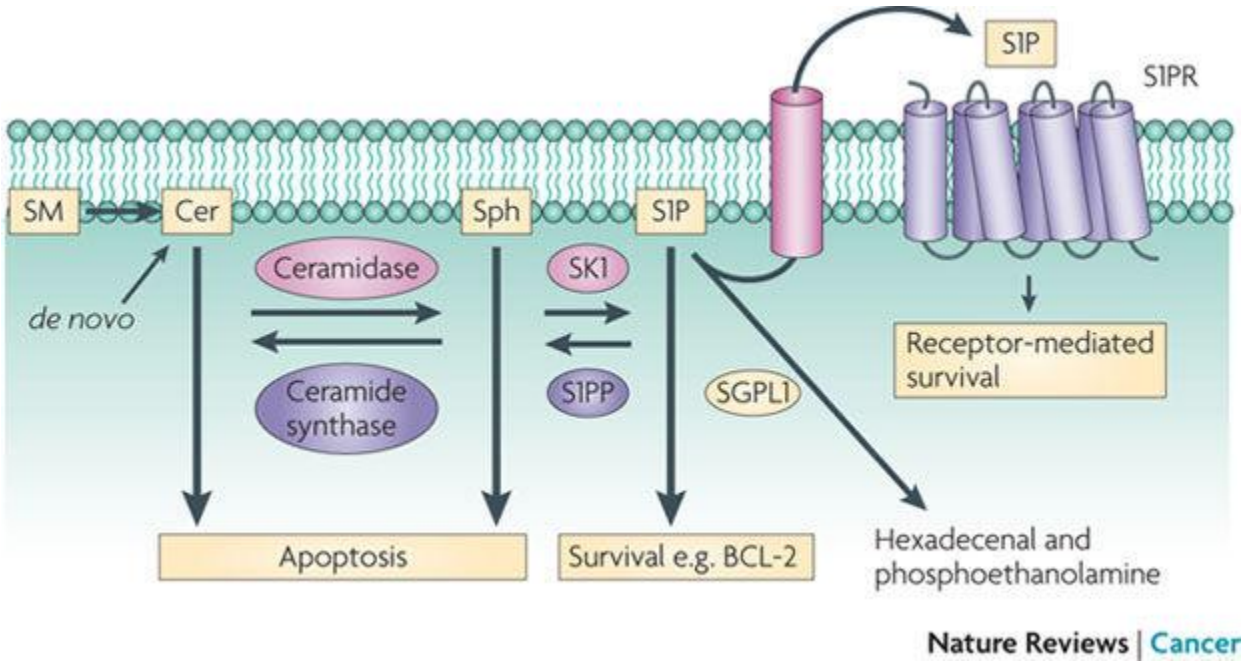

Figure 5: The relationship of ceramide – sphingosine 1-phosphate rheostat in cancer.

The balance of pro-apoptotic ceramide and pro-survival S1P is regulated by the activity of Sphk1, an 'inside-out' signaling by S1P and an S1PR-dependent mechanism. S1PP, S1P Phosphatases; S1PR, S1P receptor; SM, sphingomyelin; SGPL1, S1P lyase. (Image adopted and modified from Pyne and Pyne, 2012).

SphK1 overexpression resulted in acquisition of transformed phenotype in NIH 3T3 fibroblasts, and ability to form tumors in nude mice, suggesting a potential oncogenic effect of Sphk1[106]. Overexpression of SphK1 in MCF-7 breast cancer cells resulted in increased proliferation, decreased apoptosis, and ability to form larger tumors with higher microvessel density in nude mice in an estrogen-dependent manner. Moreover, a dominant-negative mutant of SphK1 inhibited estrogen-mediated mitogenic signaling and decreased neoplastic growth in MCF-7 cells and decreased tumor formation in nude mice[107]. SphK has also been shown to stimulate VEGF-mediated Ras activation in bladder cancer cells by favoring inactivation of Ras-GAP[108].

Sphk1 knockdown in human glioblastoma cells prevented cells from exiting G1 phase of cell cycle and increased apoptosis[109]. High Sphk1 levels and high S1P levels have also been correlated with increasing glioma grade, where S1P has been reported to be a common mitogen for glioma cells[109,110]. S1PR1 and S1PR3 enhance glioma cell migration and invasion via activation of Rac, while S1PR2 inhibited migration through Rho activation[111]. Strikingly, neutralization of extracellular S1P with a specific monoclonal antibody (known as sphingomab) suppressed lung metastasis[112], tumor growth suppression in renal cell carcinoma[113] and induced vascular remodeling in prostate cancer[114], which suggests a new therapeutic strategy to prevent cancer metastasis. Sonepcizumab, the humanized version of sphingomab, has recently completed Phase I clinical trials in cancer and advanced into Phase II safety and efficacy trials. Thus, targeting the S1P axis in the tumor would help reduce both growth and metastasis, respectively[115].

2. Materials and Methods

2.1 Materials

General Chemicals

Chemicals	Company
2-prapanol	Carl Roth GmbH, Germany
Acrylamide Mix (Rotiphorese Gel 30)	Carl Roth GmbH, Germany
Agarose	Carl Roth GmbH, Germany
Ammouniumpersulphate (APS)	Carl Roth GmbH, Germany
Beta-Mercaptoethanol	VWR International, USA
Bovine Serum Albumin	Applichem GmbH, Germany
Chloroform	Sigma-Aldrich, USA
Deoxyribo nucleotide triphosphate (dNTPs)	New England Biolabs, USA
Dimethylsulfoxide (DMSO)	Carl Roth GmbH, Germany
DEPC free water	Carl Roth GmbH, Germany
Ethanol	Sigma-Aldrich, USA
Ethidium bromide (EtBr)	Sigma-Aldrich, USA
Ethylene diamine tetra acetic acid (EDTA)	Sigma-Aldrich, USA
Hydrochloric acid (HCl)	Sigma-Aldrich, USA
Glacial Acetic Acid	Merck Millipore, USA
Laemmli Sample Buffer (6X)	New England Biolabs, USA
Luria Broth – medium	Carl Roth GmbH, Germany
Luria Broth – agar	Carl Roth GmbH, Germany
Methanol	Sigma-Aldrich, USA
Milk	Applichem GmbH, Germany
N,N,N',N'-Tetramethyl ethylene diamine (TEMED)	Sigma-Aldrich, USA
Oligonucleotide (Primer)	New England Biolabs, USA
Paraformaldehyde (PFA)	Carl Roth GmbH, Germany

Phosphate buffered saline tablets (PBS)	Applichem GmbH, Germany
Sodium Chloride (NaCl)	Carl Roth GmbH, Germany
Sodium deoxycholate	Carl Roth GmbH, Germany
Sodium dodecyl sulfate (SDS)	Carl Roth GmbH, Germany
Tris-HCl	Carl Roth GmbH, Germany
Triton X-100	G-Biosciences, USA
Tween 20	Sigma-Aldrich, USA

Equipment

Equipment	Company
Autoradiography chamber	GE Healthcare Life sciences, USA
Bacterial incubator	Memmert GmbH, Germany
Bacterial shaker	Edmund Bueler GmbH, Germany
Cell counter	Celeromics, France
Cell culture microscope	Carl Zeiss, Germany
Centrifuge 5430R	Eppendorf, Germany
FACS machine	BD Biosciences, Germany
Fluorescent microscope EVOS FL	Thermo Fischer Scientific, USA
Heat block	IKA Works, USA
iMark Spectrophotometer plate reader	BioRad Laboratories, USA
Incubator	Nuaire, UK
Laminar air flow	Thermo Fischer Scientific, USA
Luminescence reader	BMG Labtech, Germany
PCR machine	BioRad Laboratories, USA
Pipette boy	Integra Biosciences, Switzerland
Pipette Set research	Eppendorf, Germany
Power supply	BioRad Laboratories, USA
Real time PCR machine	BioRad Laboratories, USA

SDS-PAGE Electrophoresis Mini-PROTEAN	BioRad Laboratories, USA
Thermo mixer compact	Eppendorf, Germany
Transfer blotting machine	BioRad Laboratories, USA
Ultracentrifuge	Beckaman Coulter, USA
Western blot scanner	LI-COR Biotechnology GmbH, Germany

Media, solutions and accessories for Cell Culture

25X Tryspin

Accumax Cell aggregate dissociation medium

DMEM

DNase

Fetal Bovine Serum (FBS)

HEPES (with Phenol red)

HEPES (without Calcium and Magnesium)

IMDM

L-Glutamine

Penicillin/Streptomycin (Pen/Strep)

Phosphate-Buffered Saline (PBS)

Trypsin/EDTA (0.1x and 2.5x)

Consumables

0.45uM filters

1,5 ml Microcentrifuge tube

100 µl PCR Reaction tubes

2 ml Microcentrifuge tubes

384-Well PCR Plates

96-Well Plates

Cell Culture dishes and plates

Cell scraper

Cryotubes

Falcon tubes 15 ml und 50ml

Pipette tips

Pipette tips (filtered)

PVDF Transfer membrane

Sterile Injection needles

Syringe, 5ml

Whatman 3MM Paper

Kits and other materials

DC Protein assay kit, BioRad Laboratories, USA

First strand cDNA isolation kit, Thermo-Scientific, USA

Gel extraction / PCR purification kit, Macherey-Nagel, Germany

Greiss reagent assay, Sigma-Aldrich, USA

Lumi-Light Western Blotting Substrate, Roche Holding AG, Switzerland

Micro RNA isolation kit, Qiagen, Germany

NuceloBondXtra Plasmid Maxi isolation kit, Macherey-Nagel, Germany

NuceloSpin RNA isolation kit, Macherey-Nagel, Germany

NucleoSpin Plasmid Mini isolation kit, Macherey-Nagel, Germany

Super Signal West Femto Chemiluminescent Substrate kit, Thermo Scientific, Rockford, USA

Super Signal West Pico Chemiluminescent Substrate kit, Thermo Scientific, Rockford, USA

SyBr Green Master mix, BioRad Laboratories, USA

Drugs and Chemicals

Fatty acid free BSA, Sigma-Aldrich, USA

FTY720, Cayman Chemical Company, USA

FTY720-P, Cayman Chemical Company, USA

IC87114, Sigma-Aldrich, USA

JTE103, Cayman Chemical Company, USA

Lipopolysaccharide from *Escherichia coli* 0111:B4, Sigma-Aldrich, USA

Poly-L-lysine hydrobromide, Sigma-Aldrich, USA

SEW2871, Cayman Chemical Company, USA

SKI-II, Sigma-Aldrich, USA

Sphingosine 1-Phsophate, Cayman Chemical Company, USA

U73122 hydrate, Sigma-Aldrich, USA

W146, Sigma-Aldrich, USA

FACS antibodies

CD11b eBiosciences, Germany

CD45, eBiosciences, Germany

FxCycle Violet stain, eBiosciences, Germany

Primary Antibodies

Akt, Cell Signaling Technology

Alpha-Tubulin, Sigma-Aldrich, USA

EF2 (C-14) , Santa Cruz Biotechnology

IRF3, Cell Signaling Technology

IκBα, Cell Signaling Technology

NFκB-p65, Cell Signaling Technology

Phospho-Akt (Ser473), Cell Signaling Technology

Phospho-IRF3 (Ser396), Cell Signaling Technology

Phospho-NFκB-p65, Cell Signaling Technology

Phospho-STAT3 (Tyr705), Cell Signaling Technology

Phospho-TBK/NAK1 (Ser172), Cell Signaling Technology

STAT3 (sc-482), Santa Cruz Biotechnology

TBK1/NAK1, Cell Signaling Technology

Secondary Antibodies

Anti-rabbit, Dako (Agilent Technologies), USA

Anti-mouse, Dako (Agilent Technologies), USA

Anti-goat, Dako (Agilent Technologies), USA

Primers

Gene name	Primer name	Primer Sequence (5`-3`)
Human qPCR primers		
SPHK1	Sphk1_Human_F	GAG CAC CGG TGT CAT TCC
	Sphk1_Human_R	CAG ACG TGG GCT GAG CTT
GAPDH	GAPDH_Human_F	AGA AGG CTG GGG CTC ATT TG
	GAPDH_Human_R	AGG GGC CAT CCA CAG TCT TC
PPIA	PPIA_Human_F	TTC TGC TGT CTT TGG GAC CT
	PPIA_Human_R	CAC CGT GTT CTT CGA CAT TG
Mouse qPCR primers		
B2m	B2m_M FP	TTC AGT ATG TTC GGC TTC CC
	B2m_M RP	TGG TGC TTG TCT CAC TGA CC
Gapdh	GAPDH_M FP	TTG ATG GCA ACA ATC TCC AC
	GAPDH_M RP	CGT CCC GTA GAC AAA ATG GT
ActB	ActB_M FP	ATG GAG GGG AAT ACA GCC C
	ActB_M RP	TTC TTT GCA GCT CCT TCG TT
Hprt	HPRT1_M FP	CAT AAC CTG GTT CAT CAT CGC
	HPRT1_M RP	TCC TCC TCA GAC CGC TTT T
Arg1	Arg1_M for	GTG AAG AAC CCA CGG TCT GT
	Arg1_M rev	GCC AGA GAT GCT TCC AAC TG
Msr1	Msr1_M for	TTT CCC AAT TCA AAA GCT GA
	Msr1_M rev	CCT CCG TTC AGG AGA AGT TG
Il6	IL6_M FP	TGG TAC TCC AGA AGA CCA GAG G
	IL6_M RP	AAC GAT GAT GCA CTT GCA GA
Nos2	NOS2-FP	TTC TGT GCT GTC CCA GTG AG
	NOS2-RP	TGA AGA AAA CCC CTT GTG CT
Il1b	IL1b-FP	GGT CAA AGG TTT GGA AGC AG
	IL1b-RP	TGT GAA ATG CCA CCT TTT GA

Tnfalpha	TNFalpha-FP	AGG GTC TGG GCC ATA GAA CT
	TNFalpha-RP	CCA CCA CGC TCT TCT GTC TAC
Mip1aplha	MIP1alpha-FP	GTG GAA TCT TCC GGC TGT AG
	MIP1alpha-FP	ACC ATG ACA CTC TGC AAC CA
Cloning Primers		
Human *SPHK1* Overexpression	Sphk1shRNAHum-F	CCG GAC CTA GAG AGT GAG AAG TAT CCT CGA GGA TAC TTC TCA CTC TCT AGG TTT TTT TG
	Sphk1shRNAHum-R	CTA GCA AAA AAA CCT AGA GAG TGA GAA GTA TCC TCG AGG ATA CTT CTC ACT CTC TAG GT
Human *SPHK1* Knockdown	hSPHK1-A-shRNA-F	CCG GCC TGA CCA ACT GCA CGC TAT TCT CGA GAA TAG CGT GCA GTT GGT CAG GTT TTT G
	hSPHK1-A-shRNA-R	AAT TCA AAA ACC TGA CCA ACT GCA CGC TAT TCT CGA GAA TAG CGT GCA GTT GGT CAG G

Buffers

10x SDS Running buffer:

250mM Tris-HCl

1.92 M Glycine

1 % SDS

up to 1000 ml distilled water

10x Transfer buffer:

250mM Tris-HCl

1.92 M Glycine

up to 1000 ml distilled water

Separating gel buffer

45.4 g Tris Base

13.39 ml 10 % SDS

pH 8.8

up to 500 ml distilled water

Stacking gel buffer

18,9 g Tris Base

13,39 ml 10% SDS

pH 6.8

up to 500 ml distilled water

Stacking gel

5% Acrylamide

130mM Tris (pH 6,8)

0,1% SDS

0,1% APS

0,01% TEMED

in H_2O

Separating gel

8% Acrylamide

375 mMTris (pH 8,8)

0,1% SDS

0,1% APS

0,06% TEMED

in H_2O

10X Tris buffered saline (TBS) buffer

87 g NaCl

60.57 Tris-Cl, pH 7.4 - 7.6

up to 1000 ml distilled water

1X TBS-Tween

100 ml 1X TBS

1 ml Tween-20

up to 1000ml distilled water

RIPA buffer:

50 mM Tris-HCl, pH 8.0

150 mM NaCl

0.1% SDS

0.5% Sodium deoxycholate

1 tablet Protease inhibitor

1% Triton X-100

TAE (50X)

242 g Tris

18.6 g EDTA

57.1 ml Glacial acetic acid

up to 1000 ml distilled water

Genomic DNA isolation: Tail DNA buffer:

NaCl (5 M)

Tris-HCl (1 M), pH 8.0

EDTA (0.5 M), pH 8.0

SDS (10%)

In H_2O

2.2 Methods

2.2.1 Animal cell culture

2.2.1.1 Cell lines and reagents

Glioma cell lines LN229 and LN308 were cultivated in DMEM medium supplemented with 10% FCS, 1% penicillin-streptavidin at 37˚C in a 5% CO_2 humidified incubator. HEK293 cells were cultivated in IMDM medium supplemented with 10% FCS, 1% penicillin-streptavidin at 37˚C in a 5% CO_2 humidified incubator. The cells were grown generally in T-75. All cell culturing experiments were performed under a laminar flow hood. When the cells reached a confluency of 70-90%, the cells were sub cultured in a ratio of 1:3 to 1:5, depending on the requirement of the experiments. The medium was removed and changed 2 to 3 times per week. In brief, the media was aspirated by means of a suction pump. The flask were washed with PBS, to remove dead cells, debris and remaining traces of media. PBS was aspirated out and 1 ml of Typsin-EDTA solution was added. The cells were returned back to the CO_2 incubator for 5 minutes until the cells were detached. Fresh culture media was added, aspirated and dispensed into new culture flasks, depending on the subculturing ratio. RAW264.7 macrophages were cultivated in DMEM

medium supplemented with 10% FCS, 1% penicillin-streptavidin at 37˚C in a 5% CO_2humidified incubator. Subculturing of RAW264.7 was performed using a cell scraper, and split 1:5 to 1:10, depending on the requirement of the experiments.

Separate bottles of media for each cell line were maintained, to avoid risk of contamination and mixing up of cell lines. The culture medium and Trypsin-EDTA was stored at 4˚C and before working with the cells, the solutions were thawed in an water bath at 37˚C.

2.2.1.2 Freezing of cells

Before freezing, it was ensured that the cells were frozen at a low passage number, and at least 90% of the cells were viable. Approximately 1.5 - 2 X 10^6 cells were harvested from the culture flask, centrifuged and resuspended in 950 µL of fresh culture media and 50 µL of DMSO was added. The cells were transferred to a cryovial, and freezed initially at -80˚C for 24 hours and then transferred to the liquid nitrogen tank at -196˚C, where the cells were stored in the gas phase above the liquid nitrogen.

2.2.1.3 Thawing of cells

The frozen cryovial was removed from the liquid nitrogen tank and placed immediately in the water bath at 37˚C. The cells were thawed quickly (<1 minute) by gently swirling the cryovial in the water bath, and immediately transferring it into the laminar flow hood. Before opening the vial, the vial was cleaned from the outside with 70% ethanol. 1 ml of fresh culture medium was added dropwise into the vial containing the thawed cells, and contents transferred to a tube containing 8ml of media. The cell suspension was centrifuged at 1500 x g for 5 minutes, the supernatant was carefully removed without disturbing the cell pellet. The cells were resuspended in complete growth medium, and transferred into the appropriate culture vessel and incubated at 37˚C in the CO_2 incubator.

2.2.1.4 Cell counting

The cells were harvested from the culture flasks, and centrifuged at 1500 x g for 5 minutes. The supernatant was carefully removed without disturbing the cell pellet, and the cells were resuspended in 5 ml of complete growth medium. For counting of the cells, the Neubauer chamber was used. The chamber and a coverslip were cleaned with alcohol, dried and the coverslip was fixed in position on the chamber. 10 µl of resuspended cells were mixed with 10 µl

of Trypan Blue solution (dilution of 1:10), and 10 µl of the mixture was placed in the hematocytometerNeubauer chamber, without overfilling. The cells were placed in the inverted microscope under a 10X objective. The cells were counted on the four corners of the gridded square, and the average was calculated, and fitted into the following equation 1 to estimate the number of cells per ml.

$$\#\ \text{of cells/ml} = 10{,}000\ \times \mathrm{N}/4 \times \mathrm{d}$$

where,

N = # of cells counted on all 4 squares of a hematocytometer.

d = dilution factor

2.2.1.5 Microglia isolation

Murine microglia were isolated by mild trypsinization protocol as previously described (Saura et al, 2003[116]). Briefly, brains were removed from postnatal P0-P2 C57bl/6 pups, and rinsed in Hanks Balanced Salt solution (HBSS). After removal of the meninges, the brains were mechanically dissociated and digested in 0.25% Trypsin for 20 minutes. The cells were seeded in DMEM with 10% FCS (One T-75 flask per 2 brains), and cultured at 37°C in a humidified 5% CO_2/95% air. Medium was replaced every 4-5 days. Once they attained confluency after 6-8 days, the mixed glial cultures were split 1:3 and expanded for an additional week in 10cm cell culture dishes, until they attained confluency. Microglia were isolated from the mixed glial cultures by removal of astrocytes by incubation with 0.25% Trypsin-EDTA diluted 1:3 in serum-free DMEM for 45 minutes at 37°C. After removal of the floating astrocyte layer, the adherent microglia were replaced with mixed glial culture-conditioned media for 24 hours. The following day, 0.25% Trypsin-EDTA was added to adherent microglia for 10 minutes, and detached from the dishes using a Cell Lifter (Corning Inc), and replated in iBidi culture-insert 3-well at a density of 60,000 cells per well.

2.2.1.6 Co-culture model to study microglia-glioma interactions

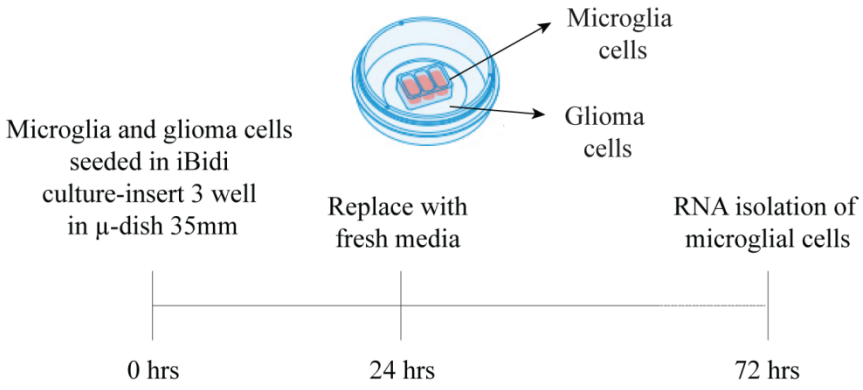

To investigate the effects of the interactions between glioma and microglia, I established an in-vitro co-culture model using the Culture-insert 3-well in µ-dish 35mm, high (iBidi GmbH, Germany). These chambers consisted of a 35mm dish, in which a 3-well biocompatible silicone insert was placed inside, allowing two cell types to be seeded separately and grown on the designated areas. The treatment schedule started by seeding the glioma cells in the 35mm dish in the area surrounding the 3-well inserts, and the primary microglia cells seeded in the 3-well inserts. After allowing the cells to attach for 24 hours, the cells were exchanged with fresh media that now covered the entire co-culture dish, allowing for exchange of soluble factors and interaction between the two cell types. The co-culture experiment was performed for 48 hours, after which RNA was isolated from primary microglial cells, and analyzed for expression of M1 and M2 markers by real-time qPCR.

2.2.1.7 Lentivirus production and infection of cells

From a healthy 90% confluent T75 flask of HEK293 cells, cells was split 1:6 in 10cm cell culture dishes and allowed to settle for 48 hours. When cells reached a 70% confluency, they are ready for transfection. A solution containing 4µg of 2nd generation packaging plasmid psPAX2, 4µg of envelope plasmid pMDG.2 and 8µg of lentiviral plasmid of interest was prepared in 250µl of OptiMEM, and briefly vortexed. Likewise, 48µl of polyethylenimine (PEI) was prepared from a 1mg/ml PEI stock in 250µl of OptiMEM, and briefly vortexed. These two solutions were mixed, vortexed thoroughly and incubated at room temperature for 20 minutes. Meanwhile, HEK293 cells were exchanged with fresh IMDM complete media. After the incubation, the solution was added dropwise to the plate, while gently swirling it. The cells were returned to the

incubator at 37˚C for 48 hours. Condition media containing the lentiviral particles was harvested after 48 hours. Glioma cells were incubated with the lentiviral supernatant for 48 hours, replaced with fresh complete media for 24hours and selected with fresh complete media containing 1 µg/µl puromycin for 48hours. The cells were replaced with fresh complete medium containing puromycin every two days. One week post selection, the overexpression or knockdown levels were analyzed by qRT-PCR or by Western blot.

2.2.2 Western blot analysis

2.2.2.1 Preparation of lysate from cell culture

The cell culture dish was placed on ice and the culture medium was aspirated out using the suction pump. The cells were washed with PBS, and quickly scraped of the plate using a cell scraper, and transferred in a micro-centrifuge tube at 800g for 5 min at 4˚C. The supernatant was carefully removed without disturbing the cell pellet, and 50 µl of ice-cold RIPA lysis buffer (50mM, TRIS-HCl pH 8, 150 mM NaCl, 0.5% sodium deoxycholate, 0.1% SDS + 1 tablet of protease inhibitor cocktail (Roche, Mannheim, Germany) was added. The cell suspension was incubated on ice for 20 minutes. The cell suspension was centrifuged at 16000 g for 20 min in a 4˚C pre-cooled centrifuge. The supernatant was carefully transferred to a fresh pre-cooled microcentrifuge tube and placed on ice, and the pellet was discarded. The lysates were either proceeded with western blot analysis or stored at -80˚C for later use.

2.2.2.2 Protein concentration determination

The protein concentration was determined using the BioRad DC Protein Assay Kit. The Albumin standards were prepared as mentioned in the kit. The unknown protein samples were diluted 1:10 in RIPA lysis buffer. 5 µl of albumin standards or unknown sample were pipetted in a 96 well microplate. 25 µl of the Reagent A' (prepared by mixing 20 µl of the Reagent S with 1 ml of Reagent A) was added to each well and the microplate was mixed thoroughly on a plate shaker for 30 s. Following, 200 µl of reagent B was added to each well, and the microplate was covered and placed at RT for 15 min. The absorbance was measured at a wavelength of 750 nm on the spectrophotometer plate reader. The absorbance was plotted against the known concentrations of the albumin standards to obtain a straight-line graph using linear regression, and the unknown protein concentrations were calculated from the graph. The volume containing 30 µg of protein was calculated from the determined protein concentrations.

2.2.2.3 Sample preparation and loading of SDS-PAGE gels

To the required volume of cell lysate containing 30 µg of protein, 5X Laemmli loading buffer was added. It was ensured that the total volume did not exceed 30 µl, otherwise it was difficult to load them on the gel. The cell lysates in loading buffer was boiled at 95˚C for 5 minutes. Equal amount of protein was loaded onto the wells of the SDS-PAGE gel, along with the 5 µl of the PageRuler Prestained Protein Ladder 10-170K (Thermo Scientific). A 10% SDS-PAGE gel was prepared. The gel was run at 90V through the stacking part of the gel, and the voltage was turned up to 120V after the proteins have gone through the stack and are migrating through the resolving gel. The migration was continued until the blue dye front from the loading buffer is at the end of the glass plates but does not migrate off the gel.

2.2.2.4 Transfer onto PVDF membrane

The Trans-Blot turbo transfer system from BioRad was used for the transfer of proteins onto Polyvinylidene difluoride (PVDF) membranes. For each gel, one piece of PVDF membrane and three pieces of Whatman 3MM Chr filter paper was cut to the dimensions of the gel. The PVDF membranes were activated by soaking them briefly in 100% ethanol for 2 minutes, and rinsing them in water and 1X transfer buffer. All the membranes were thoroughly wetted in transfer buffer prior to assembly of the gel and membrane sandwich. The Whatman filter paper was placed on top of the fiber pad. The pre-equilibrated PVDF membrane on top of the filter paper, and the SDS-PAGE gel was gently placed on top of the PVDF membrane. The roller was used to remove any air bubbles and to ensure proper contact between the gel and the membrane. The second filter paper was placed on top of the membrane. The cassette was closed and locked and placed in the tank with the latch side up, ensuring the black cassette faces the black electrode plate. The tank was filled with transfer buffer till the fill line. The transfer was run at 25V for 30 min. After the run, the membranes were briefly washed with water to remove traces of the gel, and were proceeded with blocking.

2.2.2.5 Antibody staining and detection of signals

The membranes were blocked in 5% milk powder 1X TBS containing 0.1% Tween-20 for 30minutes at RT or overnight at 4˚C. The membranes were then incubated at RT for 3 hours or overnight at 4˚C in the appropriate primary antibody in 5% milk powder in TBS/Tween, with constant shaking. The membranes were washed thrice with TBS/Tween for 10 minutes. The

membranes were then incubated with secondary antibody (goat anti-rabbit/mouse conjugated to horseradish peroxidase, DaKo, Hamburg) in 5% milk powder TBS/Tween for 1 hour. For all phospho-antibodies, membranes were blocking in 5% BSA in 1X TBS containing 0.1% Tween-20, and all further antibody dilution were prepared in the same blocking solution. The membranes were washed thrice with TBST for 10 minutes. The SuperSignal West Pico Chemiluminescent kit (Thermo Scientific) and X-ray film cassette or developing machine were used for detection.

2.2.3 Trizol based RNA isolation

This protocol was used for isolation of small quantities of RNA from samples. Briefly, the cell culture dish was removed from the incubator and the culture medium was aspirated out using the suction pump. The cells were washed with PBS, and 800 µl of PeqGoldTriFast reagent was added to the plate, and incubated at RT for 5 minutes to permit complete dissociation of the nucleoprotein complexes. The reagent was flushed across the plate and transferred into an Eppendorf tube. Subsequently, 160 µl of chloroform was added, vortexed thoroughly, incubated at RT for 2-3 minutes, and centrifuged at 13000 x g for 15 minutes at 4°C. The mixture separates into a lower red-phenol – chloroform, an interphase, and a colorless upper aqueous phase. The upper aqueous phase containing RNA was transferred into a new Eppendorf tube without disturbing the intermediate organic layer. Following, 500 µl of isopropanol and 1 µl of RNA free glycogen per 200 µl of aqueous layer was added, voretexed briefly and incubated at -20°C overnight. The following day, the solution was centrifuged at 13000 x g for 2 hours at 4°C. The supernatant was discarded, the pellet washed with 1ml cold 70% ethanol. The pellet was air-dried and dissolved in DEPC free water. RNA quality and concentration was measured by NanoDrop spectrophotometer (Peqlab, Erlangen, Germany).

2.2.4 RNA isolation using kit

Total RNA was isolated from the cell lines using the NuceloSpin RNA (Machery-Nagel, Germany) as mentioned in the kit. In brief, cells harvested were centrifuged and resuspended in 350 µl RA1 buffer + 1% β-mercapthoethanol. The lysate was filtered through the NuceloSpin Filter (violet ring) to reduce viscosity and centrifuged for 1 min at 11,000 x g. Subsequently, the NuceloSpin Filter was discarded and to the flow through an equal volume of 70% ethanol was added, mixed well by pipetting, transferred to an NucleoSpin RNA columns spin column, and

centrifuged at 11,000 x g for 30 seconds. The flow-through was discarded and the column was washed with MDB buffer, and incubated with DNase reaction mixture (diluted in DNase buffer) for 15 minutes. Subsequently, the column was washed with 200 µl of RAW2 buffer, washed twice with RA3 buffer, and eluted in RNase-free water. RNA quality and concentration was measured by NanoDrop spectrophotometer (Peqlab, Erlangen, Germany). RNA quality was assessed by photometric measurement at ratios of 260/280 and 260/230 nm.

2.2.5 First strand cDNA synthesis

First strand cDNA synthesis was performed using First strand cDNA synthesis Kit (Thermo Scientific, USA) according to the instructions in the kit. Briefly, about 1 µg of RNA was mixed with 1 µl of 1:1 mix of oligodT primer and random hexamer primer to a final volume of 11 µl. The mixture was incubated at 65°C for 5 minutes to remove secondary structures and for GC-rich RNA templates. Following, reaction buffer, RiboLock RNase Inhibitor (20 U/µl), 10 mM dNTP mix and M-MULV Reverse Transcriptase (20 U/µl) was added to the previous mixture, and incubated for 5 min at 25°C followed by 60 minutes at 37°C in a PCR machine.

2.2.6 Quantitative Real time Reverse transcriptase Polymerase Chain Reaction (qRT-PCR)

The cDNA was diluted 1:15, and mixed with a master mix containing SybrGreen and respective primers. Quantitative RT-PCR (qRT-PCR) was performed in three technical triplicates. qRT-PCR was performed using LightCycler 480 Instrument II (Roche Holding AG, Switzerland) using the following PCR program.

95˚C for 1 min
95˚C for 30 s
56˚C for 1 min } X 40 cycles
72˚C for 30 s
Melting Curve (Change to resolution 0.5°C)
4 ˚C ∞

Quantitative values were obtained from the Ct values. Ground state expression (ΔCt values) of target gene mRNA was quantified relative to mean of two housekeeping gene [mRNA value = $2^{(\text{mean Ct mean HKG - Ct mRNA target})}$]. In addition ΔΔCt values were calculated for treated cells versus solvent control; and for transfected cells versus control cells.

2.2.7 ELISA

IL-10, TNFα and IL-6 were quantified using BioLegend Mouse ELISA MAX Standard kit (BioLegend, San Diego, USA) according to the manufacturer's protocol. The cellular supernatant of microglia cultures treated with glioma conditioned media was harvested, and briefly centrifuged to remove floating cells. Briefly, a day prior to performing the ELISA, 100 µl of Capture antibody was added to half area 96-well ELISA plates, and incubated overnight at 4°C. The following day, the plate was washed four times with wash buffer by firmly tapping plate upside down on absorbent paper. The plate was further blocked with 200 µl of assay diluent, plate was sealed and incubated on a plate shaker at 500 rpm for 1 hour at RT. Plates were again washed four times with wash buffer, and 100 µl/well of standard dilutions and 100 µl /well of appropriate sample dilutions was added and incubated on a plate shaker at 500 rpm for 2 hours at RT. The plate was washed four times with wash buffer and incubated with 100 µl of Detection antibody and incubated on a plate shaker at 500 rpm for 1 hour at RT. The plate was washed four times with wash buffer and incubated with 100 µl of Avidin-HRP solution and incubated on a plate shaker at 500 rpm for 30 minutes at RT. Finally, the plate was washed four times with wash buffer and incubated with 100 µl of TMB substrate solution and incubated in the dark for 15 – 30 minutes at RT. The reaction was stopped by adding 100 µl of Stop solution and absorbance was read at 450 nm within 15 minutes. The absolute values of cytokines levels were calculated from a standard curve by plotting the standard cytokine concentration and the absorbance.

2.2.8 Flow Cytometry

For functional characterization of microglia, unspecific binding of antibodies was blocked by pre-incubating them for 15 minutes with 2% rat serum. Afterwards, samples were incubated in PBS with 2% FCS and 0.02% sodium azide (FACS buffer) containing FxCycle Violet stain (eBiosciences, Germany) to gate for dead cells for 15 minutes at 4°C, followed by washing twice with FACS buffer. Staining of the cell surface proteins CD11b and CD45 was performed with FACS buffer) for 30 minutes at 4°C, followed by washing twice with FACS buffer. Flow cytometry data was acquired on BD LSRII flow cytometer (BD Biosciences, Heidelberg). All flow cytometry data analysis was performed using FlowJo X 10.0.7 software FlowJo, Ashland, OR, USA).

2.2.9 Plasmid DNA isolation

Plasmid DNA was isolated using the NucleoSpin Plasmid isolation mini (Macherey-Nagel, Germany) according to manufacturer's instructions. Briefly, bacterial cultures grown overnight at 37°C was harvested by centrifuged the cultures at 11,000 x g for 30 seconds, resuspended in 250 µl of Buffer A1, lysed with 250 µl of Buffer A2, and neutralized with 250 µl of Buffer A3. The lysate was clarified by centrifugation at 11,000 x g for 5 minutes., and the upper clear supernatant was added to NuceloSpin Plasmid Columns in a collection tube and centrifuged at 11,000 x g for 1 minute. The column was washed with 600 µl of Buffer A4, the silica membrane dried and DNA was eluted in 50 µl of Buffer AE. RNA quality and concentration was measured by NanoDrop spectrophotometer (Peqlab, Erlangen, Germany). RNA quality was assessed by photometric measurement at ratios of 260/280 and 260/230 nm.

2.2.10 Transformation in E.coli competent cells

For transformation, the E. coli DH5α or XL10 chemical competent cells (prepared by Fabio Dietrich, AG Tews) were gently thawed on ice for 10 min. 5 µl of the ligation product was added to 50 µl of the competent cells. A heat-shock (42 °C) was given for 90 seconds and then the cells were incubated on ice again for 2 minutes. 400 µl of 1X Luria-Bertain (LB) medium was added and the samples were incubated at 37 °C for 1 hour on a shaker (500 x g). The transformed cells were then plated on Luria-Bertain (LB) plates with ampicillin. The plates were then incubated at 37 °C overnight. The transformants were then screened for the presence of the insert by picking ten colonies per plate and growing in amp-LB media for an additional cycle; isolating the plasmid DNA and appropriate restriction analysis performed.

2.2.11 Statistical analysis

Data were analyzed using Prism 8 GraphPad software. Comparisons of two different sample groups were performed using paired t-test to compare the same cell populations before and after treatment, or when comparing two cell populations within the same sample. Values of $p < 0.05$ were considered to be statistically significant. The statistical significance calculated for each data set is indicated in the figure legends. All groups show means ± SEM, unless otherwise indicated.

3. Results

3.1 High SPHK1 expression correlates with poor-survival outcome in GBM and an increased expression in mesenchymal subgroup of GBM

Lysosphospholipid signaling has emerged as important players in various fundamental biological processes. Among them, the bioactive sphingolipid metabolite S1P determines cell fate by promoting cell growth and proliferation, in contrast to ceramide and sphingolipid, which induces cell growth arrest and apoptosis[110]. Sphingosine Kinase 1 (SPHK1), the enzyme that catalyzes the phosphorylation of sphingosine to S1P plays a crucial role in maintaining this balance. SPHK1 has been shown to be frequently upregulated in multiple types of cancer and the elevated levels of SPHK1 have been associated with tumor invasion, angiogenesis and resistance to radiation and chemotherapy[117]. Increased SPHK1 has been shown to be associated with increased glioma grade, and correlates to a poor survival outcome in GBM[109,118]. I validated these observations by analyzing the survival outcomes of SPHK1 in GBM utilizing the TCGA GBM data set (Affymetrix 540 MASS 5.0-u133 array) available in the online R2: Genomics Analysis and Visualization Platform (http://r2.amc.nl). Overall free survival and Progression-free survival, assessed by Kaplan-Meier curves, showed that patients with low SPHK1 expression had higher overall survival (p=0.026) and recurrence-free survival rates (p=4.9e-0.3) compared with patients with high SPHK1 expression (**Figure 6A-B**). These results suggested that SPHK1 expression correlates to poor survival and were one of the independent prognostic factors for GBM patients.

As GBM comprises an intertumor heterogeneity characterized by distinct genetic alterations, gene expression based molecular classification of GBM identified four distinct subtypes of GBM, named Proneural, Neural, Classical and Mesenchymal[5,10]. I further analyzed the distribution of SPHK1 expression between different subtypes of GBM that showed that the mesenchymal subgroup displayed the highest expression of SPHK1 (**Figure 6C**). These results highlight the importance of SPHK1/S1P signaling in GBM physiology, as mesenchymal subtype is marked by highly aggressive tumors and associated with worst outcome usually characterized by abnormal EGFR amplification/ PTEN loss/ NF1 mutations/ Akt signaling[119]. Mesenchymal subtype of GBM has also been shown to be associated with a selective enrichment of microglia/ macrophage-related genes in adult and pediatric GBM tumors[120]. Therefore, these results also

suggested a possible role of SPHK1/S1P signaling in mediating the interactions between microglia and GBM tumors.

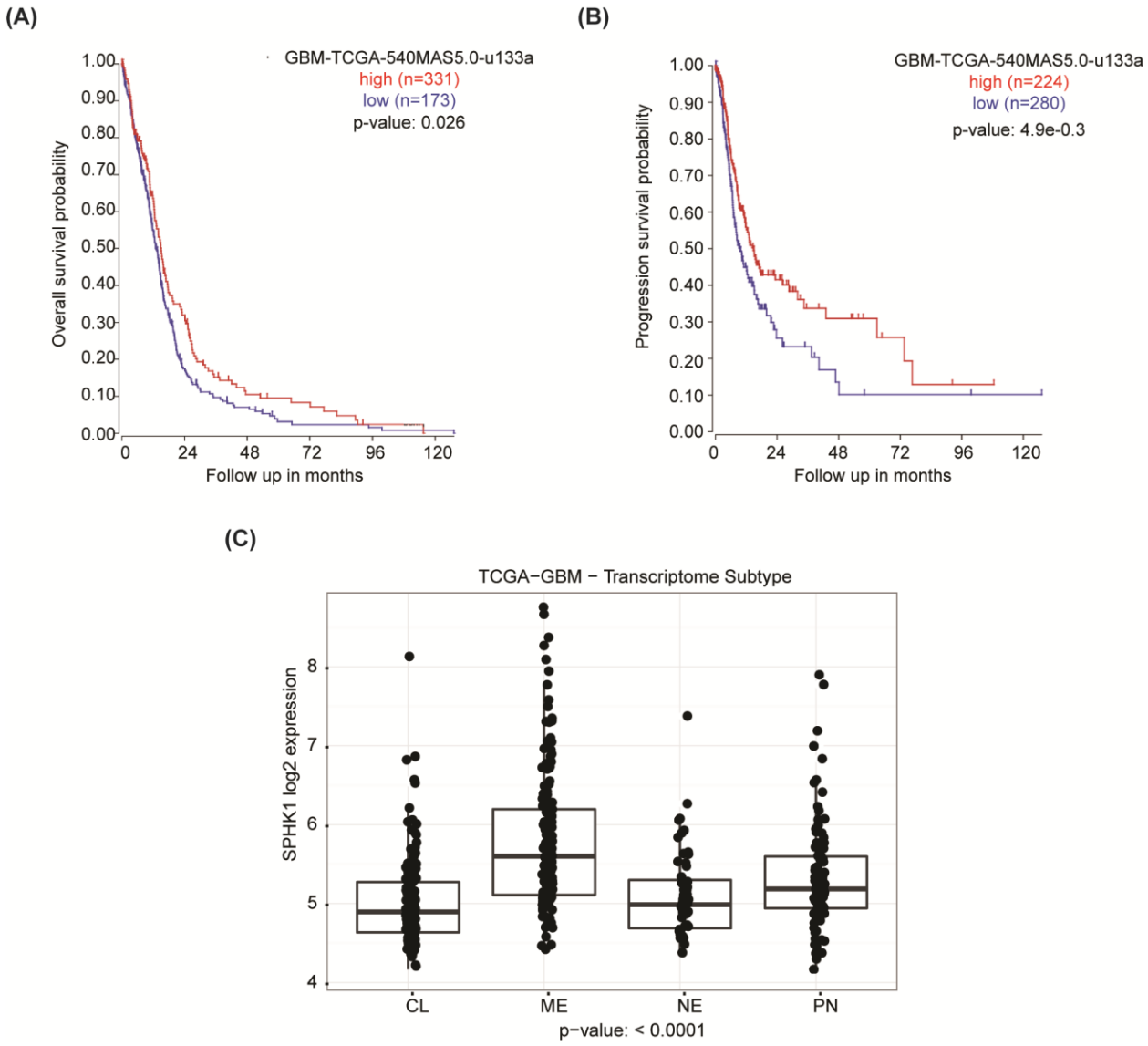

Figure 6: High SPHK1 expression correlates with poor-survival outcome in GBM and an increased expression in mesenchymal subgroup of GBM

Kaplan-Meier estimates of overall survival **(A)** and progression-free survival **(B)** in patients with glioblastoma divided into high SPHK1 and low SPHK1 expression. Data analyzed using the Affymetrix 540 MASS 5.0-u133 array available in the online R2: Genomics Analysis and Visualization Platform (http://r2.amc.nl).

(C) Boxplot of SPHK1 expression measured in CL (classical), ME (mesenchymal), NE (neural) and PN (proneural) subtypes of GBM selected from the full cohort of GBM tumors within the Affymetrix 540 MASS 5.0-u133 array.

3.2 SPHK1 expression is positively correlated to microglial gene signature

Among various factors that control the GBM physiology, tumor-microenvironment strongly influences tumor invasion and treatment resistance. The microenvironment consists of neurons, which are sustained by the glial cells: astrocytes, oligodendrocytes and microglia[121]. I therefore further analyzed the influence of SPHK1 expression in GBM on various cell types of the microenvironment. A Gene set enrichment analysis (GSEA) was performed against SPHK1 expression for differentially enriched genes of the different cell types of the microenvironment. GSEA showed that SPHK1 expression was positively associated with the microglial gene set ($p<0.0001$), with high SPHK1 correlated to expression microglial genes such as *Slco2b1*, *Csf1r*, *Gpr34* and *Tmem119* that are specifically expressed by microglial cells. Similarly, SPHK1 expression was less significantly associated with astrocyte gene set ($p=0.0086$) and oligodendrocyte gene set ($p=0.0029$) and negatively correlated with neuronal gene set ($p=0.99$) (**Figure 7**). These results suggested that SPHK1 strongly influences the microglial population over other cell types of the microenvironment, and S1P could play an important role in regulating the microglia-glioma crosstalk.

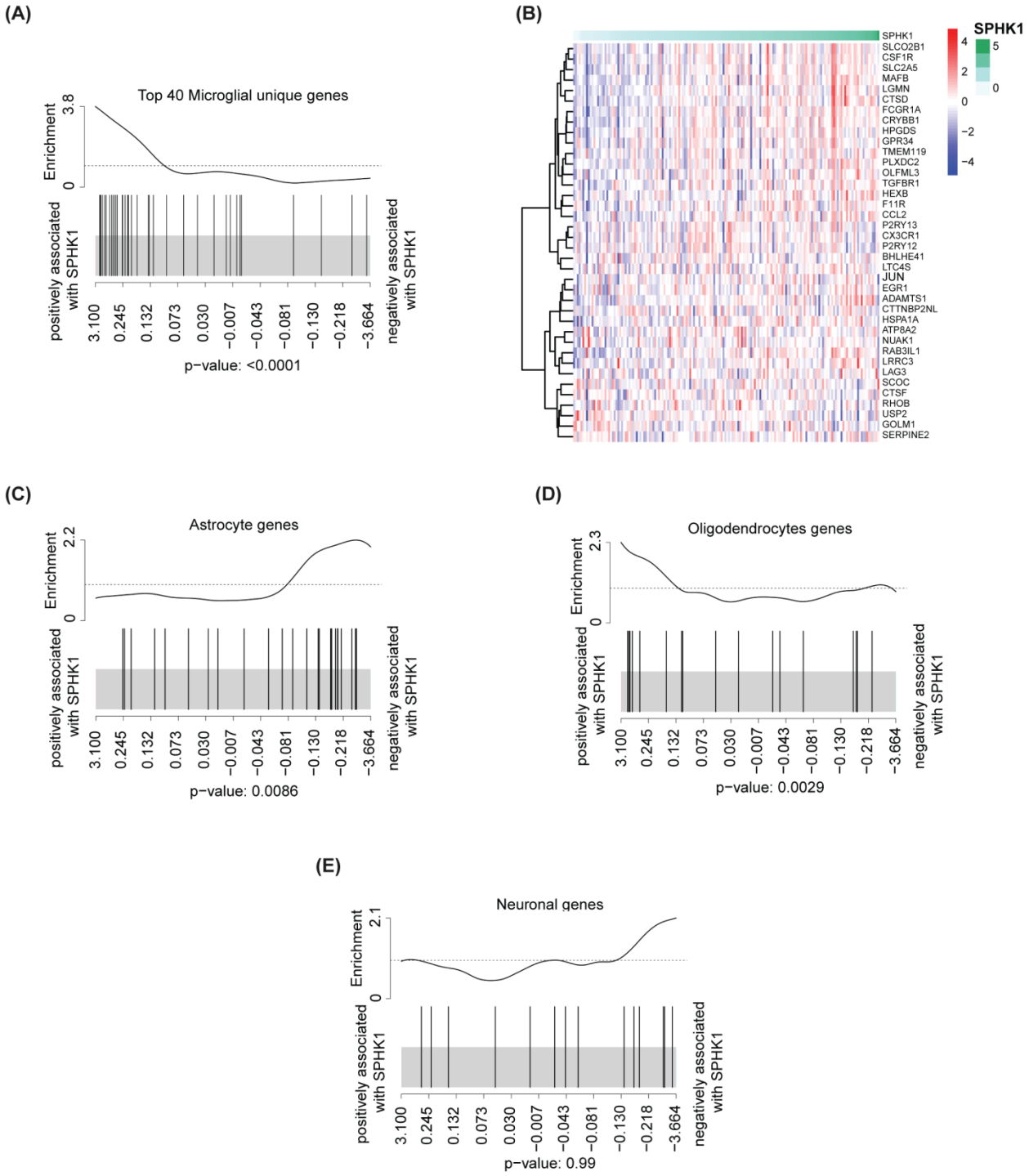

Figure 7: SPHK1 expression is positively correlated to microglial gene signature.

(A) Gene set enrichment analysis (GSEA) and corresponding heat map(B) using Affymetrix gene expression data of GBM (Affymetrix 540 MASS 5.0-u133 array) and gene sets as reported in Butovsky et al., 2013[122]against SPHK1 expression for differentially enriched genes of microglia. Gene set enrichment analysis (GSEA) against SPHK1 expression for differentially enriched genes astrocytes (C),

oligodendrocytes (D) and neurons (E). The analysis was performed in collaboration with Thomas Hielscher, Department of statistics, DKFZ.

3.3 Validation of microglia isolation by flow cytometry

As it has been shown that glioma cells produced an increased amount of the bioactive sphingolipid metabolite S1P[118], I hypothesized that S1P secreted by glioma cells contributed to the polarization of microglia/ macrophages towards an anti-inflammatory phenotype. Microglia was isolated using the mild trypsinization protocol, as mentioned before in methods. A combination of CD11b and CD45 labeling can be used to identify microglia, where ramified parenchymal microglia have been demonstrated to possess the phenotype $CD11b^{+}CD45^{low}$, while macrophages show $CD11b^{+}CD45^{high}$ phenotype[123]. The isolated microglia was validated by fluorescent activated cell sorting (FACS), where microglia was sorted for CD11b and CD45 expression. FACS analysis of microglia isolated one day after the mild trypsinization showed a 94.1% purity representing a pure population of $CD11b^{+}CD45^{low}$ microglial cells, with almost negligible astrocyte contamination represented by $CD11b^{-}CD45^{-}$ cells (**Figure 8A**). Also, microglia analyzed four days after the mild trypsinization demonstrated a 89.9% purity, indicating that even after four days of isolation there wasn't much contamination by astrocyte re-growth (**Figure 8B**). Further, FACS analysis of the mixed culture population before undergoing the mild trypsinization showed 37.6% of microglia represented by $CD11b^{+}CD45^{low}$ and a significant $CD11b^{-}CD45^{-}$ population of astrocytes (**Figure 8C**).

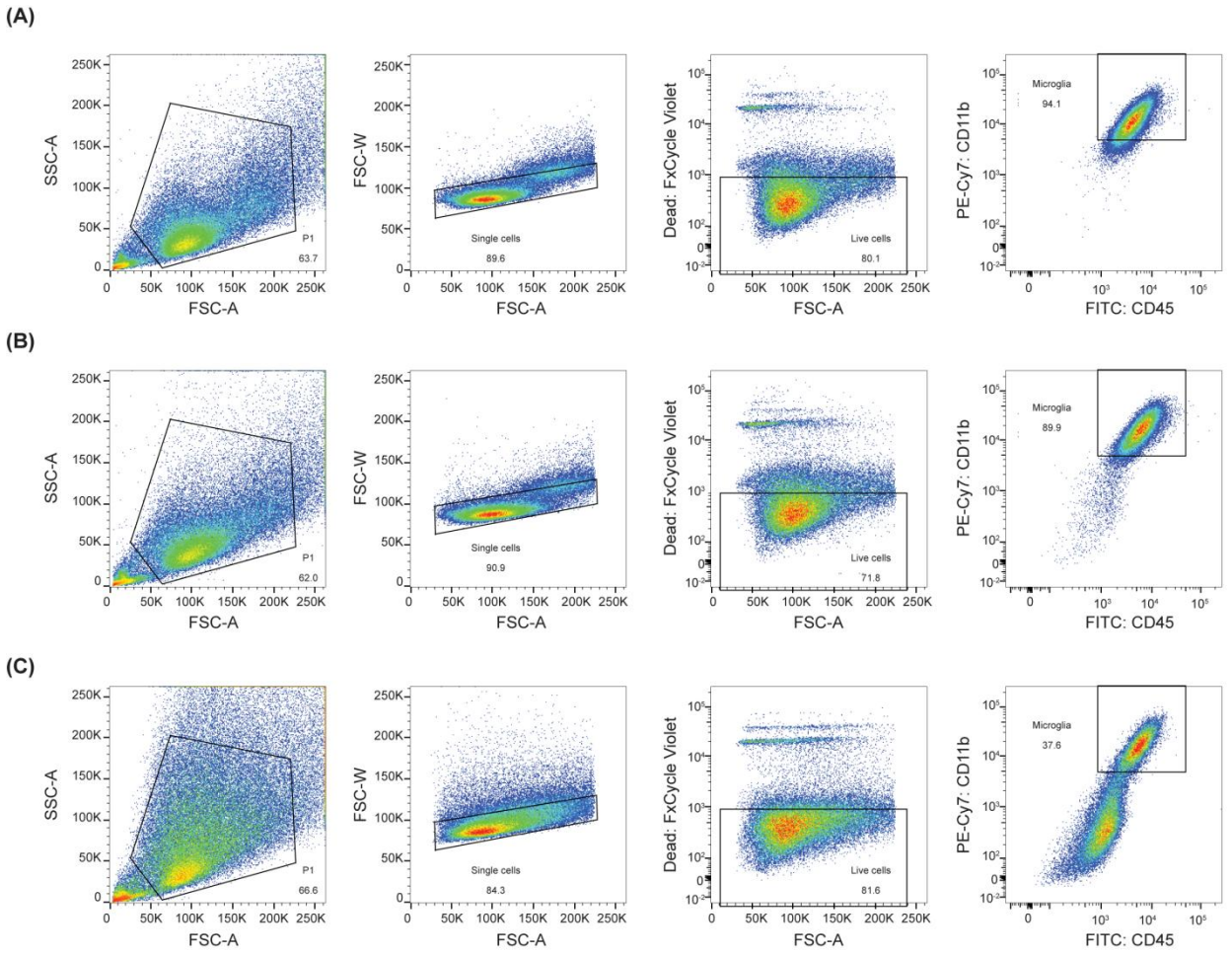

Figure 8: Validation of microglia population by flow cytometry.

(A) FACS analysis of microglia isolated one day after mild trypsinization protocol. (B) FACS analysis of microglia isolated four days after mild trypsinization protocol. (C) FACS analysis of mixed culture isolated before mild trypsinization protocol. Single cell suspensions were analyzed by flow cytometry. The cells were gated for side scatter (SSC) and forward scatter (FSC) to identify viable, single cell events; and FxCycle Violet stain to gate for dead cells. The gating strategy used to define microglia ($CD11b^{+}CD45^{low}$) is depicted. (E) Schematic representation of the *in-vitro* glioma – microglia co-culture model. The FACS analysis was performed in collaboration with MahakSinghal, Department of Vascular Oncology and Metastasis, DKFZ.

3.4 Silencing of SPHK1 in gliomas induces a pro-inflammatory phenotype in microglia/ macrophages.

In order to evaluate the effect of sphingosine kinase 1 (SPHK1), the enzyme that mainly produced S1P, I firstly generated stable SPHK1 knockdown clones in two human glioma cell

lines, LN229 and LN308 cells, using shRNA-mediated silencing technology. As shown in **Figure 9A**, the puromycin resistant clones (shSPHK1) exhibited a markedly reduced mRNA expression in both cell lines. To verify the efficiency of SPHK1 knockdown on the protein level, LN229 cells were co-transfected with over-expression of SPHK1 gene (containing a c-myc tag at its N-terminus end (SPHK1-myc), and the shRNA against SPHK1. Three days after infection and selection with puromycin, proteins were isolated and blotted for c-myc. As shown in **Figure 9B**, LN229 cells co-transfected with both SPHK1-myc and shSPHK1 showed a remarkably decreased expression of c-myc protein, as compared to cells transfected with only the virus carrying the overexpression of SPHK1 gene, thereby verifying the knockdown efficiency of the shSPHK1.

As illustrated in **Figure 10**, silencing of SPHK1 expression in gliomas resulted in a remarkably decreased expression of M2 markers, Arginase 1 (*Arg1*) and Macrophage scavenger receptor 1 (*Msr1*), in primary microglial cells co-cultured with human glioma cells, LN229 and LN308 transfected with shSPHK1, as compared to glioma cells transfected with SCR control (**Figure 10A-B**). Analysis of M1 markers although did not result in significant changes in expression of Tumor necrosis factor α (*Tnfα*) in primary microglial cells, Interleukin 6 (*IL6*) expression was significantly upregulated in primary microglial cells co-cultured with human glioma cells carrying the knockdown (shSPHK1) as compared to the SCR control (**Figure 10C-D**). These results were confirmed in another model, where RAW264.7 macrophages were co-cultured with human glioma cells, LN229 and LN308, in which silencing of SPHK1 in glioma cells resulted in a significant decrease in *Arg1* expression in RAW264.7 macrophages (**Figure 10E**). These results indicated that silencing of SPHK1 in gliomas diminished the anti-inflammatory phenotype (M2) in microglia/ macrophages promoted by glioma cells, and induced a pro-inflammatory phenotype (M1).

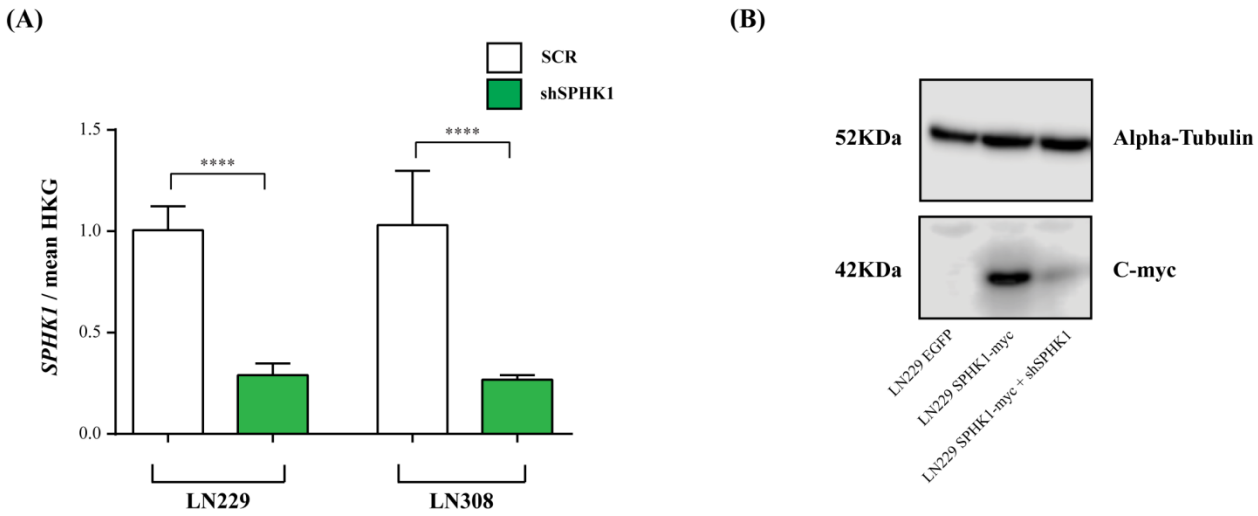

Figure 9: Validation of knockdown of SPHK1 in glioma cells.

(A) Quantitative RT-PCR analysis of *SPHK1* in human glioma cells, LN229 and LN308 stably transfected with a control (SCR) or SPHK1-targeted shRNA (shSPHK1). The mRNA expression of the target genes was normalized to the mean of two housekeeping genes (*PPIA*, *GAPDH*). Data are expressed as fold-change over SCR and are means ± sem of 3 independent experiments. Statistical analysis was performed using paired t-test. **** $p<0.0001$, *** $p<0.001$; ** $p<0.01$, * $p<0.05$, n.s.: not significant. **(B)** Western blot analysis of c-myc expression in LN229 human glioma cells transfected with either EGFP (that served as control); SPHK1-myc; or co-transfected with SPHK1-myc and SPHK1-targeted shRNA. Tubulin served as loading control.

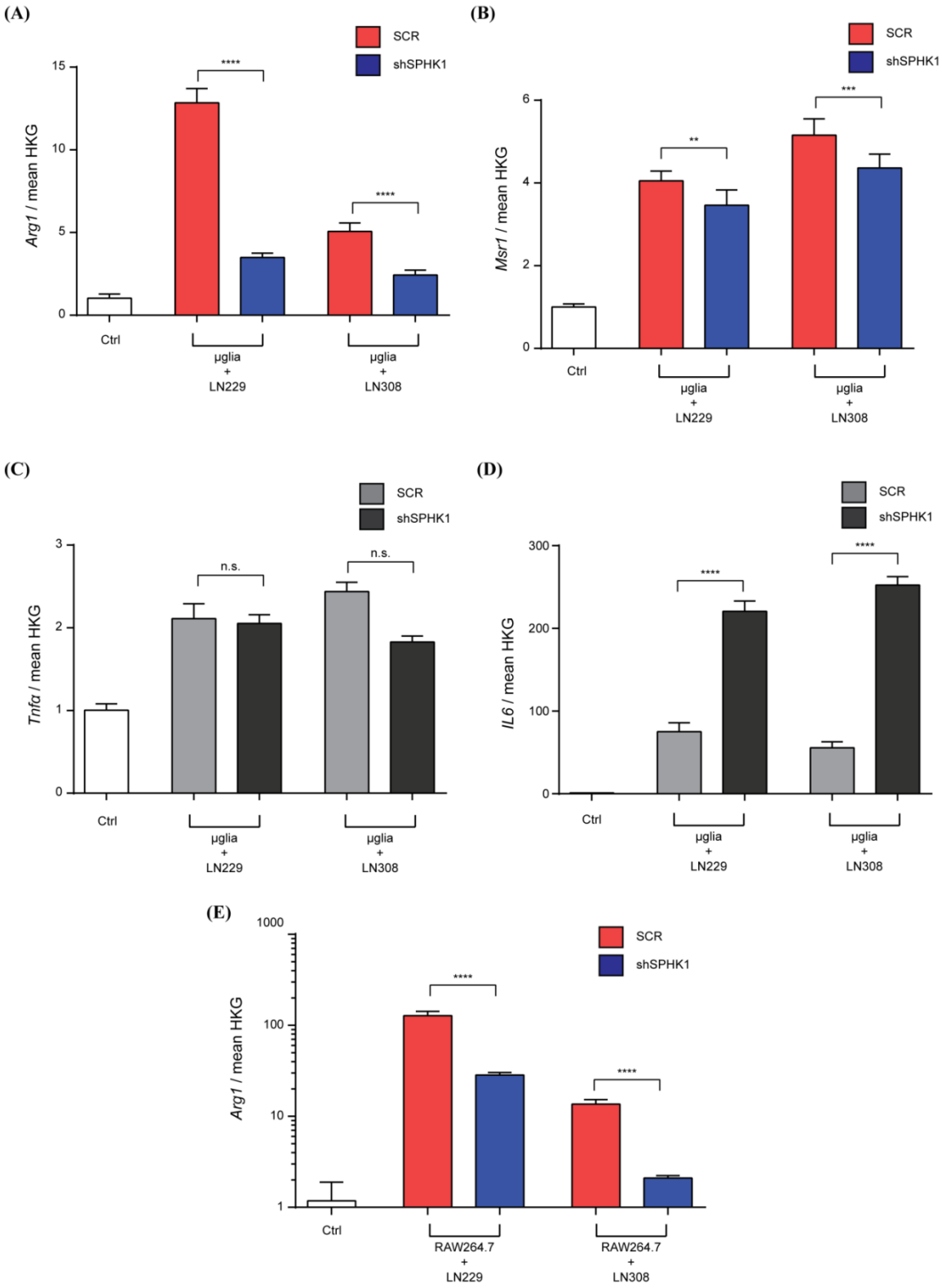

Figure 10: Silencing of SPHK1 in gliomas induces a pro-inflammatory phenotype in microglia/ macrophages.

Quantitative RT-PCR analysis of M2 markers *Arg1* **(A)** and Msr1 **(B)**; M1 markers *Tnfα***(C)** and *IL6***(D)** in murine primary microglia (μglia) co-cultured with human glioma cells, LN229 and LN308 stably transfected with control (SCR) or SPHK1-targeted shRNA (shSPHK1). **(E)** Quantitative RT-PCR analysis of M2 marker *Arg1* expression in RAW264.7 macrophages co-cultured with human glioma cells, LN229 and LN308 stably transfected with control (SCR) or SPHK1-targeted shRNA (shSPHK1).The mRNA expression of the target genes was normalized to the mean of two housekeeping genes (*B2m*, *Hprt*). Data are expressed as fold-change over control cells (Ctrl) cultured without glioma cells and are means ± sem of 3 independent experiments. Statistical analysis was performed using paired t-test. **** $p<0.0001$, *** $p<0.001$; ** $p<0.01$, * $p<0.05$, n.s.: not significant.

3.5 Over-expression of SPHK1 in glioma enhances the M2 phenotype of microglia/ macrophages.

Conversely, SPHK1 expression was modulated in human glioma cells, where cells were stably overexpressed with sphingosine kinase 1 gene carrying a myc tag at its N-terminus end (SPHK1-myc). Human glioma cells stably overexpressing EGFP served as control cells. The overexpression of SPHK1 was verified by mRNA expression of SPHK1 by real-time qPCR, that showed a remarkable increase in SPHK1 expression (**Figure 11A**). These results were further validated by western blot analysis of c-myc expression, that showed an increased expression of c-myc (**Figure 11B**); and by S1P quantification using LC-MS/MS, that showed that overexpression of SPHK1 in glioma cells resulted in considerable increase in S1P levels in LN229 glioma cells, although not statistically significant, yet tending towards an increase in LN308 cells (**Figure 11C**).

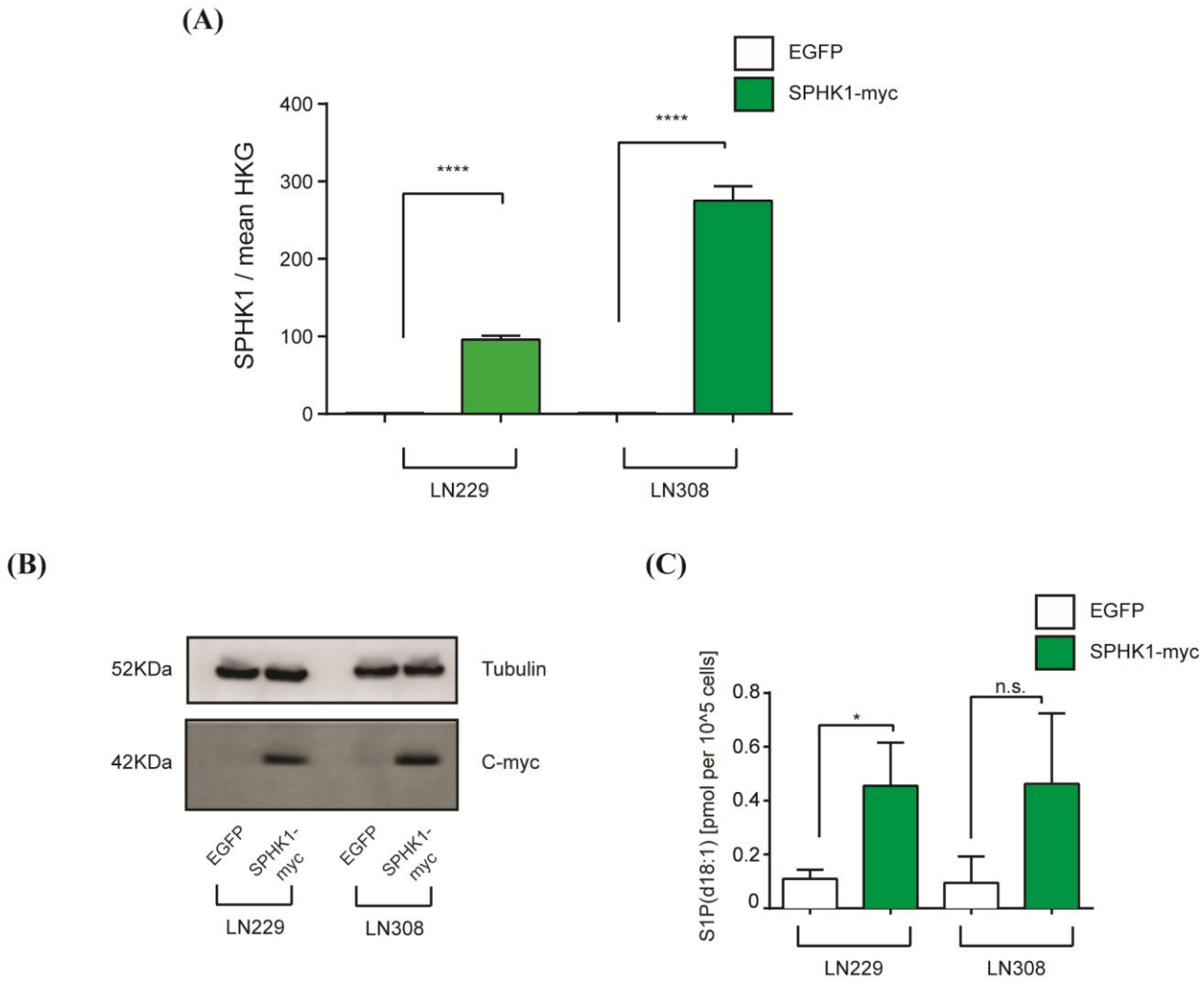

Figure 11: Verification of overexpression of SPHK1 in glioma cells.

(A) Quantitative RT-PCR analysis of *SPHK1* in human glioma cells, LN229 and LN308 stably transfected with EGFP or SPHK1-myc. The mRNA expression of the target genes was normalized to the mean of two housekeeping genes (*PPIA, GAPDH*). Data are expressed as fold-change over EGFP and are means ± sem of 3 independent experiments. **(B)** Western blot analysis of c-myc expression in human glioma cells, LN229 and LN308, stably transfected with either EGFP (that served as control) or SPHK1-myc. Tubulin served as loading control. **(C)** Quantification of S1P by LC-MS/MS in human glioma cells, LN229 and LN308 stably transfected with EGFP or SPHK1-myc. Data are expressed as S1P [d18:1] pmol per 10^5 cells and are means ± sem of 3 independent experiments. Statistical analysis was performed using paired t-test. **** $p<0.0001$, *** $p<0.001$; ** $p<0.01$, * $p<0.05$, n.s.: not significant. The LC-MS/MS analysis was performed in collaboration with Robert Pilz, Department of Cellular and Molecular Pathology, DKFZ.

As illustrated in **Figure 12**, over-expression of SPHK1 in gliomas promoted the anti-inflammatory phenotype of microglial cells, as confirmed by a further increase in mRNA expression of M2 markers, *Arg1* (**Figure 12A**) and *Msr1* expression (**Figure 12B**) in primary microglial cells co-cultured with overexpression cells as compared to EGFP control. Analysis of M1 markers did not show significant changes in mRNA expression of *Tnfα* (**Figure 12C**) and *IL6* (**Figure 12D**) in primary microglial cells co-cultured with overexpression cells as compared to control, suggesting that overexpression of SPHK1 did not alter the pro-inflammatory phenotype of primary microglia. Similarly, these results were confirmed in co-culture of RAW264.7 macrophages and human glioma cells, as observed by an increased mRNA expression of M2 marker *Arg1* (**Figure 12E**) in RAW264.7 macrophages co-cultured with SPHK1 overexpression cells as compared to EGFP control. Collectively, these results indicated that glioma derived sphingosine kinase 1 contributed to the microglial tumor-supportive activation state.

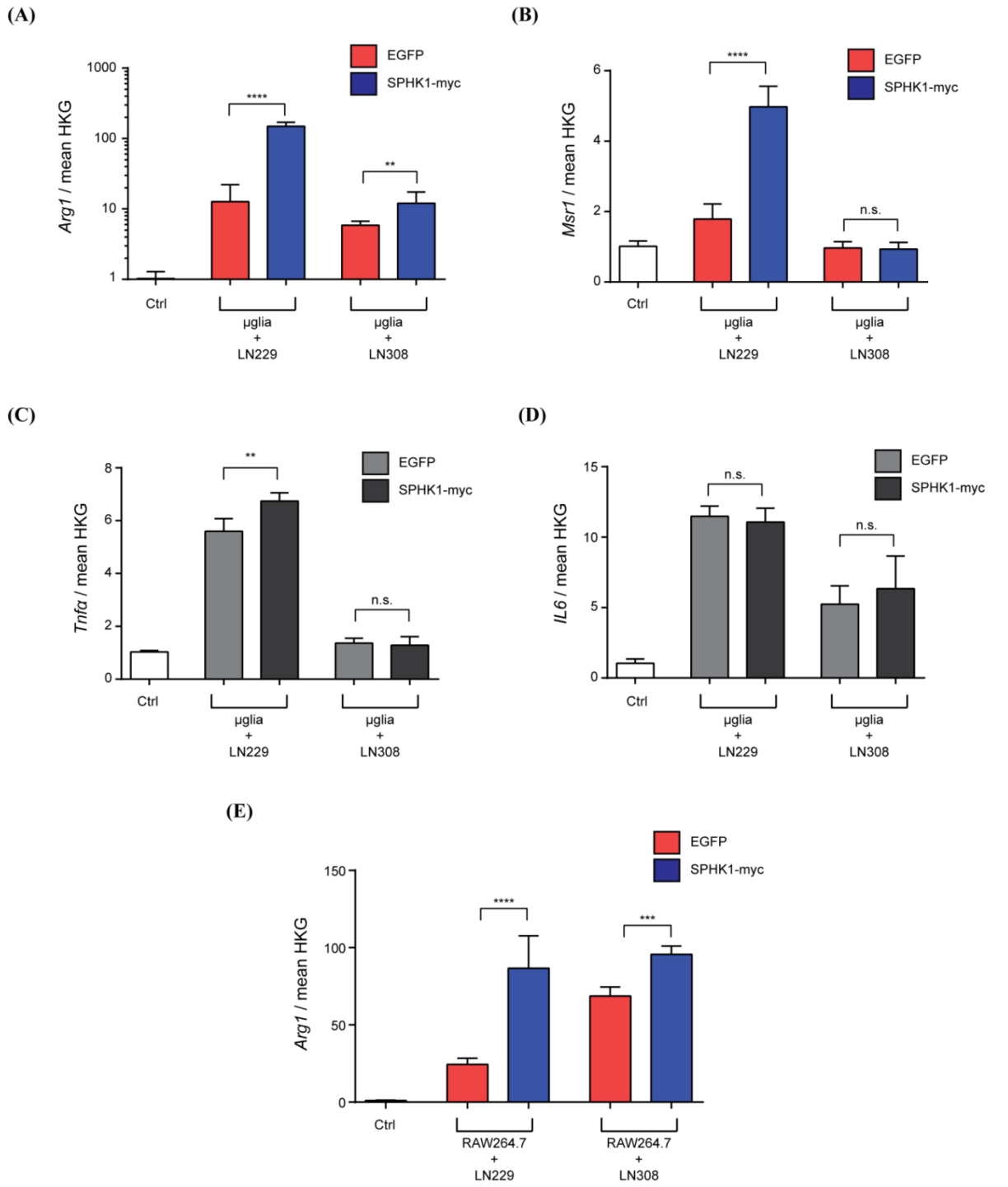

Figure 12: Over-expression of SPHK1 in glioma enhances the M2 phenotype of microglia/ macrophages.

Quantitative RT-PCR analysis of M2 markers *Arg1* **(A)** and Msr1 **(B)**; M1 markers *Tnfα***(C)** and *IL6***(D)** in murine primary microglia (µglia) co-cultured with human glioma cells, LN229 and LN308 stably transfected with EGFP or SPHK1-myc. **(E)** Quantitative RT-PCR analysis of M2 marker *Arg1* expression in RAW264.7 macrophages co-cultured with human glioma cells, LN229 and LN308 stably transfected with EGFP or SPHK1-myc.The mRNA expression of the target genes was normalized to the

mean of two housekeeping genes (*B2m*, *Hprt*). Data are expressed as fold-change over control cells (Ctrl) cultured without glioma cells and are means ± sem of 3 independent experiments. Statistical analysis was performed using paired t-test. **** p<0.0001, *** p<0.001; ** p<0.01, * p<0.05, n.s.: not significant.

3.6 Inhibition of SPHK1 in a co-culture system shifts microglia/ macrophages to an M1 phenotype.

The SPHK1 small molecule inhibitor, SKI-II, has been widely used as a SPHK1 inhibitor that blocks the binding of sphingosine and ATP to SPHK1[124]. The use of SKI-II in the context of cancer therapy has been recently reviewed[125]. Correspondingly, in a co-culture setting of murine primary microglial cells and human glioma cells treated with SPHK1 small molecule inhibitor, SKI-II, resulted in a significant decrease in expression of M2 markers, *Arg1* (**Figure 13A**) and *Msr1* (**Figure 13B**) in microglial cells. An analysis of M1 marker expression revealed a striking increase in mRNA expression of *TNFα* (**Figure 13C**) and *IL6* (**Figure 13D**). Similarly, analysis of IL10 secretion, a prominent M2 marker[126] by ELISA from cell-free supernatant of microglial cells co-cultured with human glioma cells and treated with SKI-II, displayed a marked decrease in IL10 levels in microglial cells (**Figure 14A**). These results were further substantiated by analysis of TNFα and IL6 secretion from cell-free supernatants of microglial cells that showed a remarkable decrease in secretion of these cytokines (**Figure 14A, B**). These results indicated that inhibition of SPHK1 in gliomas shifted the response of microglial cells from an anti-inflammatory phenotype (M2) within a tumor to pro-inflammatory phenotype (M1).

These results were further extended in co-culture of RAW264.7 macrophages and human glioma cells treated with SKI-II, that resulted in a decreased mRNA expression of M2 marker *Arg1* (**Figure 15A**) and an increased mRNA expression of *TNFα* (**Figure 15B**) and *IL6* (**Figure 15C**). Taken together, these data support the fact that S1P from glioma cells regulates the tumor-supportive phenotype of microglia/ macrophages, and modulation of SPHK1 expression or activity can modify the phenotype of microglial cells, and thus a potential candidate for targeted therapy.

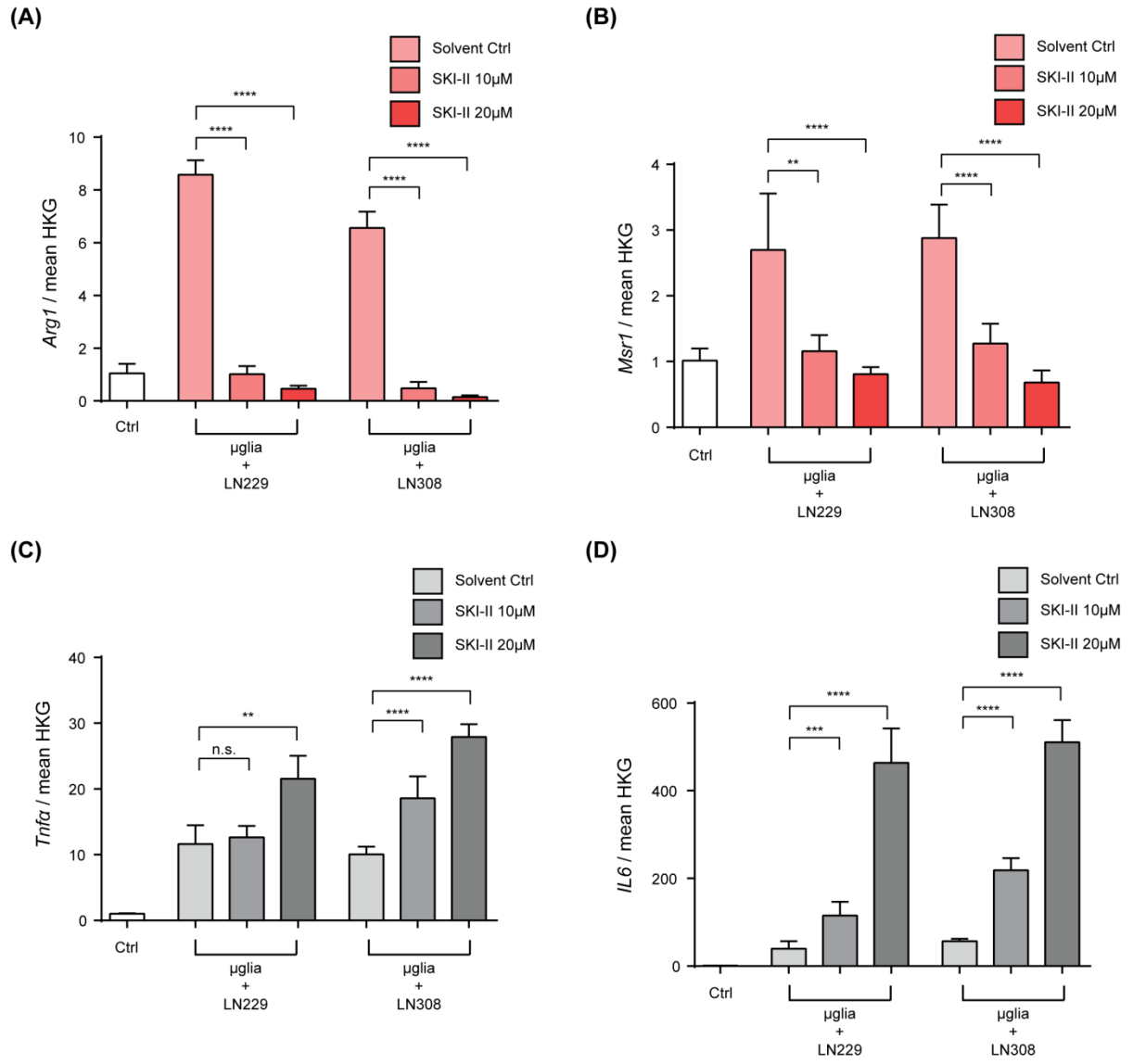

Figure 13: Inhibition of SPHK1 in gliomas modulates gene expression profile of microglia from anti-inflammatory phenotype to a pro-inflammatory phenotype

Quantitative RT-PCR analysis of M2 markers *Arg1* and *Msr1***(A, B)**, and M1 markers *Tnfα* and *IL6***(C, D)** in murine primary microglia (μglia) co-cultured with human glioma cells, LN229 and LN308 upon treatment with sphingosine kinase 1 small molecule inhibitor, SKI-II for 24 hrs. The mRNA expression of the target genes was normalized to the mean of two housekeeping genes (*B2m*, *Hprt*). Data are expressed as fold-change over primary microglial cells treated with solvent control (Ctrl) and are means ± sem of 3 independent experiments. Statistical analysis was performed using paired t-test. **** $p<0.0001$, *** $p<0.001$; ** $p<0.01$, * $p<0.05$, n.s.: not significant.

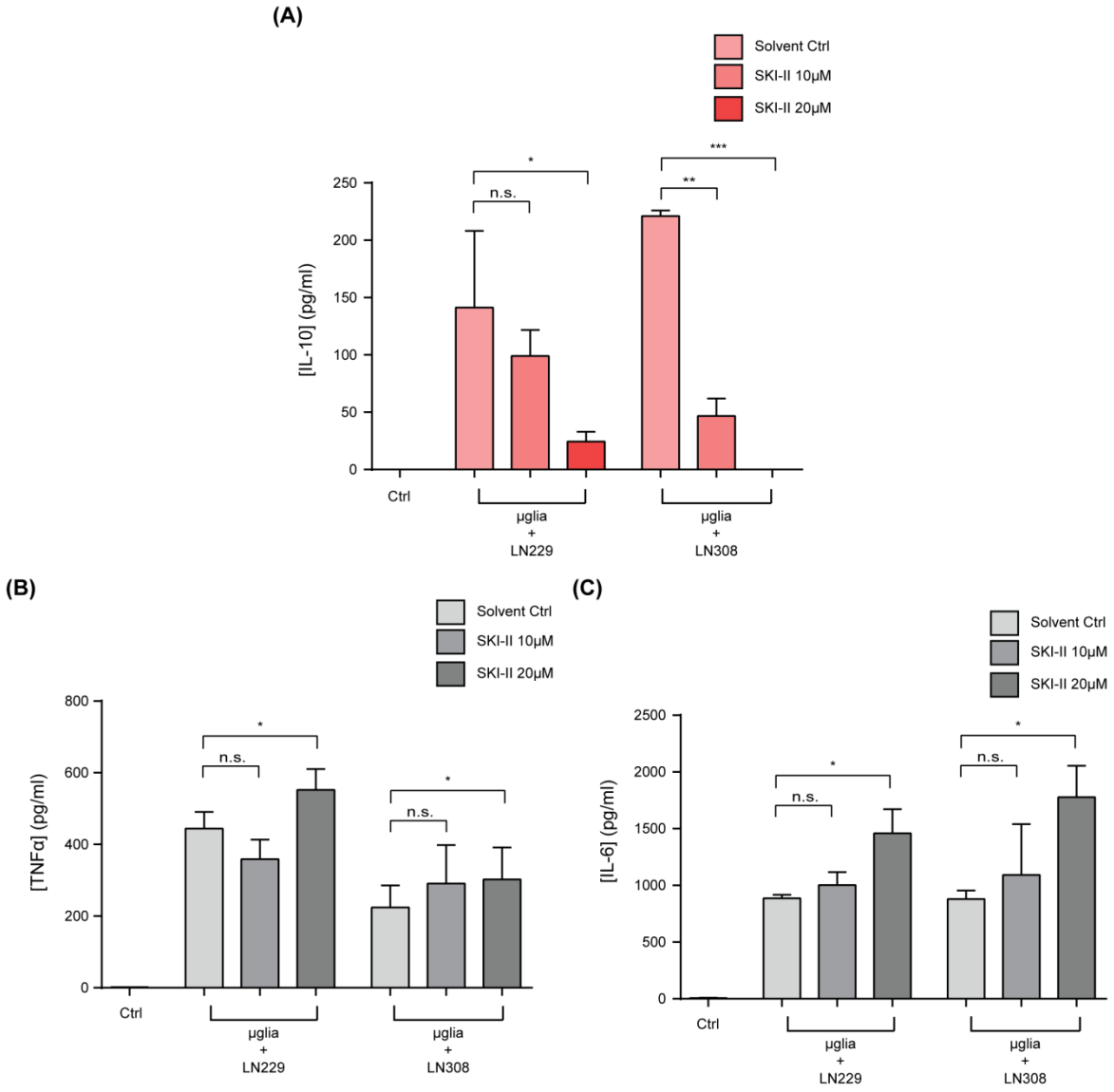

Figure 14: SKI-II treatment in gliomas induces significant changes in the secretion of inflammatory factors

Enzyme-linked immunosorbent assay (ELISA) of M2 cytokine IL10 **(A)** and M1 cytokine TNFα **(B)** and IL-6 **(C)** in cell-free supernatant of murine primary microglia (μglia) co-cultured with human glioma cells, LN229 and LN308 upon treatment with sphingosine kinase 1 small molecule inhibitor, SKI-II for 24 hrs. Data are expressed as pg/ml as plotted against a standard curve for each cytokine and are means ± sem of 3 independent experiments. Statistical analysis was performed using paired t-test. **** $p<0.0001$, *** $p<0.001$; ** $p<0.01$, * $p<0.05$, n.s.: not significant.

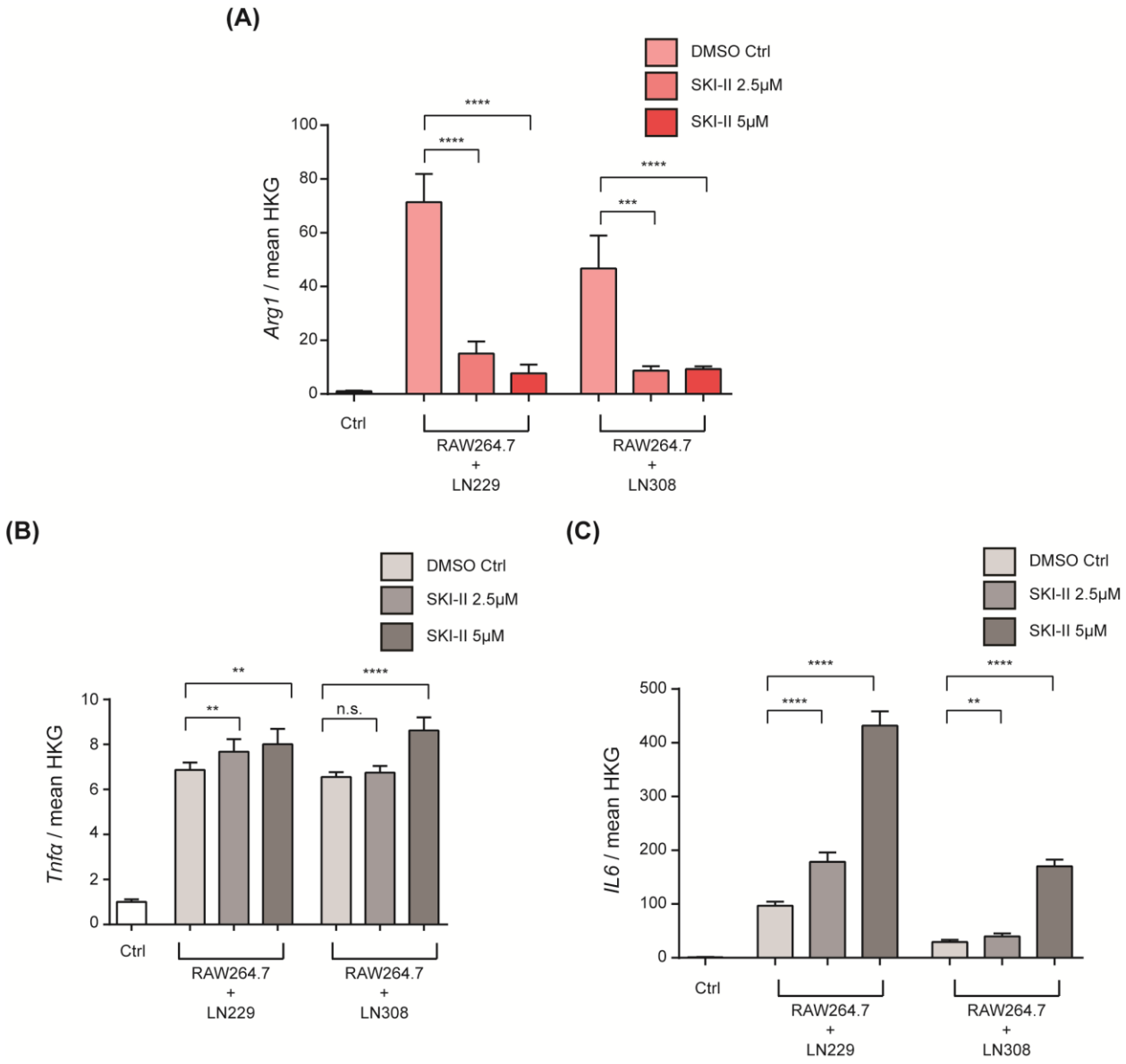

Figure 15: Inhibition of SPHK1 in gliomas shifts macrophage response to an M1 phenotype.

Quantitative RT-PCR analysis of M2 markers *Arg1* and *Msr1***(A, B)**, and M1 markers *Tnfα* and *IL6***(C, D)** in RAW264.7 macrophages co-cultured with human glioma cells, LN229 and LN308 upon treatment with sphingosine kinase 1 small molecule inhibitor, SKI-II for 24 hrs. The mRNA expression of the target genes was normalized to the mean of two housekeeping genes (*B2m, Hprt*). Data are expressed as fold-change over RAW264.7 macrophages treated with solvent control (Ctrl) and are means ± sem of 3 independent experiments. Statistical analysis was performed using paired t-test. **** $p<0.0001$, *** $p<0.001$; ** $p<0.01$, * $p<0.05$, n.s.: not significant.

3.7 Inhibition of SPHK1 in gliomas modulates important signaling pathways that regulate M1-M2 polarization of microglia/ macrophages

Among major pathways that regulate microglia/ macrophage polarization, M1 stimulus such as LPS, IFN-γ signal through activation of TLR4, IFNα, or IFN-β receptors (IFNAR), leading to the activation of transcription factors NF-κB, AP-1, IRF3 and STAT1, which in turn leads to the active transcription of pro-inflammatory genes[127]. In contrast, M2 stimuli such as IL-4 and/ or IL-13 signals via IL-4Rα, thus activating STAT6, that regulates the expression of important alternatively activated anti-inflammatory genes. IL-10 signals through its receptor IL-10R activating STAT3 triggering an M2-like macrophage polarization[127]. To elucidate the molecular pathways that mediate the shift to a pro-inflammatory phenotype in microglia/ macrophages upon SKI-II treatment in gliomas, primary microglia and RAW264.7 macrophages were treated with conditioned media harvested from human glioma cell lines, LN229 and LN308 treated with SKI-II. Total cell extracts were isolated to analyze various key signaling pathways that mediated the M1 and M2 phenotype of microglia/ macrophages.

Immunoblot analysis of primary microglia treated with conditioned media from glioma cells treated with SKI-II, showed a remarkably decreased activation of phospho-Stat3 and phospho-Akt as compared to control cells, indicating that S1P from glioma cells activates the Stat3 pathway and Akt pathway, and thereby promoting the anti-inflammatory phenotype of microglia (**Figure 16**). SKI-II treatment also showed a decreased activation of phospho-TBK1 and phospho-IRF3, demonstrating that inhibition of SPHK1 in glioma resulted in deactivation of the TBK1/ IRF3 pathway that plays an important role in regulating the anti-inflammatory polarization (**Figure 16**). On the contrary SKI-II treatment displayed an activation of the NF-κB pathway as indicated by the activation of phospho- NF-κB p65 and degradation of IκBα, suggesting that inhibition of SPHK1 in gliomas induces a pro-inflammatory polarization of microglia via activation of the NF-κB pathway (**Figure 16**). These observations were further validated in RAW264.7 macrophages that similarly illustrated that inhibition of SPHK1 in gliomas, led to decreased activation of Stat3 pathway, Akt pathway, and TBK1 / IRF3 pathway, while accompanied by an activation of the NF-κB pathway (**Figure 17**). These results taken together illustrated that S1P modulates key signaling pathways that regulate M1-M2 phenotype, thereby inducing the anti-inflammatory polarization of microglia/ macrophages.

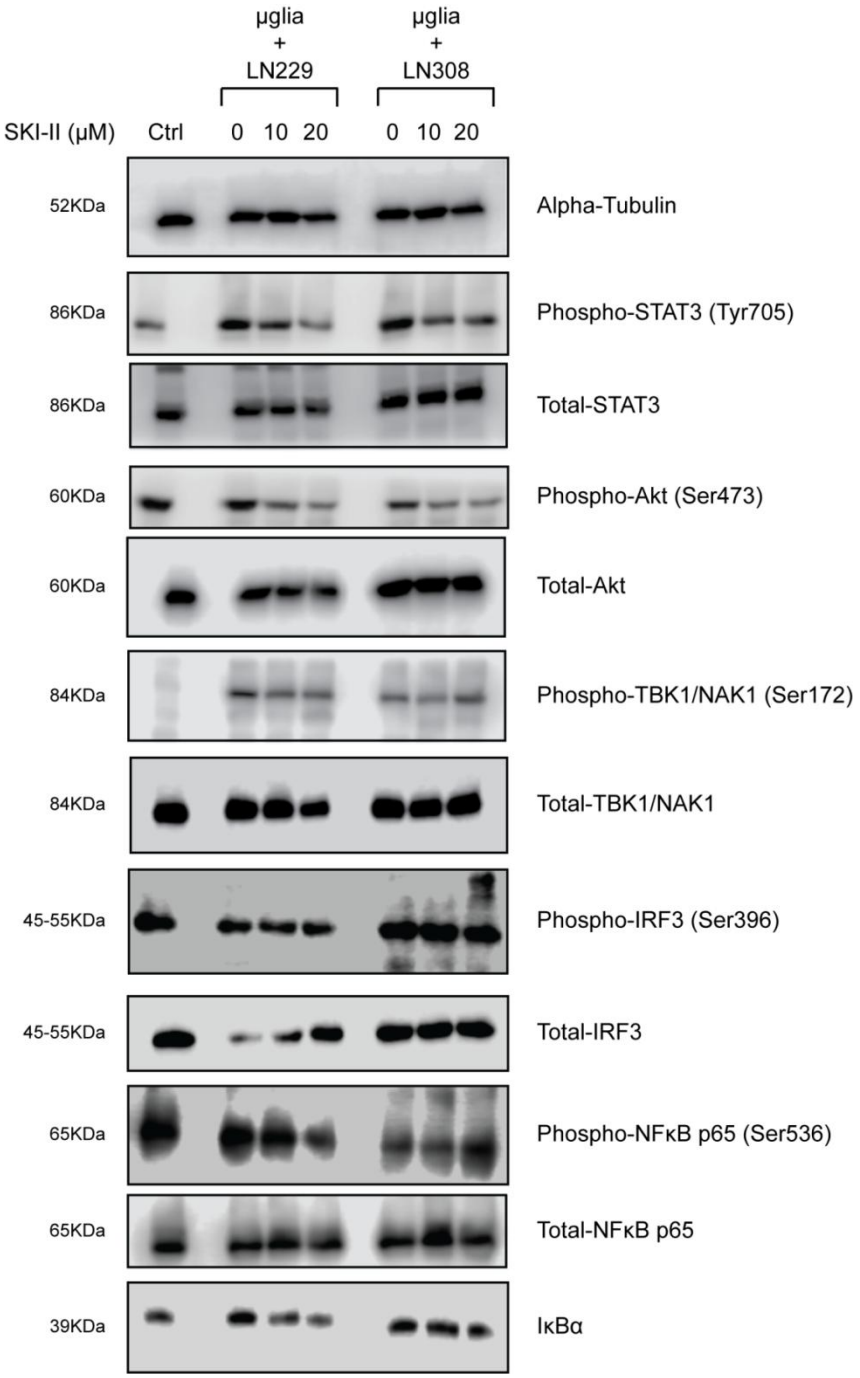

Figure 16: SKI-II treatment in glioma modulates important signaling pathways that regulate M1-M2 polarization of primary microglia

Western blot analysis of primary microglia treated for 24 hours with conditioned media harvested from human glioma cell lines, LN229 and LN308, and treated with SPHK1 small molecule inhibitor, SKI-II, assessed with anti-phospho-STAT3 (Tyr705), anti-STAT3, anti-phospho-Akt (Ser473), anti-Akt, anti-phospho-TBK1/NAK1 (Ser172), anti-TBK1/NAK1, anti-phospho-IRF3 (Ser396), anti-IRF3, anti-phospho-NFκB-p65, anti-NFκB-p65 or anti-IκBα. Alpha-tubulin served as loading control.

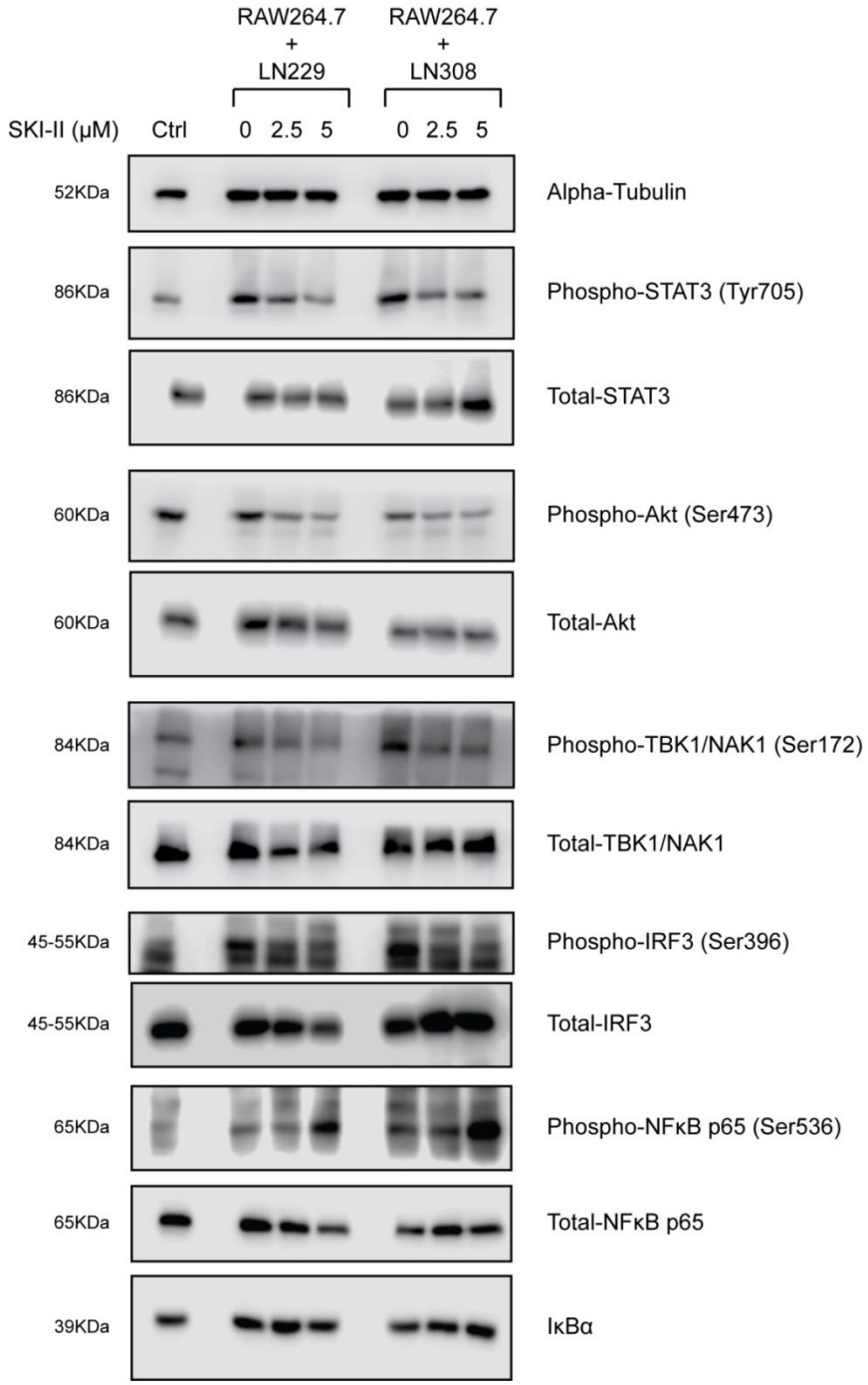

Figure 17: SKI-II treatment in glioma regulates key signaling pathways that defined the M1-M2 polarization of macrophages

Western blot analysis of RAW264.7 macrophages treated for 24 hours with conditioned media harvested from human glioma cell lines, LN229 and LN308, and treated with SPHK1 small molecule inhibitor, SKI-II, assessed with anti-phospho-STAT3 (Tyr705), anti-STAT3, anti-phospho-Akt (Ser473), anti-Akt, anti-phospho-TBK1/NAK1 (Ser172), anti-TBK1/NAK1, anti-phospho-IRF3 (Ser396), anti-IRF3, anti-phospho-NFκB-p65, anti-NFκB-p65 or anti-IκBα. Alpha-tubulin served as loading control.

3.8 Antagonism of Sphingosine 1-Phosphate receptors by FTY720 induces a pro-inflammatory phenotype of microglia/ macrophages

As previous results showed that S1P induces tumor-supportive phenotype of microglia/ macrophages in gliomas, the next experiments were aimed at targeting the receptor on microglia that mediated the anti-inflammatory responses. S1P conveys signals as an intracellular messenger and/or through a family of G-coupled receptors (S1PR1-5) expressed both on cancer cells and their surrounding microenvironment[82,128]. FTY720, an immunomodulatory drug acts as a potent antagonist of four S1P receptors (S1PR1, S1PR3, S1PR4 and S1PR5)[105,129]. FTY720 renders cells unresponsive to S1P activation by sequestering S1PR1 intracellularly[130]. For that reason, microglial cells co-cultured with glioma cells were treated with FTY720 to understand if blocking the G-coupled receptors S1PR1-5 rendered the microglial cells unresponsive to S1P, and thereby promoting a pro-inflammatory phenotype of microglia/ macrophages.

To investigate the effects of FTY720 alone on microglial cells and excluding its inhibitory effects on glioma cells, human glioma cells were initially cultured for 48 hours and the conditioned media was harvested. Primary microglia were pre-blocked with FTY720 for 24 hours, and treated with glioma-derived conditioned media for 24 hours, after which RNA was isolated. Quantitative qPCR analysis although did not result in significant changes in mRNA expression of M2 markers, *Arg1* (**Figure 18A**) and *Msr1* (**Figure 18B**) in microglial cells; analysis of M1 markers revealed a striking increase in mRNA expression of *TNFα* (**Figure 18C**) and *IL6* (**Figure 18D**). These results were further confirmed by analysis of secreted inflammatory cytokines by ELISA that showed a surprising decrease in IL10 secretion (**Figure 19A**), and a significant increase in secretion of TNFα (**Figure 19B**) and IL6 (**Figure 19C**). These results inferred that although FTY720 treatment led to a partial decrease in the anti-inflammatory phenotype, as shown by insignificant changes in expression of *Arg1* and *Msr1*, while a reduction in IL10 secretion; the drug was able to induce a pro-inflammatory state of microglia as indicated by elevated levels of TNFα and IL6 both on mRNA level and protein level.

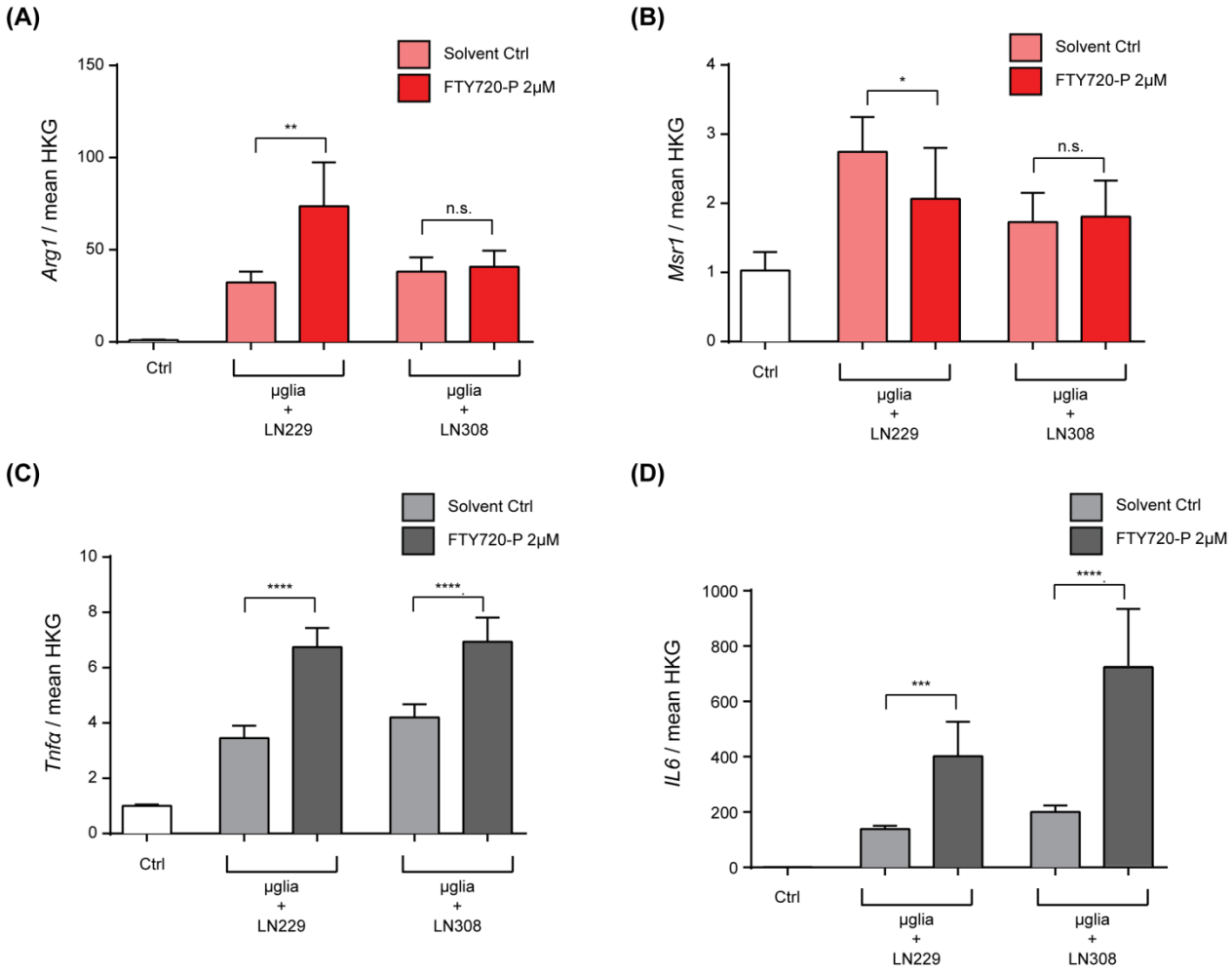

Figure 18: Inhibition of Sphingosine 1-phosphate receptors by FTY720 modulates gene expression profile of microglia by inducing a pro-inflammatory phenotype.

Quantitative RT-PCR analysis of M2 markers *Arg1* and *Msr1***(A, B)**, and M1 markers *Tnfα* and *IL6***(C, D)** in murine primary microglia (µglia) treated with conditioned media harvested from human glioma cells, LN229 and LN308; and treatment with FTY720 for 24 hrs. The mRNA expression of the target genes was normalized to the mean of two housekeeping genes (*B2m*, *Hprt*). Data are expressed as fold-change over primary microglial cells treated with solvent control (Ctrl) and are means ± sem of 3 independent experiments. Statistical analysis was performed using paired t-test. **** $p<0.0001$, *** $p<0.001$; ** $p<0.01$, * $p<0.05$, n.s.: not significant.

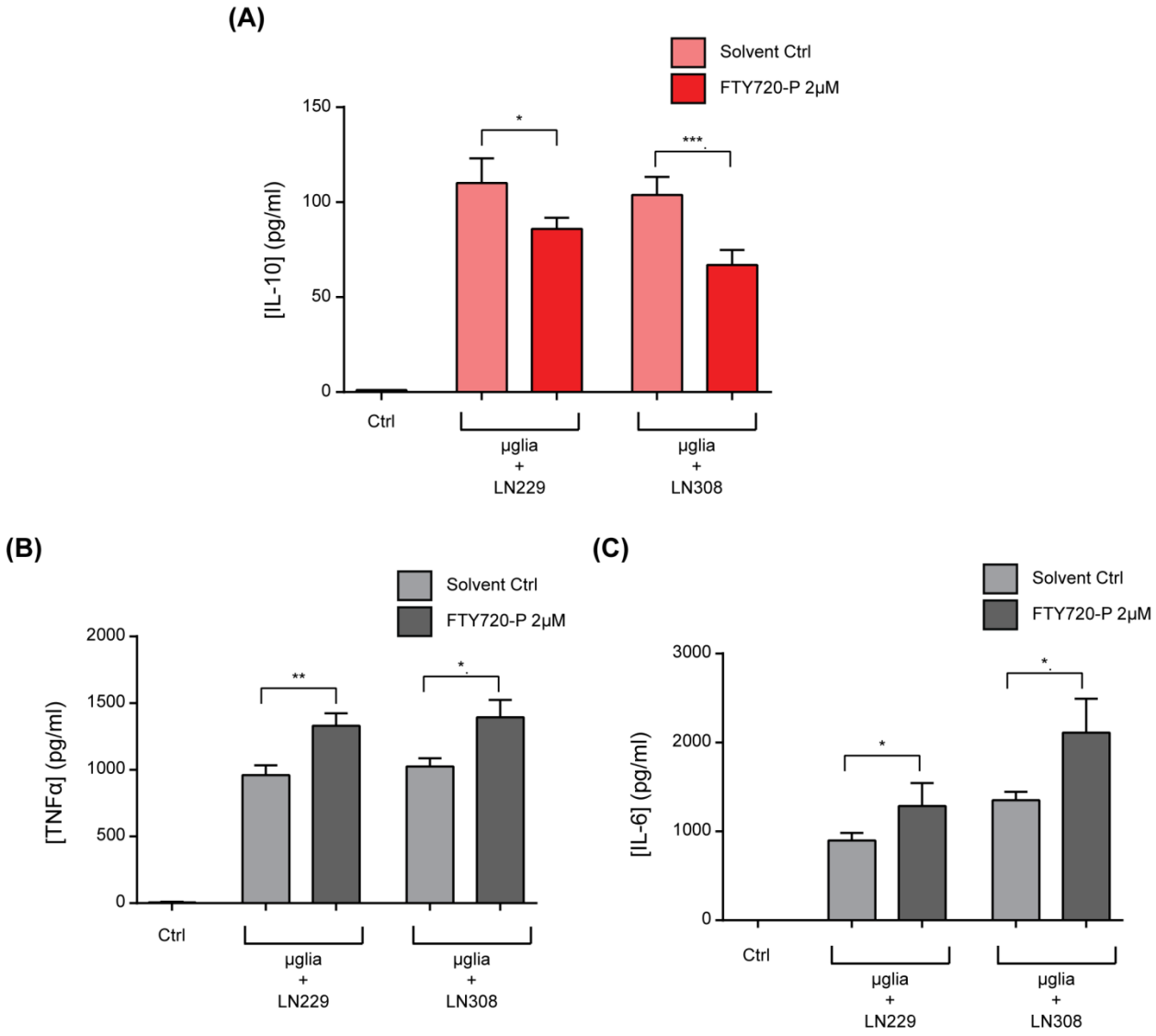

Figure 19: FTY720 treatment induces significant changes in the secretion of inflammatory factors in microglia

Enzyme-linked immunosorbent assay (ELISA) of M2 cytokine IL10 **(A)** and M1 cytokine TNFα **(B)** and IL-6 **(C)**in cell-free supernatant of murine primary microglia (µglia) treated with conditioned media harvested from human glioma cells, LN229 and LN308; and treatment with FTY720 for 24 hrs. Data are expressed as pg/ml as plotted against a standard curve for each cytokine and are means ± sem of 3 independent experiments. Statistical analysis was performed using paired t-test. **** $p<0.0001$, *** $p<0.001$; ** $p<0.01$, * $p<0.05$, n.s.: not significant.

To decipher the molecular pathways that mediate the induction of a pro-inflammatory phenotype in microglia/ macrophages upon FTY720 treatment, primary microglia were pre-treated with

FTY720 and treated with conditioned media harvested from LN229 human glioma cell line. Total cell extracts were isolated to analyze various key signaling pathways that mediated the M1 and M2 phenotype of microglia/ macrophages.

Immunoblot analysis of primary microglia treated with FTY720 and conditioned media from glioma cells, showed a remarkably decreased activation of phospho-Stat3 and phospho-Akt, indicating that blockade of the sphingosine 1-phosphate receptors by FTY720 deregulates the Stat3 pathway and Akt pathway, and play an important role in mitigation of the anti-inflammatory phenotype of microglia (**Figure 20**). FTY720 treatment also showed a decreased activation of phospho-TBK1 and phospho-IRF3, demonstrating that activation of the S1PR signaling resulted in downstream activation of the IRF3 pathway that plays an important role in regulating the anti-inflammatory polarization (**Figure 20**). On the contrary SKI-II treatment displayed an activation of the NF-κB pathway as indicated by degradation of IκBα, suggesting that inhibition of S1PR in microglia induces a pro-inflammatory polarization of microglia via activation of the NF-κB pathway (**Figure 20**). These results taken together illustrated that blockade of sphingosine 1-phosphate receptors by FTY720 modulates major signaling pathways that regulate M1-M2 phenotype, thereby inducing a pro-inflammatory phenotype of microglia/ macrophages.

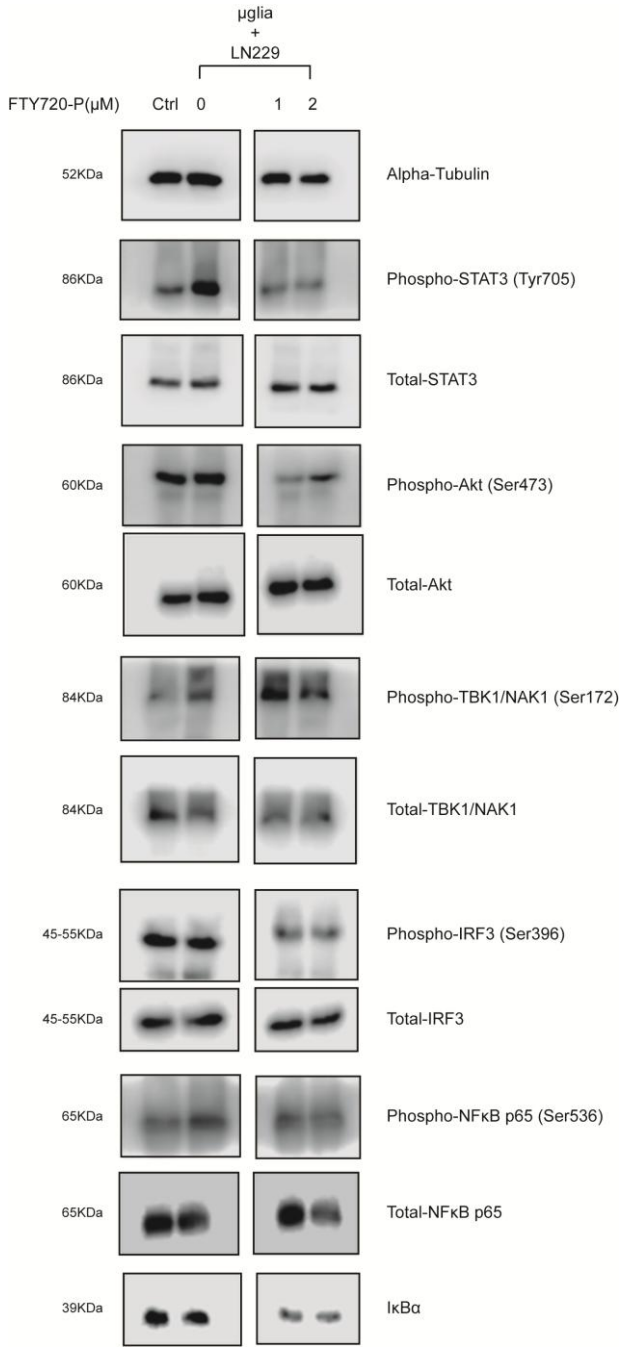

Figure 20: Antagonism of Sphingosine 1-Phosphate receptors by FTY720 in microglia modulates important signaling pathways that regulate M1-M2 polarization

Western blot analysis of primary microglia pre-treated with FTY720 for 24 hours and treated for 24 hours with conditioned media harvested from LN229 human glioma cell line, assessed with anti-phospho-STAT3 (Tyr705), anti-STAT3, anti-phospho-Akt (Ser473), anti-Akt, anti-phospho-TBK1/NAK1 (Ser172), anti-TBK1/NAK1, anti-phospho-IRF3 (Ser396), anti-IRF3, anti-phospho-NFκB-p65, anti-NFκB-p65 or anti-IκBα. Alpha-tubulin served as loading control.

3.9 S1P inhibits LPS mediated M1 phenotype of microglia/ macrophages

Following up on the previous findings that glioma derived S1P plays a key role in regulating the anti-inflammatory phenotype of microglia/ macrophages, it was plausible to investigate the potential mechanisms by which S1P maintains an anti-inflammatory phenotype in microglia/ macrophages. The canonical NF-κB pathway has primarily been considered a archetypical pro-inflammatory pathway signaling, majorly based on the role of NF-κB in the expression of important pro-inflammatory genes including cytokines, chemokines, and adhesion molecules, such as IL-6, IL-1 and TNFα[131]. NF-kappa B inhibitor alpha (IκBα), a key intermediate of the canonical NF-κB pathway activation gets phosphorylated, a pre-requisite for its proteosomal degradation[132]. This in turn releases the homo and hetero dimers of nuclear factor NF-κB that translocate into the nucleus, resulting in active target gene expression of M1 genes[132].

Direct treatment of RAW264.7 macrophages with S1P for 15 minutes – 1 hour, did not result in any significant changes in M1 phenotype as assessed by western blot analysis of IκBα (**Figure 21A**). Lipopolysaccharide (LPS), a component of the outer membrane of gram-negative bacteria, is a potent activator of NF-κB pathway [133]. RAW264.7 macrophages co-treated with LPS and S1P for 15 minutes – 1 hour, demonstrated that S1P prevented the LPS induced IκBα degradation, mainly between 45 minutes and 1 hour (**Figure 21B**), indicating that S1P was able to abrogate the LPS induced NF-κB signaling. S1P mediated decrease of NF-κB signaling was further verified by gene-expression changes of pro-inflammatory cytokines, where S1P treatment resulted in a considerable decreased mRNA expression of LPS induced M1 markers iNOS (**Figure 21C**), and TNFα (**Figure 21D**), when RAW264.7 macrophages were co-treated with LPS and S1P for 5 hours. Analysis of the production of nitric oxide, a pro-inflammatory metabolite, as measured by a modified Griess reagent assay also confirmed that co-treatment of RAW264.7 macrophages with LPS and S1P resulted in a decreased production of LPS induced nitric oxide levels (**Figure 21E**). These results were confirmed in primary microglia that showed that S1P was able to block LPS induced IκBα degradation in a concentration dependent manner, when co-treated with LPS and increasing concentrations of S1P for 1 hour (**Figure 21F**); and decreased mRNA expression of LPS induced M1 genes, TNFα (**Figure 21G**) and IL6 (**Figure 21H**) when co-treated with LPS and increasing concentrations of S1P for 5 hours. Collectively, these results indicated that S1P inhibited LPS mediated M1 phenotype of microglia/ macrophages.

To further elucidate the mechanism by which S1P inhibited LPS mediated NF-κB activation, primary microglia cells were co-treated with LPS and increasing concentrations of SEW2871, a potent and selective S1PR1 agonist for 1 hour[129]. This resulted in likewise blockade of LPS induced IκBα degradation in a concentration dependent manner (**Figure 22A**). Similarly, RAW264.7 macrophages co-treated with LPS and SEW2871 for 15 minutes – 1 hour, demonstrated that S1P prevented the LPS induced IκBα degradation, mainly between 45 minutes and 1 hour, illustrating that S1P potentially inhibited LPS induced NF-κB signaling via S1PR1 in microglia/ macrophages (**Figure 22B**) Inhibition of S1PR1 by selective antagonist W146 [129], counteracted the effect of S1P in blocking the LPS induced IκBα degradation, suggesting that S1P acted via S1PR1 in inhibiting the pro-inflammatory phenotype of microglia/ macrophages (**Figure 22C**). On the contrary, S1PR2 antagonist, JTE013 or S1PR1/ S1PR3 antagonist, VPC23019 [129], did not alter the effects of S1P modulation of NF-κB activation, suggesting that S1PR2 or S1PR3 did not play a role in mediating the inhibition of NF-κB activity upon S1P stimulation (**Figure 22C**). Furthermore, primary microglia treated with FTY720, acts as a potent antagonist of four S1P receptors (S1PR1, S1PR3, S1PR4 and S1PR5) resulted in a degradation of IκBα, indicating that FTY720 was able to induce NF-κB signaling in microglial cells (**Figure 22D**).

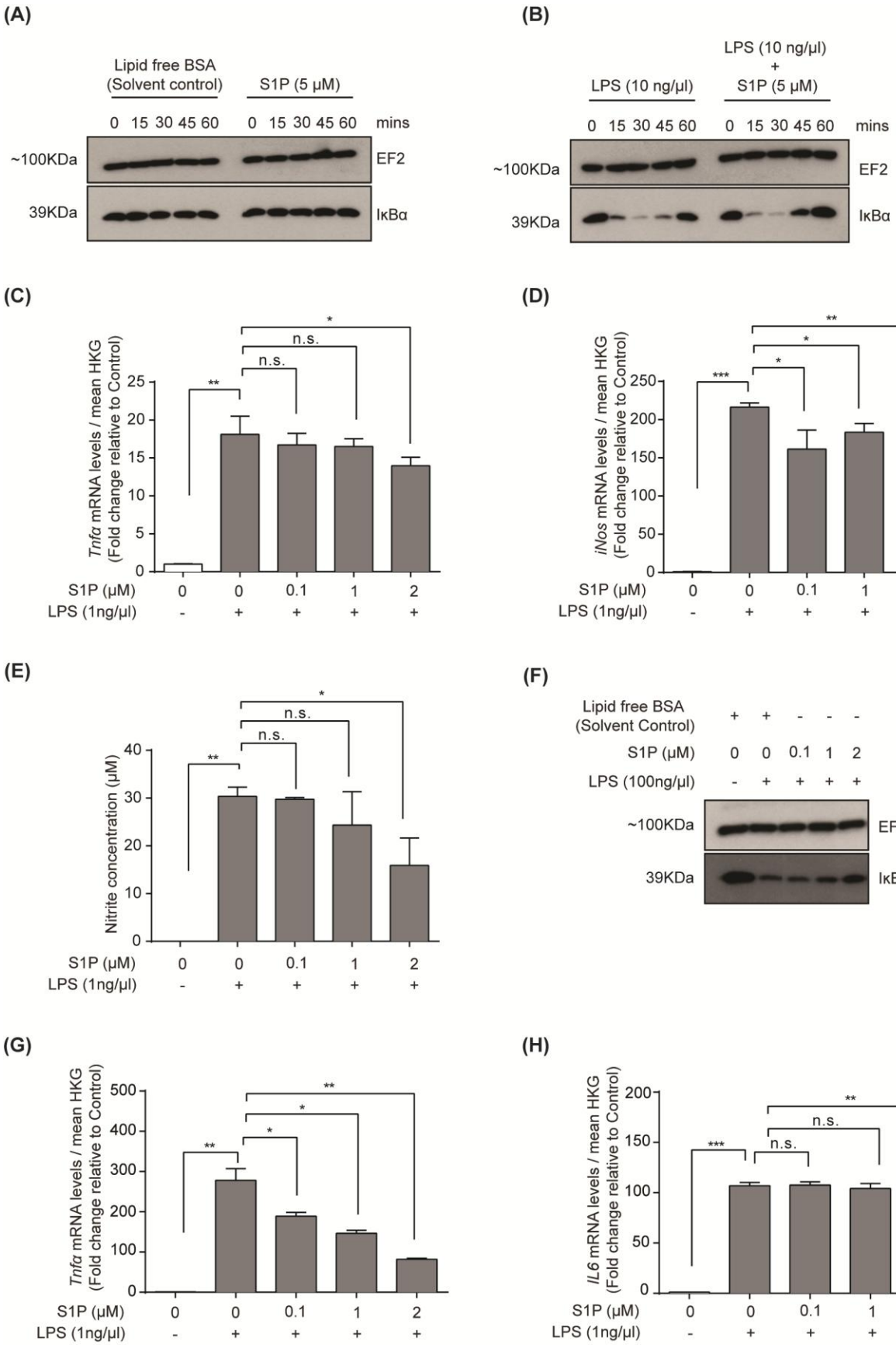
(A)
Lipid free BSA
(Solvent control)
S1P (5 μM)
0 15 30 45 60 0 15 30 45 60 mins
~100KDa
EF2
39KDa
IκBα
(B)
LPS (10 ng/μl)
LPS (10 ng/μl)
+
S1P (5 μM)
0 15 30 45 60 0 15 30 45 60 mins
~100KDa
EF2
39KDa
IκBα
(C)
Tnfa mRNA levels / mean HKG
(Fold change relative to Control)
n.s.
n.s.
S1P (μM) 0 0 0.1 1 2
LPS (1ng/μl) - + + + +
(D)
iNos mRNA levels / mean HKG
(Fold change relative to Control)
S1P (μM) 0 0 0.1 1 2
LPS (1ng/μl) - + + + +
(E)
Nitrite concentration (μM)
n.s.
n.s.
S1P (μM) 0 0 0.1 1 2
LPS (1ng/μl) - + + + +
(F)
Lipid free BSA
(Solvent Control) + + - - -
S1P (μM) 0 0 0.1 1 2
LPS (100ng/μl) - + + + +
~100KDa
EF2
39KDa
IκBα
(G)
Tnfa mRNA levels / mean HKG
(Fold change relative to Control)
S1P (μM) 0 0 0.1 1 2
LPS (1ng/μl) - + + + +
(H)
IL6 mRNA levels / mean HKG
(Fold change relative to Control)
n.s.
n.s.
S1P (μM) 0 0 0.1 1 2
LPS (1ng/μl) - + + + +

Figure 21: S1P inhibits LPS mediated M1 phenotype of microglia/ macrophage

(A) Western blot analysis of IκBα amounts in RAW264.7 macrophages treated with S1P (5 μM) for 15 min – 1 hour. EF2 served as loading control. **(B)** Western blot analysis of IκBα amounts in RAW264.7 macrophages co-treated with LPS (100 ng/μl) and S1P (5 μM) for 15 minutes – 1 hour. EF2 served as loading control. Quantitative RT-PCR analysis of M1 markers *Tnfα***(C)** and *iNos***(D)** in RAW264.7 macrophages co-treated with LPS (1 ng/μl) and increasing concentration of S1P (0 – 2 μM) for 5 hours. **(E)** Measurement of nitrite levels (NO_2^-) assessed by Griess reagent assay in RAW264.7 macrophages co-treated with LPS (1 ng/μl) and increasing concentration of S1P (0 – 2 μM) for 24 hrs. **(F)** Western blot analysis of IκBα amounts in murine primary microglia treated with LPS and increasing concentration of S1P (0 – 2 μM) for 1 hour. EF2 served as loading control. Quantitative RT-PCR analysis of M1 markers *Tnfα***(F)** and *iNos***(G)** in primary microglia co-treated with LPS(1 ng/μl) and increasing concentration of S1P (0 – 2 μM) for 5 hours. qRT-PCR data are expressed as fold standard over cells treated with solvent control and are means ± sem of 3 independent experiments. Statistical analysis was performed using paired t-test. **** $p<0.0001$, *** $p<0.001$; ** $p<0.01$, * $p<0.05$, n.s.: not significant.

Recent studies have indicated that TLR4 signaling balances the pro-inflammatory and anti-inflammatory signaling via activity of p110δ isoform of the kinase PI(3)K[74,76]. These observations suggested that p110δ limits the TLR4 mediated induction of pro-inflammatory cytokines by eliminating the plasma membrane TIRAP-anchoring lipid phosphotidylinositol-(4,5)-biphosphate ($PtdIns(4,5)P_2$), leading to the dissociation and degradation of TIRAP, and thereby mediating the endocytosis of CD14-TLR4 eventually leading to production of IFN-β and anti-inflammatory cytokine, IL-10[74,76]. Thereby, activation of p110δ shifts the balance towards a pro-inflammatory signaling. These effects are probably also mediated in unison with phospholipase C- γ (PLC-γ)[74,76]. To investigate if p110δ or PLCγ played a role in mediating the S1P modulation of TLR4 activity, RAW264.7 macrophages were pre-treated with p110δ blocker, IC87114 or PLCγ blocker, U73122 and co-treated with LPS (10 ng/ul) and S1P (5μM) for 15min – 1hr, and analyzed for expression of IκBα. Although S1P prevented the LPS induced IκBα degradation, as seen in pre-treatment with solvent control, inhibition of both p110δ and PLCγ did not abrogate these effects of S1P inhibition of NF-κB activity (**Figure 22E-F**). This indicated that S1P inhibition of the TLR4 pathway did not act via p110δ or PLCγ in microglia/ macrophages. One possible mechanism of S1P inhibition of NFκB activity could be mediated via activation of the TBK1/ IRF3 signaling, although the detailed mechanism needs further investigation.

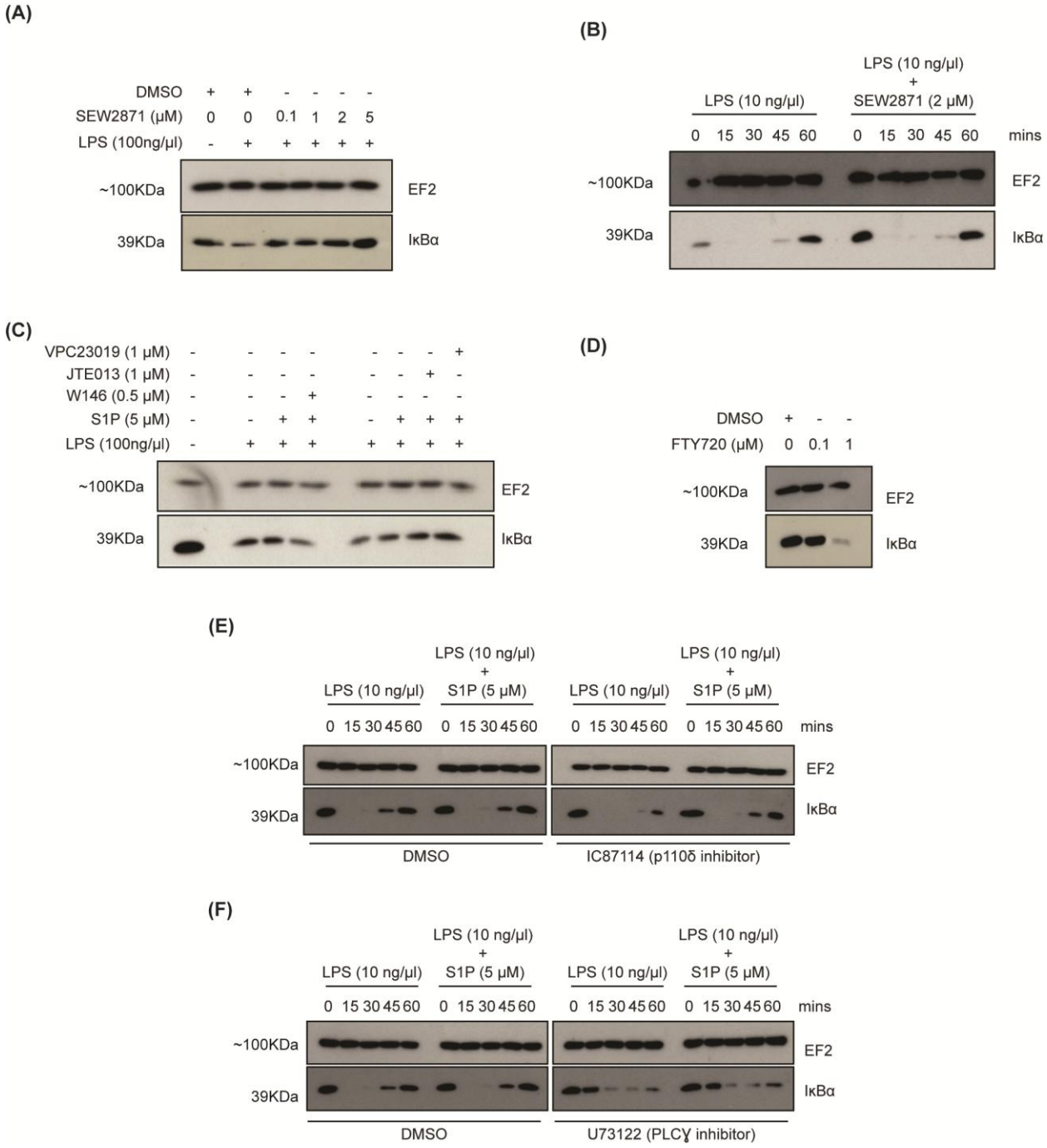

Figure 22: S1P modulates NF-κB activity in microglia/ macrophages via S1PR1

(A) Western blot analysis of IκBα in murine primary microglia co-treated with LPS (10 ng/μl) and increasing concentration of S1PR1 selective agonist SEW2871 for 1hr. EF2 served as loading control. **(B)** Western blot analysis of in IκBα in RAW264.7 macrophages co-treated with LPS (10 ng/μl) and SEW2871 (2 μM) for 15 min to 1 hr. EF2 served as loading control. **(C)** Western blot analysis of IκBα in

RAW264.7 macrophages co-treated with LPS (10 ng/µl) and S1P (5 µM) for 1 hr, where cells were pre-treated with S1PR1 antagonist, W146 (0.5 µM), S1PR2 antagonist, JTE013 (1 µM), S1PR1 and S1PR3 antagonist, VPC23019 (1 µM) or solvent control (DMSO) for 1hr. EF2 served as loading control. **(D)** Western blot analysis of IκBα in RAW264.7 macrophages treated with S1PR1,3,4,5 antagonist, FTY720 for 24 hrs. EF2 served as loading control. **(E)** Western blot analysis of IκBα amounts in RAW264.7 macrophages co-treated with LPS (10 ng/µl) and S1P (5 µM) for 1 hr, where cells were pre-incubated with p110δ blocker, IC87114 for 1 hr. EF2 served as loading control. **(F)** Western blot analysis of IκBα in RAW264.7 macrophages co-treated with LPS (10 ng/µl) and S1P (5 µM) for 1 hr, where cells were pre-incubated with PLCγ blocker, U73122 for 1 hr. EF2 served as loading control.

4. Discussion

4.1 High SPHK1 expression influences gene expression class in GBM and correlates to increased microglial gene signature

Glioblastoma multiforme (GBM) is the most common aggressive form of brain tumors occurring in adults, with a 1-year survival less than 29% and a 5-year survival less than 3%. Among several genes that are overexpressed or mutated, sphingosine kinase 1 (SPHK1) expression is upregulated in variety of cancers, including GBM, and has been associated with a poor survival for patients with GBM[109,110,118]. SPHK1 regulates the production of sphingosine 1-phosphate (S1P) by catalyzing the phoshorylation of sphingosine to S1P. S1P is a bioactive sphingolipid metabolite that has been associated with tumor pathogenesis and cancer cell fate, where S1P influences pro-survival, anti-apoptotic, and pro-angiogenic functions in tumors[82,85,115]. As shown, a higher SPHK1 expression in GBM patients resulted in an increased progression-free survival and an overall-free survival, as represented by Kaplan Meier curves in patients with GBM divided into high SPHK1 and low SPHK1. Although the progression-free survival of SPHK1 contributed to better survival outcome (p=4.9e-0.3) as compared to overall free survival (p=0.026), this could be attributed to subsequent therapies upon disease progression, tumor pathways affected by new drugs and the nature of drug and tumor interactions[134,135].

Abuhusain et al. showed that among other sphingolipid-related genes, S1P phosphatase (SGPP2) that reverse catalyzes the dephosphorylation of S1P to sphingosine was significantly downregulated in GBM contributing to decreased ceramide production and shifting the balance towards a higher S1P production in GBM; unchanged levels of CERS1 that catalyses the synthesis of ceramide C18; and a significant upregulation of Acid ceramidase (ASAH1) that converts ceramide to sphingosine. These results were further supported by quantitative sphingolipid profiling displayed by increased S1P levels and decreased total ceramide levels with increased glioma grade, and a decline of hexosylceramide (HexCer) and sulfatide levels[118]. Reduced supply of dihydroceramide and hexosylceramide, facilitated by galactosylceramidases synthetase, an ER resident protein, suppresses endoplasmic reticulum stress by interfering with the structure and function of ER[136,137]. Taken together, human gliomas displayed a metabolic shift towards S1P with increasing malignancy in expense of ceramide, indicating that the S1P-ceramide rheostat play an important role in determining cell fate[118].

Gene expression profiling of GBM identified four distinct genetic subtypes, namely Proneural, Neural, Classical and Mesenchymal based on defined subtype metagene score and characterized by aberrations in genes including PDGFRA/IDH1, EGFR, and NF1[5,138]. Analysis of data in subtypes of GBM revealed that SPHK1 was significantly higher in mesenchymal group, followed by proneural and almost an equal distribution in classical and neural subgroup. The mesenchymal subgroup is associated with highly aggressive and invasive tumors that show activation of gene expression profiles representative of cell proliferation and angiogenesis[5,138], implicating the importance of SPHK1 in this subtype. Another study showed the link between epithelial-mesenchymal transition (EMT) process and mesenchymal subtype as displayed by a negative correlation between CD133 signatures that is mostly presented by the mesenchymal subtype and EMT signatures[139]. SPHK1 has been implicated in role of induction of EMT and metastasis in non-small-cell lung cancer cells by promoting the invasive and metastatic capabilities of these cells and in hepatoma cells by stimulating autophagy via lysosomal degradation of the epithelial marker and suppressor of EMT, CDH1 in HepG2 cells[140,141].

Several studies over the past decade have witnessed the importance of brain tumor micro-environment as an important modulator of tumor progression that influences the course of tumor pathology and the outcome of malignancy. Among the different types of non-tumorgenic cells that infiltrate the tumor, mainly constituted by neurons and glial cells (like microglia, oligodendrocytes, and astrocytes), tumor associated microglia/ macrophages (TAMs) represent an important mediator of tumor growth and invasion[13,16]. A gene set enrichment analysis (GSEA) using Affymetrix gene expression data of GBM (Affymetrix 540 MASS 5.0-u133 array) and gene sets as reported in Butovsky et al., 2013[122] showed a preferentially positive association of SPHK1 to microglial gene signature ($p<0.0001$); while showing a lesser significant association to astrocyte gene set ($p=0.0086$) and oligodendrocyte gene set ($p=0.0029$) and negative correlation to neuronal gene set ($p=0.99$). High SPHK1 is positively correlated to expression of specific microglial genes such as solute carrier organic anion transporter family member 2B1 (*Slco2b1*), Colony stimulating factor 1 receptor (*Csf1r*), Gi/o protein-coupled receptor 34 of the nucleotide receptor P2Y12 -like group (*Gpr34*) and Transmembrane protein 119 (*Tmem119*). Conversely, as shown before, SPHK1 was strongly upregulated in the mesenchymal subtype of GBM, where mesenchymal subtype has been implicated with high necrosis and higher microglia/ macrophage infiltration[11,12]. These observations taken together collectively suggest the

significance of SPHK1/S1P signaling in regulating the microglia-glioma crosstalk and influencing both transcriptional regulators and gene expression class in GBM.

4.2 Modulation of SPHK1 activity in gliomas influences the polarization of microglia

Glioma associated microglia/ macrophages (GAMs) represent the major tumor infiltrating cells that are attracted towards tumor core and necrotic areas, which in response to interaction with tumor cells secrete microglia release factors and matrix secreting enzymes in the tumor microenvironment leading to accelerated glioma proliferation and invasion[71]. Several studies reported that GAMs express an "M2-like polarization" phenotype, characterized by increased production of anti-inflammatory factors (such as TGFβ1, ARG1, and IL-10), and factors influencing tissue remodeling and angiogenesis (such as VEGF, MMP2, MMP9 and MT1-MMP)[63]. As previous data suggested that SPHK1/S1P signaling in GBM could play a positive role in modulating the microglial signature, the role of SPHK1 by modulating the expression and activity of SPHK1 in gliomas was further investigated. Indeed, knockdown of SPHK1 in glioma significantly decreased mRNA expression of prominent M2 markers Arg1 and Msr1, and subsequently leading to significantly increased mRNA expression of M1 marker, IL-6 in microglia cells co-cultured with glioma cells. Although IL-6 plays a controversial role in influencing the balance between M1 and M2 macrophages, where reports also show IL-6 promoting alternative macrophage activation[142], SPHK1 knockdown led to NF-κB mediated activation as shown by activation of phospho- NF-κB p65 and degradation of IκBα , resulting in the production of pro-inflammatory genes, such as IL-6, TNFα, thereby inducing the M1 phenotype of microglia/ macrophages[143,144]. M1 microglia/macrophages are potent tumor-suppressive cells that are able to overcome the M2-associated tumor promoting functions through the expression and secretion of pro-inflammatory cytokines and chemokines such as IL-6, IL-12, CXCL9 and CXCL10, and subsequent recruitment of Th1 cells. Consequently, Th1 cells produce IFNγ, thereby promoting the classical M1 polarization of microglia/macrophages[46,47].

Conversely, overexpression of SPHK1 in glioma also significantly increased M2 marker expression of Arg1 and Msr1 in microglial cells co-cultured with glioma cells. However, overexpression of SPHK1 did not lead to much significant change in M1 marker expression of TNF and IL6, these results could be attributed to the saturation of M2-associated tumor

promoting functions that further did not influence the M1-associated tumor fighting signature in microglia. Similarly, inhibition of SPHK1 enzymatic activity by SKI-II in glioma cells correlates with a substantial reduction of M2 markers such as Arg1, Msr1 and IL-10, and conversely, a considerable increase of M1 markers such as TNFα and IL-6. These results are in line with previous report that demonstrated that the downregulation of SPHK1 in melanoma cells reduced tumor growth and modified the tumor infiltration and phenotype of macrophages[145]. Suppression of SPHK1 activity resulted in decreased populations of M2-associated MHC-II^{low}CD206^{high} TAMs, and an increased iNOS^{+}F4/80^{+} M1 macrophages, in addition to increased expression of Th1 cytokines (IL-12, TNFα, IFNγ) and chemokines (CCL5, CXCL9, CXCL10). These consequently resulted in a significant increase in NK cells and CD4^{+} and CD8^{+} tumor infiltrating T-lymphocytes (Thy1^{+}). Interestingly, macrophage depletion by clodronate-loaded liposomes abrogated the reduced tumor growth suggesting that macrophages influenced the SPHK1 mediated tumor progression. Conversely, Sphk2 mediated S1P production in apoptotic MCF-7 breast cancer cells contributed to alternative activation of macrophages and suppressed NF-κB activity[146]. Sphingosine kinase 2 deficient MCF-7 tumors in nude mice impaired M2 type macrophage polarization as evidently displayed by decreased CD206 and increased MHCII expression in macrophages, and increased nitric oxide production, indicative of M1-like activation[147].

Furthermore, the sphingosine kinase inhibitor SKI-II significantly suppressed the viability and migration of glioma cell line LN18[148]. These results are in line with other studies showing that targeting SPHK1 resulted in impairment of GBM growth and induction of apoptosis *in-vivo* via reduction of intracellular S1P levels and suppression of Akt signaling. These effects were mediated primarily as a result of reduced "inside-out signaling" of S1P, and not as a direct effect of suppression of SPHK1 enzymatic activity, resulting in decreased phosphorylation of Akt, and reduced tumor growth[149]. Neutralization of extracellular S1P using a monoclonal antibody against S1P (Sphingomab) in an *in-vivo* allograft tumor model using the B16-F10 cells markedly suppressed tumor growth, metastasis, and angiogenesis concurrently with reduced vessel formation and function. The anti-S1P antibody also suppressed the production of pro-angiogenic cytokines by inhibiting the function of VEGF and bFGF*in vivo*[150]. Similarly, therapeutic targeting extracellular S1P in prostate cancer blocked HIF-1α accumulation resulting in decreased intratumoral hypoxia and vascular normalization. The extracellular effects of S1P in

regulating HIF-1α levels were mediated by Spinster 2 (Spsn2) that is thought to be the principal transporter of S1P[114]. These results suggested that modulating SPHK1 expression in gliomas controls the balance between intracellular S1P and export of S1P, that signal through S1P receptors in paracrine and/or autocrine manner, thereby influencing and contributing to the tumor microenvironment[105]. In addition to pro-survival, anti-apoptotic and pro-angiogenic functions of S1P, S1P potentially can modulate the phenotype of tumor associated microglia/ macrophages.

The diverse functional states of microglia/macrophages are governed by a complex interplay between microenvironment signals and a differential activation of key molecular pathways that determines their identity and M1/M2 polarization. Inhibition of SPHK1 in gliomas resulted in decreased phosphorylation of anti-inflammatory signaling pathways such as STAT3, AKT, and TBK1/IRF3, with subsequent activation of pro-inflammatory NF-κB pathway through the increased phosphorylation of phosphor-p65 and degradation of IκBα in microglia/ macrophages. Decreased activity of the transcription factor STAT3 can be attributed to reduced IL-10 levels as quantified by ELISA, where binding of IL-10 to IL-10 receptor results in autophosphorylation of the receptor, consequently leading to the activation of STAT3 and inhibition of pro-inflammatory cytokine expression[151]. The IL-10/STAT3 mediated anti-inflammatory responses are cell type specific, where in macrophages IL-10/STAT3 signaling contributes to the immunosuppressive phenotype by indirect and selective inhibition of NF-κB target genes, with no significant effects in CpG frequency and expression levels of IRF members[152,153]. Conversely, in dendritic cells and mast cells, IL-10/STAT3 stimulates chromatin remodeling, with transcriptional inhibition of Irf3 and Irf7 and unaffected NF-κB transcripts[153]. IL-10 knockout represents the archetypical model for Crohn's disease displaying extensive mucosal hyperplasia, inflammatory responses, and aberrant expression of MHCII on epithelia, where most animals are growth retarded and anemic[154]. Similarly, macrophage and neutrophil specific knockdown of STAT3 developed chronic enterocolitis that are highly susceptible to LPS-induced endotoxin shock, impaired Th1 cell development and imbalanced IL-10 functions[155]. Paradoxically, both the IL-6 and IL-10 activate STAT3, although the temporal pattern and duration of STAT3 activation defines the specific cytokine response and thereby determining the end fate of macrophages towards M1or M2 phenotype[156].

AKT signaling is also associated to M2 macrophage polarization, where IL-4 signaling activates Jak1 and Jak3 through ligation to the IL-4R resulting in phosphorylation of STAT6 and recruitment of the adaptor protein IRS2. IRS2 recruits PI3K resulting in phosphorylation of PIP2 at the plasma membrane to PIP3, consequently leading to the recruitment of Akt and mTORC2 where in-turn mTORC2 phosphorylates and activate Akt[157]. Macrophage specific ablation of Akt1 resulted in hyper-sensitization to LPS exhibiting a shift towards a pro-inflammatory phenotype. Akt1 depletion also exacerbated the dextran sulfate sodium (DSS)-induced inflammatory bowel disease in mice[158]. Similarly, adenovirus mediated transfer of IRF3 in microglia suppressed expression of pro-inflammatory genes such as IL-1α, IL-1β, TNFα, IL-6, IL-8 and CXCL1 and enhanced anti-inflammatory genes (IL-1 receptor antagonist, IL-10 and IFNβ), leading to activation of PI3K/Akt pathway, suggesting that IRF3 enables M2-like macrophages[159]. Likewise, GM-CSF stimulated M1 polarization of macrophages displayed a decreased activation of the IRF3 pathway and increased activation of MyD88 dependent NF-κB pathway, while M-CSF primed macrophages that display an M2 like phenotype demonstrated a deactivated NF-κB pathway and an enhanced TRIF-mediated IRF3 induction[160,161]. Inhibition of p110δ activity, an important regulator of the balance between pro- and anti-inflammatory TLR4 signaling, diminished IRF3 activation, that are optimalfor IFN-β production and late activation of NF-κB and p38[76]. Taken together, molecular pathways such as STAT3, AKT and IRF3 play a crucial role in regulating the immunosuppressive phenotype of microglia/ macrophages.

Collectively, these results emphasize the importance of interactions between S1P-producing tumor cells with the host microenvironment that play a critical role in polarization of microglia/macrophages, and thereby driving tumor progression, and thus targeting the S1P/SPHK1 axis in tumors could be a excellent therapeutic target for treatment of GBM, presumptively in combination with other targeted therapies such as chemotherapy and radiotherapy.

4.3 FTY720 treatment stimulates a pro-inflammatory signature of microglia/ macrophages

FTY-720 (Fingolimod, Gilenya™) was developed as a first-line orally bioavailable drug for treating relapsing multiple sclerosis (MS), highlighting the significance of sphingosine-1-phosphate (S1P) signaling as a therapeutically targetable pathway in autoimmune neuroinflammation[162]. S1P signals primarily through ubiquitously expressed five cognate G

protein coupled receptors that regulates important downstream cellular processes such as proliferation, migration[82]. S1PR1 and S1PR2 have been shown to be expressed by different populations or genetic origins of macrophages and monocytes[163]. Inhibition of the sphingosine 1-phosphate receptors by FTY720 triggered a pro-inflammatory phenotype of tumor associated microglia/ macrophages, as displayed by increased production of TNFα and IL-6 and an increased production of IL-10, while also modulates important signaling pathways that regulate M1-M2 phenotype, such as deactivation of STAT3, AKT, and TBK1/IRF3 and induction of NF-κB pathway. S1P –S1PR1 axis plays an important role in lymphocyte egress from secondary lymphoid organ into the systemic circulation and chemotaxis[164]. FTY720 is phosphorylated by Sphk2, which subsequently binds to S1PR1 on T cells to induce its internalization, polyubiquitination and proteosomal degradation and, thereby preventing egress of T cells from lymph nodes. Another report showed that FTY720 also induces the proteosomal degradation of Sphk1[165,166]. STAT3 activity enhanced S1pr1 expression, where S1pr1 is a direct transcriptional activator of Stat3 and induction of S1pr1 expression reciprocally activates Stat3, while elevated S1PR1 expression in tumor cells promoted S1pr1 expression and Stat3 activation in tumor-infiltrating myeloid cells[167].

Targeted depletion of S1PR1 in tumor-associated macrophage population, defined by $Cd11b^{+}Cd206^{+}$ cells resulted in decreased pulmonary metastasis and tumor lymphangiogenesis in nonrelated methylcholanthrene-induced fibrasarcoma model. Genetic ablation of S1PR1 also reduced the expression of the inflammasome component Nlrp3 and IL-1β production[168]. Apparently, S1PR2 deficient mice showed reduced response to LPS and S1P[163], while pharmacological blockade of S1PR2 led to inhibition of macrophage pro-inflammatory cytokines in ApoE-deficient mice model of atherosclerosis[169], indicating that S1PR2 could also play an important role in modulating the anti-inflammatory phenotype of microglia/ macrophages. Liang et al[168] showed that S1PR1 and Sphk1 formed a missing link between chronic intestinal inflammation and development of colitis-associated cancer. They showed that mice deficient of Sphk2 enhanced colitis-associated tumorigensis and intestinal inflammation. These effects were attributed to Sphk2 mediated HDAC1/2 inhibition, increased expression of c-Jun, that led to a marked increase in Sphk1 expression. Inside out signaling of S1P and subsequent activation of S1PR1 and Sphk1 led to constitutive STAT3 activation[168]. FTY720 suppressed colitis and colorectal tumorigenesis associated with chronic colitis in Sphk2 deficient mice where the

Sphk1/S1P/S1PR1 feed-forward-loop is inhibited leading to abrogated STAT3 activation. Interestingly, macrophages and dendritic cells contributed to the production of tumor promoting cytokines, and inhibition of the Sphk1/S1P/S1PR1 axis by FTY720 failed to recruit macrophages in Sphk2 deficient mice contributing to suppressed colitis[168]. FTY720 synergistically reduced viability, induced apoptotic signaling in brain tumor stem cells (BTSCs), while also suppressed the growth of tumors *in-vivo* and enhanced the effects of temozolomide (TMZ) leading to enhanced survival[168]. These results first time showed that FTY720 shifts the balance of microglia towards a pro-inflammatory activation, and could represent a potential therapy approach for GBM, presumably in combination with other targeted therapies.

4.4 Sphingosine 1-phosphate induces an anti-inflammatory phenotype in microglia/ macrophages via S1PR1

Microglia/ macrophages respond to external stimuli and undergo important phenotypic and molecular changes that determine its activation state. Similarly, as previously shown in the present thesis, modulation of the SPHK1/S1P/S1PR1 axis are reciprocated by tumor associated microglia/ macrophages by undergoing significant phenotypic changes. Therefore, understanding the molecular mechanisms that govern the S1P mediated polarization is essential. Direct treatment of S1P on microglia/ macrophages did not induce any polarization of microglia/ macrophages. Thereafter, I questioned if S1P affected pre-polarized cells. Among myriad of inflammatory pathways that regulate the phenotype of microglia/ macrophages, LPS-induced TLR4 signaling are key mediators of the pro-inflammatory phenotype. The canonical NF-κB pathway has primarily been considered central players in pro-inflammatory pathway signaling and response to pathogens, predominantly as a consequence of expression of prominent pro-inflammatory genes including cytokines, chemokines, and adhesion molecules, such as IL-6, IL-1 and TNFα[131]. As contemplated, S1P inhibited LPS mediated M1 phenotype of microglia/ macrophage as evident from reduced IκBα degradation, decreased mRNA expression of LPS induced M1 genes, TNFα and IL6, and reduced nitric oxide production. Although these results are shown for the first time in microglia, these results confirmed previous findings that S1P significantly reduced LPS-mediated expression of pro-inflammatory cytokines, indicating that S1P promoted the anti-inflammatory phenotype of macrophages. Treatment of B6 peritoneal macrophages with S1P suppressed LPS-induced TNFα, MCP-1, IL-12, cyclooxygenase-2, and macrophage inflammatory protein-2 mRNA expression[170]. These effects of S1P on LPS

mediated polarization was mediated via S1PR1 as evident from SEW2871 (S1PR1 agonist) induced pro-inflammatory signaling and pharmacological inhibition of S1PR1 by W146 that abrogated the S1P mediated suppression of M1 polarization.

Similarly, another study showed that apart from inhibition of M1 polarization, S1P also induced the M2 phenotype in primary murine macrophages, shown by mRNA expression of prominent M2 markers, such as Arg1, Ym-1, IL-10 and TGF-β[171]. The induction of M2 phenotype was mediated via the IL-4 dependent phosphorylation of STAT6, increased expression of suppressor of cytokine signaling 1 (SOCS1) and suppression of SOCS3[171]. Knockdown of SOCS3 in macrophages enhanced markers associated with M2 macrophages, such as mannose receptor, TGM2, and SOCS1, while diminishing the expression of pro-inflammatory genes, such as TNFα, IL-6 and HLA-DR[172]. Monocyte/ macrophage specific SOCS3 deficient mice exhibited severe and persistent contact hypersensitivity, as displayed by enhanced ear thickness and severe inflammation in the skin. IFN-γ pretreatment attenuated M2 macrophage mediated contact hypersensitivity in a SOCS3 dependent manner, while IFN-γ-SOCS3 pathway suppressed IL-4 induced MMP-12 expression by inhibiting STAT6 activity[173].

TLR4 signaling maintains a critical balance of pro- and anti-inflammatory signaling through activation and regulation of the p110δ subunit of the kinase PI(3)K and PLCγ. A shift towards the MyD88 independent NF-κB activation results in TLR4 internalization, leading to IRF3 activation and subsequent IFN-γ and anti-inflammatory IL-10 production[174]. Human gingival epithelial cells treated with LPS and S1P resulted in increased IFN-β levels, induction of CXCL-10 and activation of IRF3[175]. Although previously shown in the present thesis that modulation of the SPHK1/S1P/S1PR1 axis affected IRF3 signaling, inhibition of p110δ and PLCγ using small molecule inhibitors did not abrogate these effects of S1P inhibition of NF-κB activity in macrophages. The detailed mechanism of suppression of LPS-induced M1 phenotype by S1P requires further investigation.

4.5 Future Outlooks

The previous few years witnessed various reports targeting tumor microenvironment, as more studies unravel the detailed mechanisms underlying the glioma-microglia interactions. While *in vitro* co-culture studies provided an insight into the role of SPHK1/S1P/S1PR1 axis in regulating microglia-glioma crosstalk, these results need further validation *in-vivo*. Furthermore, microglial

polarization state represents a complex genetic signature, therefore performing gene expression and proteome profiling can further decipher the complex molecular mechanisms governing the different activation states of microglia. A detailed understanding of the mechanisms by which S1P regulates the M1-M2 polarization would be of important interest. Thus, this study provides a strong rationale for targeting the S1P/SPHK1 axis in tumors that could be an effective targeted therapy for treatment of GBM, potentially in combination with other targeted therapies such as chemotherapy and radiotherapy.

5. Abbreviations

Arg1	Arginase 1
ATP	Adenosine triphosphate
B2M	Beta-2 microglobulin
BBB	Blood brain barrier
BSA	Bovine serum albumin
CCL	chemokines C-C motif ligand
CCR	chemokines C-C motif receptor
CD	cluster of differentiation
CNS	Central nervous system
CSF1R	Colony-stimulating factor 1 receptor
Ctrl	Control
CX3CR1	Chemokine C-X3-C motif ligand 1
DKFZ	German Cancer Research Center
DMSO	Dimethylsulfoxid
DNA	Deoxyribonucleic acid
ECM	Extracelullar matrix
EDTA	Ethylenediaminetetraacetic acid
EGFR	Epithelial growth factor receptor
ELISA	Enzyme linked immunosorbent assay

FACS	Florescent activated cell sorting
FCS	Fetal calf serum
FSC	Forward scatter
GAPDH	Glyceraldehyde-3-phoshpate dehydrogenase
GBM	Glioblastoma multiforme
GPCR	G-protein coupled receptor
GPR34 -	G-protein coupled receptor 34
GSEA	Gene set enrichment analysis
HPRT	Hypoxanthine guanine phosphoribosyl transferase
IDH1	Isocitrate dehydrogenase 1
IFNγ	Interferon gamma
IL-10	Interleukin 10
IL-6	Interleukin 6
IRF3	Interferon regulating factor 3
IκBα	NF-kappa-B inhibitor alpha
LPS	Lipopolysaccharide
MAPK	Mitogen-activated protein kinase
MMP	Matrix metalloproteinase
Msr1	Macrophage scavenger receptor 1
NF1	Neurofibromatosis type 1
NF-κB	Nuclear factor kappa-light chain enchancer of activated B-cells

PBS	Phosphate buffered saline
PDGFRA	Platelet derived growth factor
PFA	Paraformaldehyde
PI3K	Phosphatidylinositol 3-kinase
PPIA	Peptidylprolyl isomerase A
PTEN	Phosphate and tensin homolog
qRT-PCR	Quantitative reverse transcriptase polymerase chain reaction
RNA	Ribonucleic acid
S1P	Sphingosine 1-phosphate
SLCO2B1	Solute-carrier organic anion transporter family member 2B1
SPHK1	Sphingosine kinase 1
SSC	Side scatter
STAT	Signal transducer and activator of transcription
TAMs	Tumor associated microglia / macrophages
TANK	TRAF family member associated NFκB activator
TBK1	TANK-binding kinase 1
TGF-β	Transforming growth factor beta
TLR	Toll like receptor
TME	Tumor microenvironment
TMEM119	Transmembrane protein 119
TNFα	Tumor necrosis factor alpha

TRAF	TNF receptor associated factor
WT	Wildtype

6. References

1. Ostrom, Q. T. *et al.* CBTRUS Statistical Report: Primary Brain and Central Nervous System Tumors Diagnosed in the United States in 2007-2011. *Neuro. Oncol.***16,** iv1-iv63 (2014).

2. Louis, D. N. *et al.* The 2007 WHO classification of tumours of the central nervous system. *Acta Neuropathol.***114,** 97–109 (2007).

3. Wen, P. Y. & Kesari, S. Malignant gliomas in adults. *N. Engl. J. Med.***359,** 492–507 (2008).

4. Holland, E. C. Glioblastoma multiforme: The terminator. *Proc. Natl. Acad. Sci.***97,** 6242–6244 (2000).

5. Phillips, H. S. *et al.* Molecular subclasses of high-grade glioma predict prognosis, delineate a pattern of disease progression, and resemble stages in neurogenesis. *Cancer Cell***9,** 157–173 (2006).

6. Sturm, D. *et al.* Hotspot Mutations in H3F3A and IDH1 Define Distinct Epigenetic and Biological Subgroups of Glioblastoma. *Cancer Cell***22,** 425–437 (2012).

7. Sturm, D. *et al.* Paediatric and adult glioblastoma: multiform (epi)genomic culprits emerge. *Nat. Rev. Cancer***14,** 92–107 (2014).

8. Louis, D. N. *et al.* The 2016 World Health Organization Classification of Tumors of the Central Nervous System: a summary. *Acta Neuropathol.***131,** 803–820 (2016).

9. Banan, R. & Hartmann, C. The new WHO 2016 classification of brain tumors—what neurosurgeons need to know. *Acta Neurochir. (Wien).***159,** 403–418 (2017).

10. Raabe, E. H. & Eberhart, C. G. Methylome Alterations 'Mark' New Therapeutic Opportunities in Glioblastoma. *Cancer Cell***22,** 417–418 (2012).

11. Bhat, K. P. L. *et al.* Mesenchymal Differentiation Mediated by NF-κB Promotes Radiation

Resistance in Glioblastoma. *Cancer Cell***24,** 1–22 (2013).

12. Cooper, L. A. D. *et al.* The tumor microenvironment strongly impacts master transcriptional regulators and gene expression class of glioblastoma. *Am. J. Pathol.***180,** 2108–2119 (2012).

13. Quail, D. F. & Joyce, J. A. The Microenvironmental Landscape of Brain Tumors. *Cancer Cell***31,** 326–341 (2017).

14. Louveau, A., Harris, T. H. & Kipnis, J. Revisiting the concept of CNS immune privilege. *Trends Immunol.***36,** 569–577 (2015).

15. Rodriguez, F. J., Orr, B. A., Ligon, K. L. & Eberhart, C. G. Neoplastic cells are a rare component in human glioblastoma microvasculature. *Oncotarget.***3,** 98–106 (2012).

16. Nikki A, C., Holland, E. C., Gilbertson, R., Glass, R. & Kettenmann, H. The Brain Tumor Microenvironment. *Glia***60,** 502–14 (2012).

17. O'Brien, E. R., Howarth, C. & Sibson, N. R. The role of astrocytes in CNS tumors: pre-clinical models and novel imaging approaches. *Front. Cell. Neurosci.***7,** 40 (2013).

18. Abbott, N. J. Astrocyte-endothelial interactions and blood-brain barrier permeability. *J. Anat.***200,** 629–638 (2002).

19. Cabezas, R. *et al.* Astrocytic modulation of blood brain barrier: perspectives on Parkinsons disease. *Front. Cell. Neurosci.***8,** 1–11 (2014).

20. Ferraro, G. B., Kodack, D. P., Askoxylakis, V. & Jain, R. K. Closing the gap between astrocytes and brain metastasis progression. *Nat. Publ. Gr.***26,** 1–2 (2016).

21. Liu, L. *et al.* Astrocyte Elevated Gene-1 Upregulates Matrix Metalloproteinase-9 and Induces Human Glioma Invasion. *Cancer Res.***70,** 3750–3759 (2010).

22. Bajetto, A. *et al.* Glial and neuronal cells express functional chemokine receptor CXCR4 and its natural ligand stromal cell-derived factor 1. *J. Neurochem.***73,** 2348–2357 (1999).

23. Katz, A. M. *et al.* Astrocyte-specific expression patterns associated with the PDGF-

induced glioma microenvironment. *PLoS One***7,** (2012).

24. Antonios, J. P., Everson, R. G. & Liau, L. M. Dendritic cell immunotherapy for brain tumors. *J. Neurooncol.***123,** 425–432 (2015).

25. Lohr, J. *et al.* Effector T-cell infiltration positively impacts survival of glioblastoma patients and is impaired by tumor-derived TGF-β. *Clin. Cancer Res.***17,** 4296–4308 (2011).

26. Fecci, P. E. *et al.* Increased regulatory T-cell fraction amidst a diminished CD4 compartment explains cellular immune defects in patients with malignant glioma. *Cancer Res.***66,** 3294–3302 (2006).

27. Wainwright, D. A. *et al.* Durable therapeutic efficacy utilizing combinatorial blockade against IDO, CTLA-4 and PD-L1 in mice with brain tumors. *Clin. Cancer Res.***20,** 5290–5301 (2015).

28. Pyonteck, S. M. *et al.* CSF-1R inhibition alters macrophage polarization and blocks glioma progression. *Nat. Med.***19,** 1264–72 (2013).

29. Ghosh, A. & Chaudhuri, S. Microglial action in glioma: a boon turns bane. *Immunol. Lett.***131,** 3–9 (2010).

30. Kmiecik, J. *et al.* Elevated CD3+ and CD8+ tumor-infiltrating immune cells correlate with prolonged survival in glioblastoma patients despite integrated immunosuppressive mechanisms in the tumor microenvironment and at the systemic level. *J. Neuroimmunol.***264,** 71–83 (2013).

31. Liang, J. *et al.* Neutrophils promote the malignant glioma phenotype through S100A4. *Clin. Cancer Res.***20,** 187–198 (2014).

32. Perry, V. H., Nicoll, J. A. R. & Holmes, C. Microglia in neurodegenerative disease. *Nat. Rev. Neurol.***6,** 193–201 (2010).

33. Beggs, S. & Salter, M. W. SnapShot: Microglia in Disease. *Cell***165,** 1294–1294e1 (2016).

34. Salter, M. W. & Stevens, B. Microglia emerge as central players in brain disease. *Nat.*

*Med.***23,** 1018–1027 (2017).

35. Cherry, J. D., Olschowka, J. A. & O'Banion, M. Neuroinflammation and M2 microglia: the good, the bad, and the inflamed. *J. Neuroinflammation***11,** 98 (2014).

36. Penfield, W. Microglia and the process of phagocytosis in gliomas. *Am. J. Pathol.* (1925).

37. Kettenmann, H., Hanisch, U.-K., Noda, M. & Verkhratsky, A. Physiology of Microglia. *Physiol. Rev.***91,** 461–553 (2011).

38. Ransohoff, R. M. A polarizing question: do M1 and M2 microglia exist? *Nat. Neurosci.***19,** 987–991 (2016).

39. Tremblay, M. Ě., Lowery, R. L. & Majewska, A. K. Microglial interactions with synapses are modulated by visual experience. *PLoS Biol.***8,** (2010).

40. Hristovska, I. & Pascual, O. Deciphering Resting Microglial Morphology and Process Motility from a Synaptic Prospect. *Front. Integr. Neurosci.***9,** 1–7 (2016).

41. Guedes, J., Cardoso, A. L. C. & Pedroso De Lima, M. C. Involvement of MicroRNA in microglia-mediated immune response. *Clin. Dev. Immunol.***2013,** (2013).

42. Walker, D. G. & Lue, L.-F. Immune phenotypes of microglia in human neurodegenerative disease: challenges to detecting microglial polarization in human brains. *Alzheimers. Res. Ther.***7,** 56 (2015).

43. Tang, Y. & Le, W. Differential Roles of M1 and M2 Microglia in Neurodegenerative Diseases. *Mol. Neurobiol.***53,** 1181–1194 (2016).

44. Raivich, G. *et al.* Neuroglial activation repertoire in the injured brain: Graded response, molecular mechanisms and cues to physiological function. *Brain Res. Rev.***30,** 77–105 (1999).

45. Bell-Temin, H. *et al.* Novel molecular insights into classical and alternative activation states of microglia as revealed by SILAC-based proteomics. *Mol. Cell. Proteomics***14,** 1–36 (2015).

46. Krausgruber, T. *et al.* IRF5 promotes inflammatory macrophage polarization and TH1-TH17 responses. *Nat. Immunol.***12,** 231–238 (2011).

47. Goldmann, T. & Prinz, M. Role of microglia in CNS autoimmunity. *Clin. Dev. Immunol.***2013,** (2013).

48. Duque, G. A. & Descoteaux, A. Macrophage cytokines: Involvement in immunity and infectious diseases. *Front. Immunol.***5,** 1–12 (2014).

49. Gordon, S. Alternative activation of macrophages. *Nat. Rev. Immunol.***3,** 23–35 (2003).

50. Rodero, M. *et al.* Polymorphism in the microglial cell-mobilizing CX3CR1 gene is associated with survival in patients with glioblastoma. *J. Clin. Oncol.***26,** 5957–5964 (2008).

51. Kerber, M. *et al.* Flt-1 signaling in macrophages promotes glioma growth in vivo. *Cancer Res.***68,** 7342–7351 (2008).

52. Strik, H. M., Stoll, M. & Meyermann, R. Immune Cell Infiltration of Intrinsic and Metastatic Intracranial Tumours. *Anticancer Res.***24,** 37–42 (2004).

53. Li, W. & Graeber, M. B. The molecular profile of microglia under the influence of glioma. *Neuro. Oncol.***14,** 958–78 (2012).

54. Markovic, D. S., Glass, R., Synowitz, M., Rooijen, N. Van & Kettenmann, H. Microglia stimulate the invasiveness of glioma cells by increasing the activity of metalloprotease-2. *J. Neuropathol. Exp. Neurol.***64,** 754–62 (2005).

55. Markovic, D. S. *et al.* Gliomas induce and exploit microglial MT1-MMP expression for tumor expansion. *Proc. Natl. Acad. Sci. U. S. A.***106,** 12530–5 (2009).

56. Watanabe, A. *et al.* Critical Role of Transient Activity of MT1-MMP for ECM Degradation in Invadopodia. *PLoS Comput. Biol.***9,** (2013).

57. Chen, X. *et al.* RAGE Expression in Tumor-associated Macrophages Promotes Angiogenesis in Glioma. *Cancer Res.***74,** 7285–7297 (2014).

58. da Fonseca, A. C. C. *et al.* Increased expression of stress inducible protein 1 in glioma-associated microglia/macrophages. *J. Neuroimmunol.***274,** 71–77 (2014).

59. Wesolowska, A. *et al.* Microglia-derived TGF-b as an important regulator of glioblastoma invasion—an inhibition of TGF-b-dependent effects by shRNA against human TGF-b type II receptor. *Oncogene***27,** 918–930 (2008).

60. Coniglio, S. & Eugenin, E. Microglial Stimulation of Glioblastoma Invasion Involves Epidermal Growth Factor Receptor (EGFR) and Colony Stimulating Factor 1 Receptor (CSF-1R) Signaling. *Mol. Med.***18,** 1 (2012).

61. Pyonteck, S. M. *et al.* CSF-1R inhibition alters macrophage polarization and blocks glioma progression. *Nat. Med.***19,** 1264–1272 (2013).

62. Gabrusiewicz, K. *et al.* Characteristics of the alternative phenotype of microglia/macrophages and its modulation in experimental gliomas. *PLoS One***6,** e23902 (2011).

63. Szulzewsky, F. *et al.* Glioma-associated microglia/macrophages display an expression profile different from M1 and M2 polarization and highly express Gpnmb and Spp1. *PLoS One***10,** 1–27 (2015).

64. Rodrigues, J. C. *et al.* Normal human monocytes exposed to glioma cells acquire myeloid-derived suppressor cell-like properties. *Neuro. Oncol.***12,** 351–365 (2010).

65. Wu, A. *et al.* Glioma cancer stem cells induce immunosuppressive macrophages/microglia. *Neuro. Oncol.***12,** 1113–1125 (2010).

66. Wei, J., Gabrusiewicz, K. & Heimberger, A. B. The Controversial Role of Microglia in Malignant Gliomas. *Clin. Dev. Immunol.***2013,** (2013).

67. Dzaye, O. D. A. *et al.* Glioma stem cells but not bulk glioma cells upregulate IL-6 secretion in microglia/brain macrophages via toll-like receptor 4 signaling. *J. Neuropathol. Exp. Neurol.***75,** 429–440 (2016).

68. Bao, S. *et al.* Glioma stem cells promote radioresistance by preferential activation of the

DNA damage response. *Nature***444,** 756–760 (2006).

69. Brennan, C. *et al.* Glioblastoma subclasses can be defined by activity among signal transduction pathways and associated genomic alterations. *PLoS One***4,** (2009).

70. Hu, F. *et al.* Glioma-associated microglial MMP9 expression is upregulated by TLR2 signaling and sensitive to minocycline. *Int. J. Cancer***135,** 2569–2578 (2014).

71. Hambardzumyan, D., Gutmann, D. H. & Kettenmann, H. The role of microglia and macrophages in glioma maintenance and progression. *Nat. Neurosci.***19,** 20–27 (2016).

72. Vaure, C. & Liu, Y. A comparative review of toll-like receptor 4 expression and functionality in different animal species. *Front. Immunol.***5,** 1–15 (2014).

73. Billack, B. Macrophage activation: Role of Toll-like receptors, nitric oxide, and nuclear factor kappa B. *Am. J. Pharm. Educ.***70,** (2006).

74. Siegemund, S. & Sauer, K. Balancing pro- and anti-inflammatory TLR4 signaling. *Nat. Immunol.***13,** 1031–1033 (2012).

75. Mosser, D. M. & Edwards, J. P. Exploring the full spectrum of macrophage activation David. *Nat. Rev. Immunol.***8,** 958–969 (2008).

76. Aksoy, E. *et al.* The p110δ isoform of the kinase PI(3)K controls the subcellular compartmentalization of TLR4 signaling and protects from endotoxic shock. *Nat. Immunol.***13,** 1045–1054 (2012).

77. Valledor, A. F., Comalada, M., Santamaría-Babi, L. F., Lloberas, J. & Celada, A. Macrophage Proinflammatory Activation and Deactivation. A Question of Balance. *Adv. Immunol.***108,** 1–20 (2010).

78. Smale, S. T. & Natoli, G. Transcriptional Control of Inflammatory Responses. *Cold Spring Harb Perspect Biol***6,** 1–11 (2014).

79. Zhou, W. *et al.* Histone H2A Monoubiquitination Represses Transcription by Inhibiting RNA Polymerase II Transcriptional Elongation. *Mol. Cell***29,** 69–80 (2008).

80. De Santa, F. *et al.* The Histone H3 Lysine-27 Demethylase Jmjd3 Links Inflammation to Inhibition of Polycomb-Mediated Gene Silencing. *Cell***130,** 1083–1094 (2007).

81. Xing, X. Q. *et al.* Sphingosine kinase 1/sphingosine 1-phosphate signalling pathway as a potential therapeutic target of pulmonary hypertension. *Int. J. Clin. Exp. Med.***8,** 11930–11935 (2015).

82. Spiegel, S. & Milstien, S. Sphingosine-1-phosphate: an enigmatic signalling lipid. *Nat. Rev. Mol. Cell Biol.***4,** 397–407 (2003).

83. Gault, C. R., Obeid, L. M. & Hannun, Y. A. An overview of sphingolipid metabolism: From synthesis to breakdown. *Adv. Exp. Med. Biol.***688,** 1–23 (2010).

84. Futerman, A. H. & Hannun, Y. A. The complex life of simple sphingolipids. *EMBO Rep.***5,** 777–782 (2004).

85. Zhang, H. *et al.* Sphingosine-1-phosphate, a novel lipid, involved in cellular proliferation. *J. Cell Biol.***114,** 155–167 (1991).

86. Meyer zu Heringdorf, D. *et al.* Sphingosine kinase-mediated Ca 2+ signalling by G-protein-coupled receptors. *EMBO J.***17,** 2830–2837 (1998).

87. Cuvillier, O. *et al.* Suppression of ceramide-mediated programmed cell death by sphingosine-1-phosphate. *Nature***381,** 800–803 (1996).

88. Imai, H. & Nishiura, H. Phosphorylation of sphingoid long-chain bases in Arabidopsis: Functional characterization and expression of the first sphingoid long-chain base kinase gene in plants. *Plant Cell Physiol.***46,** 375–380 (2005).

89. Mandala, S. M. *et al.* Sphingoid base 1-phosphate phosphatase: a key regulator of sphingolipid metabolism and stress response. *Proc. Natl. Acad. Sci. U. S. A.***95,** 150–155 (1998).

90. Spiegel, S. & Milstien, S. Sphingosine 1-phosphate, a key cell signaling molecule. *J. Biol. Chem.***277,** 25851–25854 (2002).

91. Kim, S., Fyrst, H. & Saba, J. Accumulation of phosphorylated sphingoid long chain bases

results in cell growth inhibition in Saccharomyces cerevisiae. *Genetics***156,** 1519–1529 (2000).

92. Wang, Z. *et al.* Molecular Basis of Sphingosine Kinase 1 Substrate Recognition and Catalysis. *Structure***21,** 798–809 (2013).

93. Hait, N. C., Fujita, K., Lester, R. L. & Dickson, R. C. Lcb4p sphingoid base kinase localizes to the Golgi and late endosomes. *FEBS Lett.***532,** 97–102 (2002).

94. Funato, K., Lombardi, R., Vallée, B. & Riezman, H. Lcb4p is a key regulator of ceramide synthesis from exogenous long chain sphingoid base in Saccharomyces cerevisiae. *J. Biol. Chem.***278,** 7325–7334 (2003).

95. Maceyka, M., Harikumar, K. B., Milstien, S. & Spiegel, S. Sphingosine-1-phosphate signaling and its role in disease. *Trends Cell Biol.***22,** 50–60 (2012).

96. Jarman, K. E., Moretti, P. A. B., Zebol, J. R. & Pitson, S. M. Translocation of sphingosine kinase 1 to the plasma membrane is mediated by calcium- and integrin-binding protein 1. *J. Biol. Chem.***285,** 483–492 (2010).

97. Neubauer, H. A. & Pitson, S. M. Roles, regulation and inhibitors of sphingosine kinase 2. *FEBS J.***280,** 5317–5336 (2013).

98. Hait, N. C. *et al.* Regulation of Histone Acetylation in the Nucleus by Sphingosine-1-Phosphate. *Scienc***325,** 1254–1257 (2009).

99. Igarashi, N. *et al.* Sphingosine Kinase 2 Is a Nuclear Protein and Inhibits DNA Synthesis. *J. Biol. Chem.***278,** 46832–46839 (2003).

100. Maceyka, M. *et al.* SphK1 and SphK2, sphingosine kinase isoenzymes with opposing functions in sphingolipid metabolism. *J. Biol. Chem.***280,** 37118–37129 (2005).

101. Chipuk, J. E. *et al.* Sphingolipid Metabolism Cooperates with BAK and BAX to Promote the Mitochondrial Pathway of Apoptosis. *Cell***148,** 988–1000 (2012).

102. Brinkmann, V. Sphingosine 1-phosphate receptors in health and disease: Mechanistic insights from gene deletion studies and reverse pharmacology. *Pharmacol. Ther.***115,** 84–

105 (2007).

103. Blaho, V. A. & Hla, T. An update on the biology of sphingosine 1-phosphate receptors. *J. lipid reseach***55,** 1596–608 (2014).

104. Mehling, M., Kappos, L. & Derfuss, T. Fingolimod for multiple sclerosis: Mechanism of action, clinical outcomes, and future directions. *Curr. Neurol. Neurosci. Rep.***11,** 492–497 (2011).

105. Takabe, K. & Spiegel, S. Export of Sphingosine-1-Phosphate and Cancer Progression. *J. lipid reseach***55,** 1839–46 (2014).

106. Xia, P. *et al.* An oncogenic role of sphingosine kinase. *Curr. Biol.***10,** 1527–1530 (2000).

107. Sukocheva, O. a *et al.* Sphingosine kinase transmits estrogen signaling in human breast cancer cells. *Mol. Endocrinol.***17,** 2002–12 (2003).

108. Wu, W., Shu, X., Hovsepyan, H., Mosteller, R. D. & Broek, D. VEGF receptor expression and signaling in human bladder tumors. *Oncogene***22,** 3361–3370 (2003).

109. Van Brocklyn, J. R. *et al.* Sphingosine kinase-1 expression correlates with poor survival of patients with glioblastoma multiforme: roles of sphingosine kinase isoforms in growth of glioblastoma cell lines. *J Neuropathol Exp Neurol***64,** 695–705 (2005).

110. Shida, D., Takabe, K., Kapitonov, D., Milstien, S. & Spiegel, S. Targeting SphK1 as a new strategy against cancer. *Curr. Drug Targets***9,** 662–73 (2008).

111. Young, N. & Van Brocklyn, J. R. Roles of sphingosine-1-phosphate (S1P) receptors in malignant behavior of glioma cells. Differential effects of S1P2 on cell migration and invasiveness. *Exp. Cell Res.***313,** 1615–1627 (2007).

112. Ponnusamy, S. *et al.* Communication between host organism and cancer cells is transduced by systemic sphingosine kinase 1/sphingosine 1-phosphate signalling to regulate tumour metastasis. *EMBO Mol. Med.***4,** 761–775 (2012).

113. Zhang, L. *et al.* Anti-S1P antibody as a novel therapeutic strategy for VEGFR TKI resistant renal cancer. *Clin. Cancer …***21,** 1925–1934 (2015).

114. Ader, I. *et al.* Neutralizing S1P inhibits intratumoral hypoxia, induces vascular remodelling and sensitizes to chemotherapy in prostate cancer. *Oncotarget***6,** 13803–21 (2015).

115. Milstien, S. & Spiegel, S. Targeting sphingosine-1-phosphate: a novel avenue for cancer therapeutics. *Cancer Cell***9,** 148–50 (2006).

116. Saura, J., Tusell, J. M. & Serratosa, J. High-yield isolation of murine microglia by mild trypsinization. *Glia***44,** 183–189 (2003).

117. Guillermet-Guibert, J. *et al.* Targeting the sphingolipid metabolism to defeat pancreatic cancer cell resistance to the chemotherapeutic gemcitabine drug. *Mol. Cancer Ther.***8,** 809–820 (2009).

118. Abuhusain, H. J. *et al.* A metabolic shift favoring sphingosine 1-phosphate at the expense of ceramide controls glioblastoma angiogenesis. *J. Biol. Chem.***288,** 37355–37364 (2013).

119. Verhaak, R. G. W. *et al.* An integrated genomic analysis identifies clinically relevant subtypes of glioblastoma characterized by abnormalities in PDGFRA, IDH1, EGFR and NF1. *Cancer Cell***17,** 98 (2010).

120. Engler, J. R. *et al.* Increased microglia/macrophage gene expression in a subset of adult and pediatric astrocytomas. *PLoS One***7,** e43339 (2012).

121. Barcellos-hoff, M. H., Newcomb, E. W., Zagzag, D. & Narayana, A. Therapeutic Targets in Malignant Glioblastoma Microenvironment. *Semin Radiat Oncol***19,** 163–170 (2009).

122. Butovsky, O. *et al.* Identification of a unique TGF-β–dependent molecular and functional signature in microglia. *Nat. Neurosci.***17,** 131–143 (2013).

123. Bennett, M. L. *et al.* New tools for studying microglia in the mouse and human CNS. *Proc. Natl. Acad. Sci.***113,** E1738–E1746 (2016).

124. Cingolani, F. *et al.* Inhibition of dihydroceramide desaturase activity by the sphingosine kinase inhibitor SKI II. *J. Lipid Res.***55,** 1711–1720 (2014).

125. Truman, J. P., García-Barros, M., Obeid, L. M. & Hannun, Y. A. Evolving concepts in

cancer therapy through targeting sphingolipid metabolism. *Biochim. Biophys. Acta - Mol. Cell Biol. Lipids***1841,** 1174–1188 (2014).

126. Lobo-Silva, D., Carriche, G. M., Castro, A. G., Roque, S. & Saraiva, M. Balancing the immune response in the brain: IL-10 and its regulation. *J. Neuroinflammation***13,** 297 (2016).

127. Biswas, S. K. & Mantovani, A. Macrophage plasticity and interaction with lymphocyte subsets: cancer as a paradigm. *Nat. Immunol.***11,** 889–896 (2010).

128. Milstien, S. & Spiegel, S. Targeting sphingosine-1-phosphate: A novel avenue for cancer therapeutics. *Cancer Cell***9,** 148–150 (2006).

129. Kunkel, G. T., Maceyka, M., Milstien, S. & Spiegel, S. Targeting the sphingosine-1-phosphate axis in cancer, inflammation and beyond. *Nat. Rev. Drug Dsicovery***12,** 688–702 (2013).

130. LaMontagne, K. *et al.* Antagonism of sphingosine-1-phosphate receptors by FTY720 inhibits angiogenesis and tumor vascularization. *Cancer Res.***66,** 221–231 (2006).

131. Lawrence, T. The nuclear factor NF-kappaB pathway in inflammation. *Cold Spring Harb. Perspect. Biol.***1,** 1–10 (2009).

132. Hoesel, B. & Schmid, J. A. The complexity of NF-κB signaling in inflammation and cancer. *Mol. Cancer***12,** 86 (2013).

133. Chow, J. C. *et al.* Toll-like Receptor-4 Mediates Lipopolysaccharide-induced Signal Transduction. *J. Biol. Chem.* 10689–10693 (1999). doi:10.1074/jbc.274.16.10689

134. Ballman, K. V *et al.* The relationship between six-month progression-free survival and 12-month overall survival end points for phase II trials in patients with glioblastoma multiforme. *Neuro. Oncol.***9,** 29–38 (2007).

135. Gutman, S., Piper, M., Grant, M. & Al., E. Progression-free survival: what does it mean for psychological well-being or quality of life? *Methods Res. Rep.* 21 (2013).

136. Rao, R. P. *et al.* Ceramide transfer protein deficiency compromises organelle function and

leads to senescence in primary cells. *PLoS One***9,** (2014).

137. Mullen, T. D. *et al.* Selective knockdown of ceramide synthases reveals complex interregulation of sphingolipid metabolism. *J. Lipid Res.***52,** 68–77 (2011).

138. Verhaak, R. G. W. *et al.* Integrated Genomic Analysis Identifies Clinically Relevant Subtypes of Glioblastoma Characterized by Abnormalities in PDGFRA, IDH1, EGFR, and NF1. *Cancer Cell***17,** 98–110 (2010).

139. Zarkoob, H., Taube, J. H., Singh, S. K., Mani, S. A. & Kohandel, M. Investigating the Link between Molecular Subtypes of Glioblastoma, Epithelial-Mesenchymal Transition, and CD133 Cell Surface Protein. *PLoS One***8,** (2013).

140. Ni, M. *et al.* Epithelial mesenchymal transition of non–small–cell lung cancer cells A549 induced by SPHK1. *Asian Pac. J. Trop. Med.***8,** 142–146 (2015).

141. Liu, H., Ma, Y., He, H., Zhao, W. & Shao, R. SPHK1 (sphingosine kinase 1) induces epithelial-mesenchymal transition by promoting the autophagy-linked lysosomal degradation of CDH1/E-cadherin in hepatoma cells. *Autophagy***8627,** 900–913 (2017).

142. Mauer, J. *et al.* Interleukin-6 signaling promotes alternative macrophage activation to limit obesity-associated insulin resistance and endotoxemia. *Nat. Immunol.***15,** 423–430 (2014).

143. Wang, N., Liang, H. & Zen, K. Molecular mechanisms that influence the macrophage M1-M2 polarization balance. *Front. Immunol.***5,** 1–9 (2014).

144. Wang, W., Tan, M., Yu, J. & Tan, L. Role of pro-inflammatory cytokines released from microglia in Alzheimer's disease. *Ann. Transl. Med.***3,** 1–15 (2015).

145. M., M. *et al.* Downregulation of sphingosine kinase-1 induces protective tumor immunity by promoting M1 macrophage response in melanoma. *Oncotarget***7,** 71873–71886 (2016).

146. Weigert, A. *et al.* Tumor Cell Apoptosis Polarizes Macrophages—Role of Sphingosine-1-Phosphate. *Mol. Biol. Cell***18,** 3810–3819 (2007).

147. Weigert, A. *et al.* Sphingosine kinase 2 deficient tumor xenografts show impaired growth and fail to polarize macrophages towards an anti-inflammatory phenotype. *Int. J.*

*Cancer***125,** 2114–21 (2009).

148. Bien-Möller, S. *et al.* Expression of S1P metabolizing enzymes and receptors correlate with survival time and regulate cell migration in glioblastoma multiforme. *Oncotarget***7,** 13031–46 (2016).

149. Kapitonov, D. *et al.* Targeting Sphingosine Kinase 1 inhibits AKT signaling, induces apoptosis, and suprresses growth of human glioblastoma cells and xenografts. *Cancer Res.***69,** 6915–6923 (2010).

150. Visentin, B. *et al.* Validation of an anti-sphingosine-1-phosphate antibody as a potential therapeutic in reducing growth, invasion, and angiogenesis in multiple tumor lineages. *Cancer Cell***9,** 225–238 (2006).

151. Hutchins, A. P., Diez, D. & Miranda-Saavedra, D. The IL-10/STAT3-mediated anti-inflammatory response: Recent developments and future challenges. *Brief. Funct. Genomics***12,** 489–498 (2013).

152. Murray, P. J. The primary mechanism of the IL-10-regulated antiinflammatory response is to selectively inhibit transcription. *Proc. Natl. Acad. Sci. U. S. A.***102,** 8686–91 (2005).

153. Hutchins, A. P., Takahashi, Y. & Miranda-Saavedra, D. Genomic analysis of LPS-stimulated myeloid cells identifies a common pro-inflammatory response but divergent IL-10 anti-inflammatory responses. *Sci. Rep.***5,** 9100 (2015).

154. Kühn, R., Löhler, J., Rennick, D., Rajewsky, K. & Müller, W. Interleukin-10-deficient mice develop chronic enterocolitis. *Cell***75,** 263–274 (1993).

155. Takeda, K. *et al.* Enhanced Th1 activity and development of chronic enterocolitis in mice devoid of stat3 in macrophages and neutrophils. *Immunity***10,** 39–49 (1999).

156. Braun, D. A., Fribourg, M. & Sealfon, S. C. Cytokine response is determined by duration of receptor and signal transducers and activators of transcription 3 (STAT3) activation. *J. Biol. Chem.***288,** 2986–2993 (2013).

157. Covarrubias, A. J., Aksoylar, H. I. & Horng, T. Control of macrophage metabolism and

activation by mTOR and Akt signaling. *Semin Immunol.***27,** 286–296 (2015).

158. Arranz, A. *et al.* Akt1 and Akt2 protein kinases differentially contribute to macrophage polarization. *Proc. Natl. Acad. Sci.***109,** 9517–9522 (2012).

159. Tarassishin, L., Suh, H.-S. & Lee, S. C. Interferon regulatory factor 3 plays an anti-inflammatory role in microglia by activating the PI3K/Akt pathway. *J. Neuroinflammation***8,** 187 (2011).

160. Biswas, S. K. *et al.* A distinct and unique transcriptional program expressed by tumor-associated macrophages (defective NF-?Band enhanced IRF-3/STAT1 activation). *Blood***107,** 2112–22 (2006).

161. Günthner, R. & Anders, H. J. Interferon-regulatory factors determine macrophage phenotype polarization. *Mediators Inflamm.***2013,** (2013).

162. Garris, C. S. *et al.* Defective sphingosine-1-phosphate receptor 1 (S1P1) phosphorylation exacerbates TH 17-mediated autoimmune neuroinflammation. *Nat. Immunol.***14,** 1166–1172 (2013).

163. Rivera, J., Proia, R. L. & Olivera, A. THE ALLIANCE OF SPHINGOSINE-1-PHOSPHATE AND ITS RECEPTORS IN IMMUNITY. *Nat Rev Immunol***8,** 753–763 (2008).

164. Matloubian, M. *et al.* Lymphocyte egress from thymus and peripheral lymphoid organs is dependent on S1P receptor 1. *Nature***427,** 355–360 (2004).

165. Myat, L. O. *et al.* Immunosuppressive and anti-angiogenic sphingosine 1-phosphate receptor-1 agonists induce ubiquitinylation and proteasomal degradation of the receptor. *J. Biol. Chem.***282,** 9082–9089 (2007).

166. Kharel, Y. *et al.* Sphingosine kinase 2 is required for modulation of lymphocyte traffic by FTY720. *J. Biol. Chem.***280,** 36865–36872 (2005).

167. Lee, H. *et al.* Stat3-induced S1PR1 expression is critical for persistent Stat3 activation in tumors. *Nat. Med.***16,** 1421–1428 (2010).

168. Liang, J. *et al.* Sphingosine-1-Phosphate Links Persistent STAT3 Activation, Chronic Intestinal Inflammation, and Development of Colitis-Associated Cancer. *Cancer Cell***23,** 107–120 (2013).

169. Wang, F. *et al.* Sphingosine-1-phosphate receptor-2 deficiency leads to inhibition of macrophage proinflammatory activities and atherosclerosis in apoE-deficient mice. *J. Clin. Invest.***120,** 3979–3995 (2010).

170. Hughes, J. E. *et al.* Sphingosine-1-phosphate induces an antiinflammatory phenotype in macrophages. *Circ. Res.***102,** 950–958 (2008).

171. Park, S. J. *et al.* Sphingosine 1-phosphate induced anti-atherogenic and atheroprotective M2 macrophage polarization through IL-4. *Cell. Signal.***26,** 2249–2258 (2014).

172. Gordon, P., Okai, B., Hoare, J. I., Erwig, L. P. & Wilson, H. M. SOCS3 is a modulator of human macrophage phagocytosis. *J. Leukoc. Biol.***100,** 771–780 (2016).

173. Meguro, K. *et al.* SOCS3 Expressed in M2 Macrophages Attenuates Contact Hypersensitivity by Suppressing MMP-12 Production. *J. Invest. Dermatol.***136,** 649–657 (2016).

174. Aksoy, E. *et al.* The p110δ isoform of the kinase PI(3)K controls the subcellular compartmentalization of TLR4 signaling and protects from endotoxic shock. *Nat. Immunol.***13,** 1045–54 (2012).

175. Eskan, M. A., Rose, B. G., Benakanakere, M. R., Lee, M.-J. J. & Kinane, D. F. Sphingosine 1-phosphate 1 and TLR4 mediate IFN-beta expression in human gingival epithelial cells. *J. Immunol.***180,** 1818–1825 (2008).

7. Acknowlegdement

I would like to express my deep gratitude to Dr. Bjorn Tews for giving me the opportunity to conduct my PhD thesis in his division. I extremely value his guidance, encouragement and unlimited support. I thank him in particular for the mentorship and career advice that he provided all the time, and I am grateful for his patience and for offering me the freedom to pursue my research ideas.

I especially thank Prof. Dr. Peter Angel and PD Dr. Roger Sandhoff for their contribution in my thesis examination and TAC committees, and for providing their immense knowledge and vital input to the project.

Furthermore, I thank Prof. Dr. Ana Martin-Villalba for her willingness to participate in my thesis examination committee.

Moreover, I thank Thomas Hielscher from Department of statistics, DKFZ for providing his valued expertise on genomic analysis, and Mahak Singhal from Department of Vascular Oncology and Metastasis, DKFZ for his excellent proficiency with FACS staining and isolations.

My very sincere thanks go to all members of Molecular Mechanisms of Tumor Invasion (V077) lab, especially Dr. Julia Bode, Dr. Peter Wirthschaft, Dr. Lavinia Arseni, Himanshu Soni, Deepthi Nagalla, Fabio, Gordon and other current and former members of the lab for their tremendous support, stimulating discussions, the collaborative spirit and the friendly environment throughout my time as a fellow PhD student.

This journey wouldn’t have been possible without the support of my dearest friends from Heidelberg, Mahak Singhal, Ashik Abdul Pari, Sakeena Quraishi, Dr. Ashwin Sriram, Nalini Srinivas, Dr. Pranav Shah, Dr. Shariq Ansari, and Dr. Marta Fratini. Thank you for your encouragement, advices, debates, dinners, and game nights. I shall never forget the support you’ve given me through hard times together, cheered on me, and celebrated each accomplishment, thanks guys for always being there.

Finally and most importantly, I would like to thank my parents and my sister, who mean the world to me, for their unconditional love and support, and encouraging me in all my pursuits and inspiring me to follow my dreams. I always knew that you believed in me and wanted the best in me. I consider myself the luckiest in the world to have such a supportive family, standing behind me with their love and support.

Rakesh Sharma